GA-8375

EXPERIMENTAL INVESTIGATION OF THE FUNDAMENTAL MODES OF A COLLISIONLESS PLASMA

FINAL REPORT FOR THE PERIOD
10 March 1964 through 31 October 1967

by

John H. Malmberg, Dilip K. Bhadra, David L. Book
C. David Moore, L. Donald Pearlstein, and Charles B. Wharton

Prepared for
National Aeronautics and Space Administration
under Contract NAS7-275

N68-22847 (ACCESSION NUMBER) (THRU)
129 (PAGES) 1 (CODE)
CR-94430 (NASA CR OR TMX OR AD NUMBER) 25 (CATEGORY)
FACILITY FORM 602

GPO PRICE $
CFSTI PRICE(S) $
Hard copy (HC) 3.00
Microfiche (MF) .65
ff 653 July 65

MAR 1968
RECEIVED
NASA STI FACILITY
INPUT BRANCH

Gulf General Atomic
Incorporated
P.O. Box 608, San Diego, California 92112

Gulf General Atomic
Incorporated
P.O. Box 608, San Diego, California 92112

GA-8375

EXPERIMENTAL INVESTIGATION OF THE FUNDAMENTAL MODES OF A COLLISIONLESS PLASMA

FINAL REPORT FOR THE PERIOD
10 March 1964 through 31 October 1967

Work done by:

John H. Malmberg
Dilip K. Bhadra
David L. Book
Norris W. Carlson
William E. Drummond
T. Kenneth Fowler
C. David Moore
Thomas M. O'Neil
L. Donald Pearlstein
Marshall N. Rosenbluth
Norman Rostoker
Charles B. Wharton

Report written by:

John H. Malmberg
Dilip K. Bhadra
David L. Book
C. David Moore
L. Donald Pearlstein
Charles B. Wharton

Contract NAS7-275
National Aeronautics and Space Administration
Western Operations Office
150 Pico Boulevard
Santa Monica, California
Gulf General Atomic Project 407

November 23, 1967

FOREWARD

This final report was prepared by Gulf General Atomic, Incorporated, San Diego, California, under NASA Contract NAS7-275, "Experimental Investigation of the Fundamental Modes of a Collisionless Plasma." Research was conducted during the period 10 March 1964 through 31 October 1967. The Gulf General Atomic Principal Investigator for the contract is Dr. John H. Malmberg, and its project number is 407.

ABSTRACT

This report summarizes results of a three year program of experimental and theoretical research to investigate propagation of electron cyclotron waves in a collisionless plasma and to investigate the origin and effects of low frequency noise in the plasma. The theoretical work concentrates on the application of the linear theory of plasma waves to geometries encountered experimentally, where the size is finite, and the density is a function of position. A perturbation method is derived for predicting the Landau damping (or growth) of electron cyclotron waves in terms of the electron velocity distribution function and the potential and density profiles. The dispersion, damping, and beam induced growth of the waves have been measured as a function of the plasma parameters and the plasma boundary conditions. The results are compared to theory. An electronic device for analyzing composite interferograms composed of two or more damped sine waves is described. Measurements on the origin and effects of low frequency noise in the plasma (10-300 kc) are presented. Methods are given for reducing the low frequency noise which result in a simultaneous order-of-magnitude reduction in anomalous diffusion of the plasma.

PRECEDING PAGE BLANK NOT FILMED.

CONTENTS

	Page
I. INTRODUCTION	1
II. SUMMARY OF RESULTS	3
2.1 Rotation, Diffusion and Noise	3
2.2 Plasma Waves: Theory	5
2.3 Plasma Waves: Experimental	8
APPENDICES	
I - "Rotation, Diffusion, and Noise of a Column of Plasma," by J. H. Malmberg	13
II - "Rotation and Diffusion of a Column of Plasma in a Magnetic Field," by J. H. Malmberg and C. B. Wharton	33
III - "Landau Damping and Growth of Electrostatic Modes with Effects of Spatial Variation," by David L. Book GA-6513	37
IV - "The Dispersion of the Upper Hybrid Mode in a Spatially Inhomogeneous Plasma," by L. D. Pearlstein and D. Bhadra GA-8347	45
V - "Cyclotron Waves in a Collisionless Plasma," by C. B. Wharton and J. H. Malmberg GA-6584	75
VI - "Cyclotron Waves in a Collisionless Plasma," by C. B. Wharton and J. H. Malmberg	91
VII - "Comparison of the Electron Cyclotron Wave Dispersion for Various Boundary Conditions," by J. H. Malmberg	95
VIII - "Curve Resolver for Mixtures of Damped Sine Waves," by C. D. Moore and J. H. Malmberg	113

PRECEDING PAGE BLANK NOT FILMED.

I
INTRODUCTION

This report summarizes research at Gulf General Atomic, Incorporated sponsored by the National Aeronautics and Space Administration (Contract NAS7-275), conducted from 10 March 1964 through 31 October 1967, on the fundamental modes of collisionless plasma. The general objectives of this research program, which was part of the plasma turbulence project at Gulf General Atomic, were to systematically develop the theory of plasma turbulence and to provide a series of detailed experimental checks of the theory. This tested theory would provide a firm foundation for predicting the behavior of plasmas in more complex situations, and especially for predicting the anomalously large transport coefficients associated with plasma turbulence which are encountered in actual plasmas. Significant theoretical and experimental results to this end have been obtained from the research.

The detailed objectives of the NASA program are succinctly summarized by combining the statement of work from the contract authorizing the program and the statements from modifications authorizing its extension:

1. Measurement of the dispersion relations of plasma waves near the electron cyclotron frequency;
2. Measurement of the spatial damping of these waves;
3. Measurement of the coupling of these waves to an electron beam;
4. Measurement of the effects on the waves as the plasma properties are systematically varied;
5. Experimental investigation of the "low frequency" dynamics of the plasma used for the wave experiments;
6. Development of theoretical dispersion relations for plasma waves in nonuniform plasmas; and
7. Comparing the results of 1-5 with theory.

Despite the inevitable shifts in emphasis on various aspects of the program that occurred as our knowledge increased, comparison of the specific accomplishments listed in the results with the statement of work guiding the research indicates that most of the particular calculations and measurements attempted were successful. The appendices to this report consist of the principal scientific papers arising from the research. These papers present in detail the advances in our understanding of plasma dynamics resulting from this project.

The contents of the papers are summarized briefly in Section II. This summary gives an overall view of the research and emphasizes essential results. It is intended that it provide orientation for a study of the scientific papers. In Section II and the appendices, research on noise and diffusion is presented first, the theory of waves second, and experiments on waves last. This ordering is chosen for clarity of exposition. All the papers given in the appendices except one describe work supported wholly or in part by the NASA program. The exception, Appendix IV, describes theoretical work which was undertaken to explain some of the NASA experimental results but supported by a related program. It is included as a convenience to the reader, since this theory is essential for understanding part of the experimental results and since the theory has not yet been published.

II

SUMMARY OF RESULTS

2.1 Rotation, Diffusion and Noise

In almost every experimental case, plasmas diffuse at a rate that is much too large to be explained by binary collision processes. This "anomalous diffusion" determines the characteristics of plasma devices in many cases. It is known that anomalous diffusion is caused by fluctuating electric fields (often associated with instabilities), but the effect is not understood in detail. Anomalous diffusion is observed in the Gulf General Atomic Plasma Turbulence machine, and asymmetric plasma rotation is also observed. In similar experiments, the asymmetric rotation has been associated with a theoretically predicted instability caused by the presence of neutral particles and has been considered to be the cause of the anomalous diffusion.

In the present work, probe studies demonstrated that the plasma rotates asymmetrically in the $E \times B$ direction with frequency in the range 30 to 50 kHz. The frequency and direction are consistent with the radial electric field produced by the plasma potential and the longitudinal magnetic field due to the main coils. By rearranging the bias voltages on the duoplasmatron anode, it was possible to turn off the rotation. When the mean radial electric field is reduced to zero, the rotation stops and the low frequency noise in probe signals is greatly reduced. However, the diffusion of the plasma is unchanged.

We have also observed that the probe signals caused by the asymmetric rotation of the plasma are of smaller amplitude or absent if the neutral background pressure is made sufficiently small, even with an anode bias which would normally allow the rotation. When the background pressure is increased rotation becomes more pronounced. This result is expected from the three fluid theory, which relies on a difference between the drag on the ions and the drag on the electrons caused by a third fluid, the neutral particles, to generate the instability leading to the asymmetry in the rotation.

Most of the anomalous diffusion may be eliminated by modifying the magnetic field of the machine. When a cusp magnetic field is interposed between the source and the main part of the machine and properly adjusted, there is a spectacular reduction in the radial diffusion of the plasma, as indicated by a nearly constant plasma density along the central axis. The broadband noise observed by a downstream probe in the 10 to 50 kc range also decreases by about an order of magnitude when the cusp is properly adjusted. The onset of both effects is rather abrupt and occurs approximately as the central field of the cusp goes through zero. The hypothesis which best explains the experimental results assumes that the 0.12 mm diameter plasma-emitting surface at the anode of the duoplasmation is subject to noisy modulation. Magnetic lines through different parts of the surface have different potentials, which persist down the whole length of the machine. Ions passing near the center of the plasma experience a large, noisy electric field due to potential differences between different magnetic field lines, and are thus diffused radially. When the cusp is turned on, most of the magnetic lines passing through the source intersect the stainless steel cylinder bounding the plasma, and electrons on these lines cannot get past the cusp. Thus, most of the electrons in the downstream plasma come from a small area of the source and large potential fluctuations do not appear between adjacent magnetic lines. Ions pass through the cusp non-adiabatically and so are not much affected, except that those having a large gyroradius strike the wall and are lost. This hypothesis agrees both qualitatively and quantitatively with all our present observations. Thus, we now have a rather complete understanding of the anomalous diffusion mechanism in this case. We also have a method for greatly reducing the diffusion.

These experimental results and their theoretical explanation are described in detail in Appendix I. The abstract of a paper given at a meeting of the Plasma Physics Division of the American Physical Society on this subject is reproduced in Appendix II.

2.2 Plasma Waves: Theory

The theory of electrostatic waves in a cold, collisionless, uniform plasma has been known for a long time. These waves have also been studied for the case of a column of cold plasma of uniform density with finite radius. To apply the theory to our experiments, it was necessary that it be redeveloped for a hot plasma column of nonuniform density. In addition, we need the theory for the case when an electron beam with a radially dependent velocity is injected into the plasma.

The geometry to be considered is a long column of plasma bounded in the radial direction by a good conductor. The plasma is immersed in a uniform finite magnetic field parallel to the axis of the plasma column. The plasma density is a function of radius, but its temperature is not.

One approach is to calculate the Landau damping (or growth) by a perturbation procedure in terms of the plasma velocity distribution function and potential and density profiles. For a zero-temperature plasma, no Landau damping or growth occurs. When a finite spread (finite temperature) is introduced in the velocity distribution of the electrons, the eigenfrequencies become complex; however, if the spread in the distribution is small, γ, the imaginary part of the wave frequency, will be small and the shape of the potential eigenmodes of the system as functions of transverse coordinates will not be greatly altered. The effect of wave-particle resonance is to cause the zero-temperature eigenmodes to grow or decay slowly in time as a whole, without changing otherwise. The rate of decay or growth depends on the slope of the velocity distribution function at the velocities where resonance can take place, weighted by the electrostatic energy as a function of transverse displacement and averaged over the density profile of the plasma. The average is quite insensitive to the exact shape of the transverse profile, and the resulting formula for γ is not qualitatively different from that obtained for infinite homogeneous plasmas. It can be applied to predict the growth or decay of plasma waves in an electron plasma confined by a magnetic field, provided that the density and potential profiles, shape of the electron velocity distribution and dependence of the real part of the wave frequency on $k_{\parallel}$ are known.

For a thermal plasma γ is negative and damping occurs. If an electron beam is injected into the plasma with radially dependent velocity determined by the transverse variation in potential, the averaging process described above smears it into a "gentle bump" on the tail of the Maxwellian, so that waves with the proper phase velocity experience slow growth, just as in the idealized gentle bump problem with an infinite homogeneous plasma. This theory is given in detail in Appendix III.

The variational approach of Appendix III provides only the damping or growth of the waves, not their dispersion. It also approximates the radial density profile. For these reasons, we decided to make a computer code to integrate the dispersion relation directly. This is done as follows. We specify the properties of the plasma by the dielectric tensor relating the displacement to the electric field $(\vec{D} = \vec{\vec{\epsilon}} \cdot \vec{E})$. For waves having phase velocity small compared to the velocity of light, $\nabla \times E$ may be neglected and the electric field calculated from a scalar potential, Ψ. When the plasma is regarded as a dielectric, there are no <u>free</u> charges and

$$\nabla \cdot \vec{D} = \nabla \cdot (\vec{\vec{\epsilon}} \cdot \vec{E}) = - \nabla \cdot (\vec{\vec{\epsilon}} \cdot \nabla \Psi) = 0 \ . \tag{1}$$

The frequency is sufficiently high that the motion of ions may be ignored. The electron gyroradius is assumed small compared to $(1/n)\ (dn/dr)$, where n is the electron density, so the dielectric tensor is a local quantity. Since n is a function of radial position, $\vec{\vec{\epsilon}}$ is also. In addition, $\vec{\vec{\epsilon}}$ is a function of the wave frequency and the magnetic field. A suitable solution for Ψ is

$$\Psi = \varphi(r) e^{i(kz + m\theta)} \ , \tag{2}$$

where k is the complex wave number describing the wave.

Substituting (2) into (1) yields

$$\frac{\partial^2 \varphi}{\partial r^2} + \left[\frac{1}{r\epsilon_{rr}} \frac{\partial}{\partial r} (r\epsilon_{rr}) \right] \frac{\partial \varphi}{\partial r} + \left[\frac{im}{r} \frac{\partial \epsilon_{r\theta}}{\partial r} \right] \varphi - \left[\left(\frac{m}{r} \right)^2 + k^2 \frac{\epsilon_{zz}}{\epsilon_{rr}} \right] \varphi = 0, \tag{3}$$

where ϵ_{zz}, ϵ_{rr}, and $\epsilon_{r\theta}$ are components of the dielectric tensor.

The eigenfunction φ must satisfy the boundary conditions, φ equals zero at the conducting wall, φ equals some given finite normalization factor at the origin and $\partial\varphi/\partial r = 0$ at the origin. In general, φ is complex. The complex eigenvalues, $k = k_r + ik$, computed for a series of real frequencies ω, give the dispersion and Landau damping of the waves.

We have made a computer program to integrate Eq. (3) numerically, subject to the given boundary conditions, for the experimentally observed radial electron-density distribution. For the lower-branch wave (near the plasma frequency), the real part of the parallel dielectric constant, ϵ_{zz}, goes through zero at some radius for some of the frequencies of interest. However, this does not make the equation singular, and so there are no difficulties in integration. The dispersion and damping of the lower-branch wave are accurately predicted by this calculation. For the upper-branch wave (near the electron cyclotron frequency), the real part of the perpendicular component of the dielectric tensor, ϵ_{rr}, goes through zero for some of the frequencies of interest. Since ϵ_{rr} is the coefficient of the highest order derivative, Eq. (3) is almost singular in this case. (Only a small imaginary part of ϵ_{rr} keeps it from being actually singular.) This gives rise to difficulties in the computer code, because of numerical errors near this radius. These numerical problems could be overcome by treating the problem analytically near the singularity and having the computer join this analytic form to the numerical solution. However, these numerical difficulties are the symptoms of a much more serious disease. They indicate that the eigenfunction is changing very rapidly in space near the singularity. But the assumption has been made in deriving the fundamental equations that the electron Larmor radius is small compared to the spatial changes of the eigenfunction. Thus, it is not clear that the code is correct in principle. To answer this question, the theory must be derived to one higher order. We have done this calculation.

For the case in which the density varies in a direction orthogonal to the uniform magnetic field, it becomes necessary to solve a differential equation which is characterized by the vanishing of the coefficient of the second derivative of the perturbed potential at a frequency near the local upper hybrid frequency. Since the differential equation is obtained (in the

small Larmor radius limit) from a convergent expansion of an integral equation it is now necessary to go to higher order in the derivatives of the perturbed potential. In general, such an analysis leads to a fourth order differential equation in which the coefficient of the fourth derivative is down by the Larmor radius squared; however, due to the accidental cancellation in the second derivative, the higher order term can no longer be neglected.

In the present calculation we incorporate the effect of wavelengths parallel to the magnetic field. We concern ourselves with two different regimes. In one, the plasma is Maxwellian and Landau damping is introduced. In the other, a beam with a velocity parallel to the ambient magnetic field is superimposed upon a Maxwellian plasma and instability occurs.

The theory for the spatially inhomogeneous Maxwellian plasma predicts the presence of a mode whose frequency increases with increasing parallel wavenumber for the least damped mode in agreement with the experiment. The frequency drops with increasing parallel wavenumber in the homogeneous infinite medium limit. The theory also predicts an unstable beam mode for frequencies above and below the upper hybrid frequency, whereas the infinite medium solution beam mode is unstable only for frequencies below the upper hybrid frequency. In general, theory and experiment are in qualitative agreement for both the stable and unstable modes of operation.

Our method of solution is a WKBJ analysis of the fourth order differential equation. Since it turns out that the eigenmode is exponentially small outside the turning point of the fourth order equation, but well within the plasma, the analysis leads to reliable values of the eigenvalue but not of the eigenfunction. The answer occurs as an integral from the origin to the turning point of a modified phase equal to $(n + \frac{1}{2})\pi$. The details of this calculation are given in Appendix IV.

The WKBJ analysis provides a convincing explanation of the features of the data but does not have sufficient precision to make an accurate quantitative comparison. The fourth order equation would have to be integrated numerically to obtain such a comparison. This has not been done.

2.3 Plasma Waves: Experimental

The dispersion and damping of the waves near the electron cyclotron frequency have been measured, and their interaction with an electron beam

injected into the plasma has been observed. The measurements have been made for a variety of plasma parameters.

In a first series of measurements, at least three (and perhaps more) distinct waves having resonances (wave number becoming large) or cutoffs near the electron cyclotron frequency have been catalogued. Two waves lie above the cyclotron frequency. One has a high phase velocity, $(v_\varphi > c)$, and is a forward wave. The other is a "slow wave," having a phase that retards with frequency, i.e., a backward wave. The fast wave apparently is an electromagnetic waveguide mode, perturbed by the plasma. The slow wave apparently is the C_{01} cyclotron wave having a propagation cutoff at the upper hybrid frequency, $f_{uh} = (f_b^2 + f_p^2)^{\frac{1}{2}}$.

Below the cyclotron frequency there appear to be several waves. The fastest of these, fairly certainly, is a plasma perturbed TE_{mn} waveguide mode, mentioned above. Its dispersion curve matches that for a TE_{11} mode in a waveguide whose cross-section is 1/10 filled with plasma. The dispersion for this wave is very similar to that for a whistler.

The other "cyclotron waves" are strong waves, having only moderate damping. One of them, having a cutoff frequency between 200 and 300 Mc, seems to be a wave pair, with a frequency-separation depending on density. We have measured effects of various plasma densities and cyclotron frequencies on the cyclotron family of waves. The resonances and cutoffs of the waves move in the expected manner as the plasma and cyclotron frequencies are adjusted. This series of experiments is described in Appendix V. The abstract of a paper on this work given at a American Physical Society meeting is reproduced in Appendix VI.

We have also used a variety of radial boundary conditions for the plasma. This introduced an unexpected complication. In the first series of experiments, the conducting boundary was a cylindrical pipe 10 cm in diameter with two longitudinal slots almost full length for manipulating the probes. The slots coupled into a large diameter ($\sim$ 60 cm) stainless steel vacuum chamber containing essentially no absorbing material. In addition, the chamber was not very uniform, since various mechanical structures (e.g., probe manipulators) protruded into the machine. In this case various waves were observed, including the backward electron cyclotron wave for which we were searching. The appearance of more than one wave

at a given frequency greatly complicated the measurements, as did the appearance of electromagnetic cavity resonances of the machine. Thus, for a second series of measurements one slot was closed and the main chamber lined with wave absorbing material. This change completely removed the high phase velocity wave previously observed above the cyclotron frequency, but the cyclotron wave also changed character. It became much more heavily damped and appeared to break up into a number of different modes. The wave damping also gives evidence of a complicated mode structure. For a third series of measurements, we went all the way and closed the slot in the tube surrounding the plasma with an electrical contactor which opens as the probe approaches and closes behind it. We also provided coaxial shielding of the probes to within one millimeter of their tip. With this geometry the dispersion of the backward wave was no longer measurable, but a well-defined forward wave associated with the electron cyclotron frequency appeared. The dispersion of the forward wave has been measured as a function of plasma parameters, and its interaction with an electron beam has been studied. The experimental data on this forward wave are very clear and unambiguous - just as good as the lower branch data.

We believe the explanation of these changes in wave character as the boundary condition is modified is associated with the fact that the singularity in the second order dispersion equation makes it difficult for the plasma wave to find an eigenmode of the system which matches the boundary condition at the wall and still behaves properly at the singularity. Thus, as the boundary is made more symmetric, the eigenmodes are strongly affected. The lower branch waves, which do not have this singularity, are hardly changed at all by the changes in boundary condition. It is not possible to be sure of this explanation without extensive further experimentation and numerical integration of the fourth order eigenvalue equation. However, the fourth order WKBJ theory provides a qualitative explanation of the observed dispersion of the forward wave and of its interaction with an electron beam injected into the plasma. Detailed experimental data on the cyclotron waves for various boundary conditions are given in Appendix VII. As has already been mentioned, the theory is presented in Appendix IV.

For much of the electron cyclotron wave data, the output of the interferometer is a curve which is the sum of two or more damped sine waves,

and the curve must be reduced to its component parts to be accurately interpreted. The interferometer circuitry converts the signals to a curve $I(z)$ vs z, where z is the position in the plasma and $I(z)$ is of the form

$$I(z) = \sum_i A_i \exp(-\alpha_i z)\sin(k_i z+\varphi_i). \tag{4}$$

The problem is to extract the amplitudes, A_i, damping constants, α_i, wave numbers, k_i, and phases, φ_i, from the composite curve. We have developed an analogue system for doing this analysis. The instrument generates a series of damped sine waves of variable amplitude, frequency, damping constant, and phase. These waveforms are added to obtain a waveform which matches the original data. The component waveforms are then analyzed one at a time. This system is described in Appendix VIII.

APPENDIX I

ROTATION, DIFFUSION, AND NOISE OF A COLUMN OF PLASMA

by

J. H. Malmberg

August 6, 1967

PRECEDING PAGE BLANK NOT FILMED.

Rotation, Diffusion, and Noise of a Column of Plasma

J. H. Malmberg

Gulf General Atomic, Incorporated
P. O. Box 608
San Diego, California 92112

I. INTRODUCTION

In almost every experimental case, plasmas diffuse at a rate that is much too large to be explained by binary collision processes. This "anomalous diffusion" determines the characteristics of plasma devices in many cases. It is known that anomalous diffusion is caused by fluctuating electric fields (often associated with instabilities), but the effect is not understood in detail. Anomalous diffusion is observed in the Gulf General Atomic, Incorporated, Plasma Turbulence machine, and asymmetric plasma rotation is also observed. In similar experiments[1], the asymmetric rotation has been associated with a theoretically predicted instability caused by the presence of neutral particles[2] and has been considered to be the cause of the anomalous diffusion. The present experiments establish that the asymmetry vanishes when the neutral particles are removed, that the diffusion is not altered when the rotation is removed, that the diffusion may be eliminated by modifying the magnetic field, and that the most probable explanation of the diffusion is that it has a subtle connection with source noise. Thus, a reasonably detailed picture of the diffusion process emerges in this case.

PRECEDING PAGE BLANK NOT FILMED.

In Section II of this paper the characteristics of the machine are described. Data on plasma rotation and a method for suppressing it are given in Section III. Section IV presents data on the effects that modification of the magnetic field geometry has on diffusion and noise in the plasma, and proposes a theoretical explanation of the results.

II. MACHINE DESCRIPTION

A schematic diagram of the machine which produces the plasma[3] is given in Fig. 1. The plasma is produced in a duoplasmatron arc source and drifts from it into a long, uniform magnetic field of a few hundred gauss. Since the duoplasmatron has a magnetic field of approximately 3 kG at its orifice, there is a strong magnetic mirror at the source end of the machine. At the other end, the ions are attracted to the negatively charged end plate and die, but the electrons are reflected by the electrostatic field and return to the magnetic mirror. Some electrons are contained at one end by a magnetic mirror and at the other end by an electrostatic field. The ions are not contained; they simply flow through the machine, providing a background of positive charge. The entire machine is steady state. The suppressor grid is held 25 V negative with respect to the end plate to prevent the secondary electrons, which are due to ions striking the end plate, from being injected into the plasma.

The density of ions and electrons in the plasma must be approximately equal, both in the main part of the machine and in the collision-dominated orifice of the duoplasmatron. The ions acquire a much larger Larmor radius than the electrons at the point of injection, and some electrons are contained while the ions are not. Both effects tend to increase the relative electron density. To maintain quasineutrality, the center of the plasma charges negatively with respect to the duoplasmatron anode by roughly 3 kT_e. When the duoplasmatron anode is grounded, the center of the plasma is thus

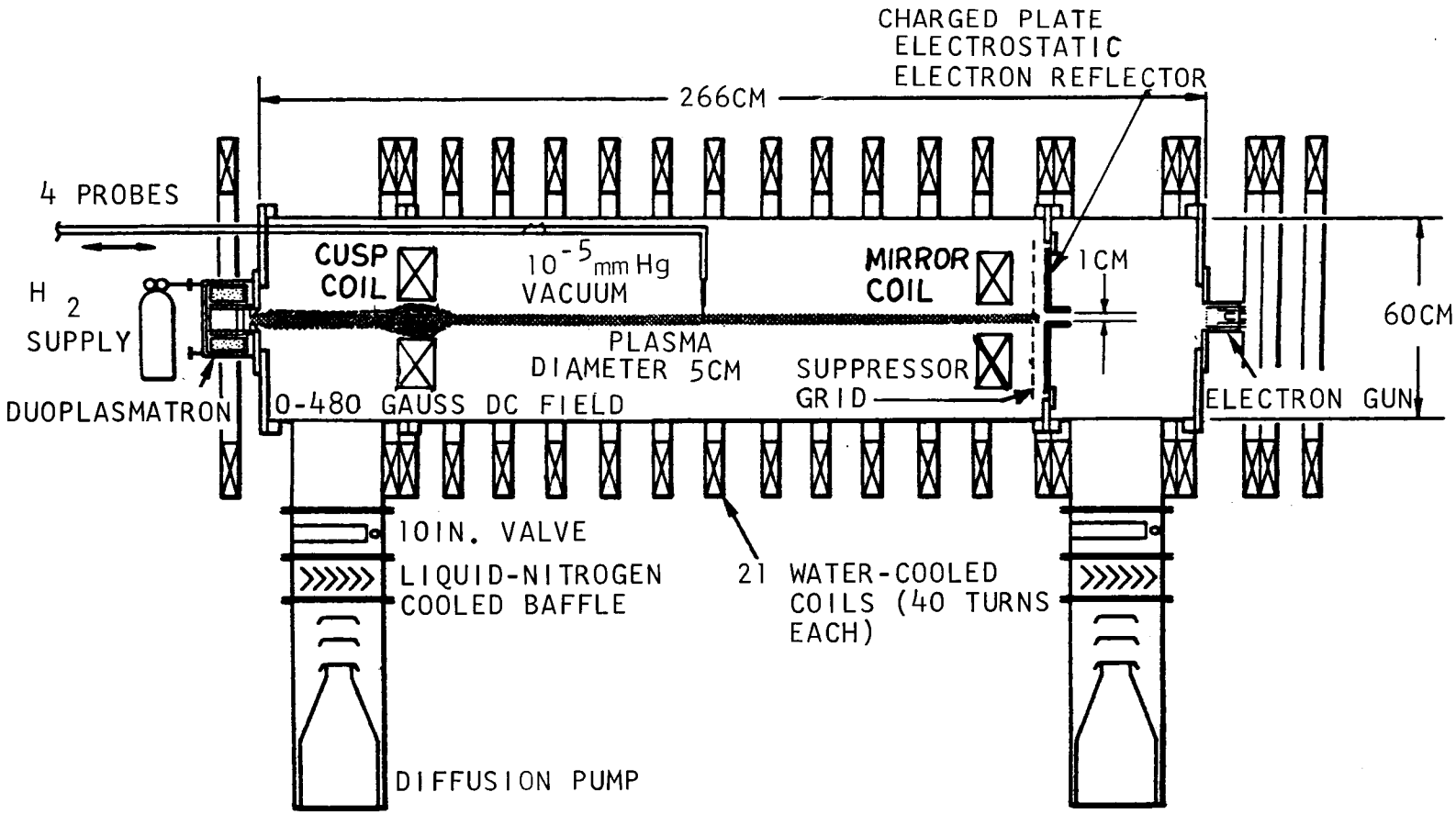

Fig. 1--Schematic diagram of the machine. The 10 cm diameter stainless steel tube surrounding the plasma is not shown

about 3 kT_e negative with respect to the grounded stainless steel cylinder bounding the plasma, and a radial electric field of a few volts per centimeter is established.

Since the 1 mm diam. orifice of the duoplasmatron is collision-dominated, the center of the plasma is very well connected electrically to the anode. The spatial potential along the axis remains almost constant with respect to the duoplasmatron anode as the end plate potential is varied over a wide (negative) range and as the anode potential is varied with respect to the grounded stainless steel cylinder which bounds the plasma radially.

The difference between the duoplasmatron anode potential and the spatial potential at the center of the plasma provides an electric field which extracts ions from the source and injects them through the magnetic mirror into the plasma. The dimensions of the mirror region are not large compared with the Larmor radius and the electric field is not exactly parallel to the magnetic field. Thus, the injection is nonadiabatic; some ions acquire substantial perpendicular energy in their transit through the mirror. The spatial distribution of plasma density is not determined by the magnetic transformation between the duoplasmatron orifice and the main part of the machine; rather, it is determined by the distribution of ion Larmor radii.

For a given gas in the arc (usually H_2), the plasma temperature is determined almost entirely by the relationship of pressure in the duoplasmatron to arc current. At a fixed current, the temperature rises as the pressure is reduced, at first very slowly and then rapidly, until a point is reached at which the arc goes out. Temperatures range from 5 to 20 eV. The radial distribution of plasma density is influenced by the

adjustments of the machine, especially by the magnitude of the magnetic field. The central density is typically 10^8 - 10^9 electrons/cm^3. In the pressure range where the temperature is not very sensitive to arc current, the density of the plasma is almost directly proportional to arc current. The density is also a function of longitudinal position, since the ions diffuse radially as they drift down the machine. This diffusion process is much too fast to be the result of two-body collisions. Typically the central density decreases by a factor of two from one end of the machine to the other.

The machine is pumped by two 10-inch diameter oil diffusion pumps with liquid-nitrogen-cooled baffles to remove neutrals escaping from the source and neutralized ions which have hit the end plate. The background pressure is typically 1.6×10^{-5} torr (mostly hydrogen). The electron mean free path for electron-ion collisions is of the order of 1000 m and for electron-neutral collisions is about 40 m. Debye length is typically 1 mm, and the number of particles in a Debye sphere is about 10^6.

III. ROTATION EXPERIMENTS

The stability of a long axisymmetric column of plasma immersed in a longitudinal magnetic field has been the subject of extensive theoretical[2] and experimental[1] research. This geometry has been widely used for plasma-wave experiments, studies of plasma diffusion, and the investigation of various instabilities. If the plasma is weakly ionized and carries a sufficient longitudinal current, it is, above a certain critical magnetic field, subject to the "screw-instability" which has been explained theoretically and observed experimentally. Large, very regular, periodic variations in plasma density at a fixed radius and azimuth are often observed (with probes) even in experiments having negligible longitudinal current. Analysis of the probe measurements shows that the column of plasma is rotating and is not symmetric about the axis of rotation. The rotation is generally associated with the existence of a radial electric field. The asymmetry is normally explained in terms of some plasma instability expected in a symmetric geometry.

The measurements are best explained by assuming the system is in some "dynamically stable" state of rotation. This state is presumably the nonlinear limit of some instability which may be computed from the linearized theory. The particular instability predicted in this case by Simon and by Hoh[2] is due to a differential drag on the ions and electrons caused by collisions with neutral particles. Some authors believe this behavior causes the anomalous diffusion usually observed in such systems; others do not believe that a coherent rotation can cause diffusion.

The motion of the plasma is deduced from Langmuir probe measurements. First, we discuss measurements taken with the duoplasmatron anode grounded. The fluctuating component of the saturation ion current as a function of time to a glass-covered 0.02 mm diameter tungsten wire with 1 mm exposed at the end is given in Fig. 2 (top trace). Such traces exhibit remarkable coherence and amplitude stability, leading to the interpretation that the motion is "dynamically stable." Such a result cannot be the turbulent end product of random noise growing to a high level. The phase of the signal from a fixed probe was compared with the phase on a second probe as the latter was moved longitudinally the full length of the machine (1.8 m). Within the experimental accuracy (± 10 deg) there is no phase shift. Thus, the asymmetry is not a corkscrew but a straight flute. Comparison of phases between the fixed probe signal and from a probe which may be rotated 360 deg in azimuth (inserted from the end of the machine) shows that the repetition pattern observed on the oscilloscope corresponds to one complete (360 deg) rotation of the plasma. The direction of rotation is given by $\vec{E} \times \vec{B}$, where B is the longitudinal magnetic field and E is the inwardly directed radial electric field.

The anode of the duoplasmatron may be biased with respect to ground without changing arc current or voltage. As the anode voltage is increased, the spatial potential in the plasma along the axis changes from a value of approximately $3\ kT_e$ negative to zero and then to a positive value. As this change is made the plasma rotation slows, stops, and then begins again in the opposite direction. This effect is shown in Fig. 2. The nonrotating state is obtained when the axial potential is approximately zero with respect to the grounded wall.

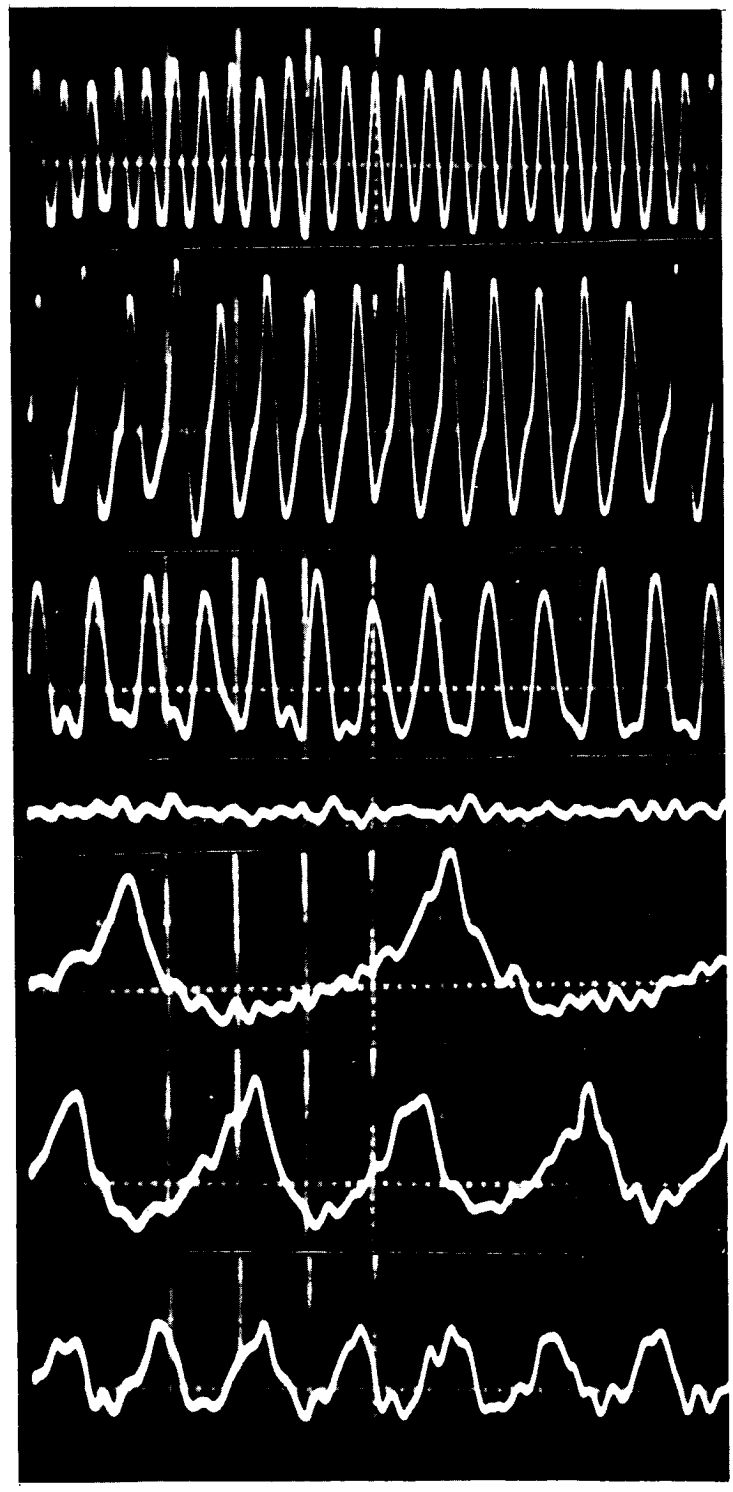

Fig. 2--Probe current, showing column rotation, at various bias voltages on the duoplasmatron anode. DC component, ~ 50 μA; AC component, 5 μA/cm. Time scale, 50 μsec/dm

The spatial potential as a function of radius may be understood qualitatively by considering the processes that keep the plasma "quasi-neutral." As has been explained previously, along the axis the arc is a copious source of electrons. The plasma density here is determined by the ion density. This is an "electron-rich" region. At the instant the machine is turned on, a few extra electrons enter this region, charging it sufficiently negative to prevent more electrons from the duoplasmatron from entering, except for a small flow to compensate losses.

The region well away from the axis receives ions by radial diffusion. Electrons cannot easily diffuse from the central region because their Larmor radius is very small. This region is "electron-poor." In the outer region, the plasma charges positively (by building up sheaths at the ends of the machine) and thus retains for a long time the few electrons it does receive from diffusion, photoionization, etc. Thus, adjusting the anode potential so that the center of the plasma and the wall are at the same potential does not eliminate radial electric fields, except on the average. However, in the latter case, counter-rotating cylindrical shells of plasma would be generated by the $E \times B$ drift. This phenomenon would not be expected intuitively when the Larmor radius is large, and it is not observed. The deductions of the plasma potential as a function of radius and duoplasmatron anode potential given above agree with probe observations of the potential.

The radial electric field can be removed by coating the end plate with a suitable emissive coating which is heated so that it becomes a source of electrons. (The duoplasmatron anode must be covered with a suitable insulator to prevent excessive longitudinal currents from being drawn.) When this experiment was performed, the radial electric field was

suppressed as expected. With appropriate biases on the end plate and duoplasmatron anode, the rotation is also stopped. However, this set of biases stops the rotation whether the end plate is hot (emitting) or not, although the settings are much less critical and the plasma noise level is lower with the plate hot.

The asymmetric rotation becomes progressively more difficult to observe as the background pressure in the machine is reduced. At the lowest background pressure (5×10^{-6} torr) the effect is not observable. When this condition is obtained, the asymmetric rotation may be restored by an increase in chamber pressure with no other machine changes. The existence of the asymmetric rotation depends on the presence of neutrals as predicted by the theory.

The ions diffuse radially at the same time they are drifting axially away from the duoplasmatron. This diffusion manifests itself as a spreading of the radial density distribution and a drop in the axial density downstream from the source. The central density as a function of longitudinal position is given in Fig. 3. Since the electrons do not diffuse radially as rapidly as the ions, but have a larger axial velocity, an electric field is established longitudinally which keeps the electron and ion densities approximately equal according to the equation

$$n = n_o \exp \frac{-e\varphi}{kT_e} , \qquad (1)$$

where n is the electron number density, n_o is the electron density at the point where φ is zero, φ is the spatial potential, T is the electron temperature, and e and k are the electron charge and Boltzmann's constant,

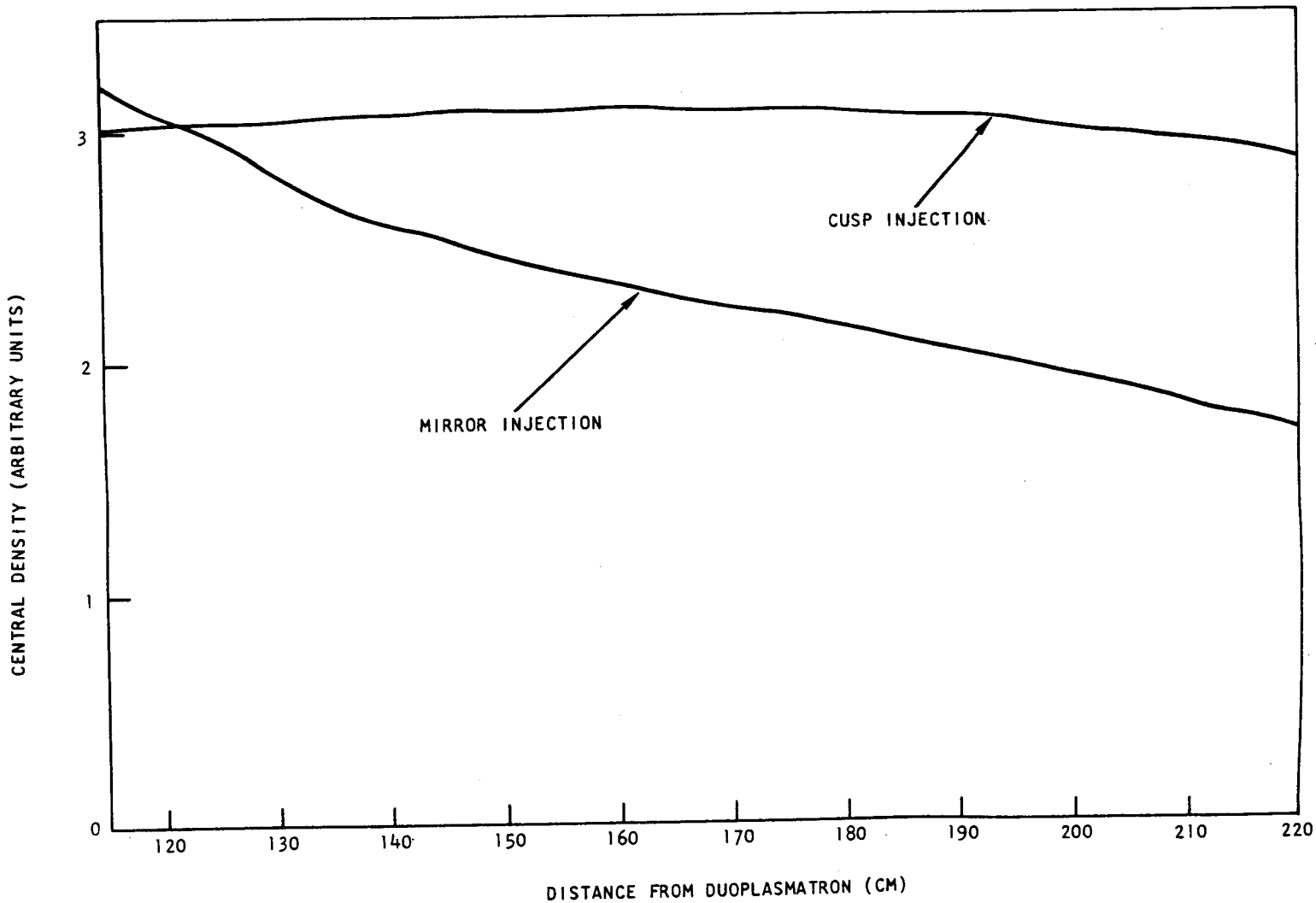

Fig. 3--Plasma density as a function of longitudinal position

respectively. (It has been demonstrated in other experiments that the electron velocity distribution in the machine is Maxwellian.[4]) We note in passing that this electric field, which is parallel to the magnetic field, extends over a distance of about 2 m in a plasma whose Debye length is about 1 mm.

The observed diffusion, which causes a factor-of-two drop in the central density over the length of the machine, is too rapid by a factor of 100 to be explained by binary collisions. The decrease in central density, which is a sensitive measure of the ion diffusion, is not much changed by turning off the rotation of the plasma. Thus, the diffusion is not caused by this rotational "instability." This phenomenon, which has been blamed for the anomalous diffusion in other experiments, is not the cause in our machine.

IV. CUSP EXPERIMENTS

The anomalous diffusion can be dramatically reduced by rearranging the magnetic field configuration of the machine. We have installed two independent magnetic coils near each end of the machine. These coils, which may be operated to provide either mirrors or cusps in the longitudinal magnetic field, immediately surround the 4 in. diameter stainless steel liner which bounds the plasma. They are located a few inches inside each end of the plasma column. The geometry is shown in Fig. 1. When the upstream coil (the one near the source) is connected so as to produce a mirror in this region, very little effect is observed on the plasma. However, when this coil is connected to produce a cusp, there is a spectacular reduction in the radial diffusion of the plasma, as indicated by a nearly constant plasma density along the central axis. A plot of the central density as a function of longitudinal position with and without the cusp field is shown in Fig. 3.

The broadband noise observed by a downstream probe in the 10 to 50 kc range decreases by about an order of magnitude when the cusp is properly adjusted. The onset of both effects is rather abrupt and occurs approximately as the central field of the cusp goes through zero. Even when the field of the upstream cusp is fairly close to the critical value, turning on the downstream cusp has little or no effect on the density profile or noise.

There are various possible explanations of the reduction in diffusion. One is that ions with a large Larmor radius simply are not able to enter the machine through the cusp, and as a result the average ion has a much smaller Larmor radius in the cusp case than in the mirror case. Since the diffusion length is expected to scale with the ion Larmor radius, this would result in a much smaller diffusion coefficient. However, when the upstream cusp is adjusted to a value that produces a reasonably flat density profile and the downstream coil is operated as a mirror, some of the ions that would normally leave the machine at the downstream end are reflected, indicating that their Larmor radii are applicable. In addition, the radius of the downstream plasma remains the order of one centimeter when the cusp is on, an indication that the ion Larmor radius is still large. Thus, this explanation for the result appears unlikely.

A second hypothesis is that the plasma exhibits some low frequency instability (for example, the universal instability) in the mirror case, and this instability is stabilized by an average minimum-B field condition introduced by the cusp. But the fact that the downstream cusp has so little influence on the diffusion makes it appear unlikely that the effect of the cusp is to provide an average minimum-B field.

A third possibility is that with the cusp field inserted it is much more difficult for electrons to go from the source into the machine. Thus, for high frequencies, we would expect that the source would be somewhat disconnected electrically from the main body of the plasma. With the normal configuration, variations in plasma density or temperature at the source produce corresponding variations in potential at the center of the plasma in the machine. These potential fluctuations cause an associated fluctuating radial electric field which would cause the ions to diffuse

rapidly across the magnetic field lines. If electrons from the source find it difficult to get into the main part of the machine, the potential fluctuations and electric field would be reduced and the diffusion less.

We observe a potential difference of about 3 kT across the cusp, with the main body of the plasma more positive than the plasma at the source end. This reinforces the view that electrons have a difficult time getting through the cusp. The order of magnitude reduction in noise when the cusp is turned on also favors this explanation. In addition, low frequency noise transmission experiments through the cusp (using probe antennas) show an order of magnitude attenuation when the cusp is turned on. However, there are two difficulties with the third explanation. If the idea is correct, it should be possible to increase the diffusion by driving the duoplasmatron anode with a broadband noise signal; we tried this without success. It is possible that the driving signal was too small, but the calculation indicated it was sufficient. In addition, this model implies that the noisy electric field in the plasma should be highly correlated at all positions in the machine. For usual values of the main magnetic field, the noise observed with probes is almost completely uncorrelated even when the probes are within a few millimeters of each other. This result cannot be attributed to noise in sheaths around the probes. Sheath noise could not be reduced by the cusp.

A fourth hypothesis, which seems to be the best explanation of all the experimental results, assumes that the 0.12 mm diameter plasma-emitting surface at the anode of the duoplasmatron is subject to noisy modulation. Magnetic lines through different parts of the surface have different potentials, which persist down the whole length of the machine.

Ions passing near the center of the plasma experience a large, noisy electric field due to potential differences between different magnetic field lines, and are thus diffused radially. When the cusp is turned on, most of the magnetic lines passing through the source intersect the stainless steel cylinder bounding the plasma, and electrons on these lines cannot get past the cusp. Thus, most of the electrons in the downstream plasma come from a small area of the source and large potential fluctuations do not appear between adjacent magnetic lines. Ions pass through the cusp non-adiabatically and so are not much affected, except that those having a large gyroradius strike the wall and are lost. This hypothesis agrees both qualitatively and quantitatively with all our present observations.

As a test of these ideas, we performed a further probe noise correlation measurement. Probes were constructed which measure the noise at a single radius (our previous probes averaged over radius). These new probes are in the form of an insulated rigid coaxial cable with overall diameter of 0.028 in. One millimeter of the center conductor projects beyond the shield conductor. These probes sample the potential in a sphere of radius of about one millimeter. When the main magnetic field of the machine is reduced so that the magnetic transform of the orifice of the duoplasmatron is much larger than two millimeters, the noise on these probes is correlated when they are on the same field line and not otherwise, as expected from theory. In summary, we now have a rather complete understanding of the anomalous diffusion mechanism in this case. We also have a method for greatly reducing the diffusion.

APPENDIX I

REFERENCES

1. J. Bonnal, G. Briffod, and C. Manus, Phys. Rev. Letters 6, 665 (1961); F. F. Chen, and A. W. Cooper, Phys. Rev. Letters 9, 333 (1962); H. Lashinsky, Phys. Rev. Letters 12, 121 (1964); D. L. Morse, Phys. Fluids 8, 516 (1965); and K. I. Thomassen, Phys. Rev. Letters 14, 587 (1965).
2. F. C. Hoh, Phys. Fluids 6, 1184 (1963); A. Simon, Phys. Fluids 6, 382 (1963); and D. L. Morse, Phys. Fluids 8, 1339 (1965).
3. J. H. Malmberg, *et al.*, *Proceedings* of the Sixth International Conference on Ionization Phenomena in Gases, Paris, 1963, edited by P. Hubert (S.E.R.M.A., Paris, 1964), Vol. 4, p. 229.
4. J. H. Malmberg, C. B. Wharton, and W. E. Drummond, Plasma Physics and Controlled Nuclear Fusion Research 1, 485 (1966).

APPENDIX II

ROTATION AND DIFFUSION OF A COLUMN OF PLASMA IN A MAGNETIC FIELD

by

J. H. Malmberg and C. B. Wharton

ABSTRACT

Presented at the Division of Plasma Physics
American Physical Society Meeting
Boston, Massachusetts, November 2-5, 1966

Published in
Bulletin of American Physical Society
Volume 12, 797 (1967)

Rotation and Diffusion of a Column of Plasma in a Magnetic Field

J. H. Malmberg and C. B. Wharton

ABSTRACT

The dynamics of a long axisymmetric column of plasma immersed in a longitudinal magnetic field has been investigated experimentally. Large, very regular, periodic variations in plasma density are observed (with probes) at a given radius and azimuth. Analysis of the probe measurements shows that the column of plasma is rotating and is not symmetric about the axis of rotation. The rotation is associated with the existence of a radial electric field. When the mean radial electric field is set to a certain critical value, the rotation stops and the low frequency noise in probe signals is greatly reduced. The diffusion of the plasma is about 100 times too large to be explained by binary collisions and is not changed by stopping the rotation.

In a second (and successful) attempt to reduce the anomalous diffusion, the plasma is injected into the main part of the machine through a cusp. This results in a spectacular reduction in the radial diffusion of the plasma, as indicated by a nearly constant plasma density along the central axis. Possible explanations of this result will be discussed.

PRECEDING PAGE BLANK NOT FILMED.

APPENDIX III

LANDAU DAMPING AND GROWTH OF ELECTROSTATIC MODES WITH EFFECTS OF SPATIAL VARIATION

by

David L. Book

General Atomic Report
GA-6513
June 29, 1965

Published in
The Physics of Fluids
Volume 10, 198 (1967)

PRECEDING PAGE BLANK NOT FILMED.

Reprinted from
THE PHYSICS OF FLUIDS VOLUME 10, NUMBER 1 *Printed in U.S.A.*
JANUARY 1967

Landau Damping and Growth of Electrostatic Modes with Effects of Spatial Variation

DAVID L. BOOK
General Atomic Division, General Dynamics Corporation, John Jay Hopkins Laboratory for Pure and Applied Science, San Diego, California
(Received 29 July 1965; final manuscript received 16 September 1966)

For a plasma with finite cross section of the sort which occurs typically in laboratory plasma waves experiments, in a constant magnetic field, the Landau damping (or growth) is obtained by a perturbation procedure in terms of the plasma velocity distribution function and potential and density profiles. The result is applied to the damping associated with the upper and lower branches of the dispersion curve for longitudinal electron plasma waves in the case of a Maxwellian velocity distribution in slab and cylindrical geometries. Application is also made to the growth rates resulting from a low-density electron beam with radially dependent energy superposed on a Maxwellian.

I. INTRODUCTION

THEORETICAL investigations of the dispersion relations and damping of longitudinal electron plasma waves[1] have been carried out in considerable detail for the case of homogeneous finite-temperature collisionless plasma. However, it is of interest to extend these considerations to inhomogeneous systems as well, since laboratory experiments[2] always employ bounded plasmas.

A number of other papers have treated this subject. Trivelpiece and Gould[3] considered a cylindrical cold plasma inside a concentric cylindrical conducting surface in the quasi-static (low β) approximation. The boundary conditions lead to a dispersion relation with two branches, a lower one corresponding to Langmuir oscillation, and an upper one, the "backward wave," near the cyclotron frequency. Gould[4] generalized this result for the lower branch in the case of strong magnetic field ($\Omega_e \gg \omega_{pe}$), using the finite-temperature dielectric tensor and treating a smoothly varying cross-sectional density profile instead of a step function. The effect of finite temperature is to introduce Landau damping and to permit ω to become greater than ω_{pe} for large $k_\parallel$, just as in the homogeneous case.

Lichtenberg and Jayson[5] consider one- and two-stream Maxwellian plasmas, keeping lowest-order finite temperature terms in the dielectric tensor. For a cylindrical plasma with constant density bounded at $r = R$ (step-function dependence), they solve the dispersion relation for the decay (growth) rate in terms of frequency, wavelength, and plasma density, temperature and radius. The contribution to this growth rate comes from resonance between electrons and three plasma modes: the Langmuir oscillations, the $n = 1$ cyclotron mode (backward wave), and the $n = -1$ mode.

In this paper an approach similar to that of Lichtenberg and Jayson is employed. In Sec. II a variational technique is used to calculate the decay rate γ as a small perturbation correction to the wave frequency. Here a Maxwellian electron distribution is assumed, but the density and electric potential are arbitrary slowly varying functions of position, regarded as being obtained from measurements. They enter in the final expression for γ only in two rather insensitive averages. The result describes damping in both upper and lower branches. Formulas for the growth rate in both two-dimensional (slab) and cylindrical geometry are derived, for strong ($\Omega_e > \omega_{pe}$) and weak ($\Omega_e < \omega_{pe}$) magnetic field.

In Sec. III, this calculation is modified to include the effect of a low-density electron beam. The beam is injected axially with a very narrow velocity spread about a mean velocity which is a function of position. This injected beam is shown to lead to an instability of the lower branch mode which may be made quite gentle, so as to be describable by the quasi-linear theory.[6]

II. DECAY RATE FOR MAXWELLIAN PLASMA

We consider a plasma which is uniform in the direction along the uniform constant magnetic field (the z direction) and inhomogeneous in the transverse direction. We restrict ourselves to low β (quasi-static) systems, so that the perturbed electric field is derivable from a potential. If the plasma were

[1] See, for example, T. H. Stix, *The Theory of Plasma Waves* (McGraw-Hill Book Company, Inc., New York, 1962).
[2] J. H. Malmberg and C. B. Wharton, Phys. Rev. Letters **13**, 184 (1964).
[3] A. W. Trivelpiece and R. W. Gould, J. Appl. Phys. **30**, 1784 (1959).
[4] R. W. Gould (unpublished).
[5] A. J. Lichtenberg and J. S. Jayson, J. Appl. Phys. **36**, 449 (1965).
[6] W. E. Drummond and D. Pines, Nucl. Fusion Suppl. Pt. 3, 1049 (1962).

PRECEDING PAGE BLANK NOT FILMED.

homogeneous in the transverse direction as well as along the field lines, we would, of course, be able to integrate the linearized Vlasov equation along the unperturbed particle orbits to obtain Poisson's equation in the form

$$\nabla\cdot\boldsymbol{\varepsilon}\cdot\nabla\varphi = 0, \tag{1}$$

where $\boldsymbol{\varepsilon}$ is independent of the coordinates. This equation is still valid for spatially varying temperature and density, provided that the scale lengths for the variation are large compared with the electron Larmor radius. This can be seen most easily[7] by noting that the zero-order or "background" electron distribution function f_0 must be a function of the single particle constants of motion $X = x + v_y/\Omega_e$ and $Y = y - v_x/\Omega_e$ if it is to exhibit transverse spatial dependence. The first-order perturbed distribution function f_1 is equal to

$$f_1 = \int_{-\infty}^{t} dt' \left[\frac{e}{m} E(x')\cdot\nabla_{v'} f_0\right], \tag{2}$$

where x' and v' are related to t' by the unperturbed orbit equation. If f_0 depends on the coordinates through X and Y, then (for example) the x component of $\nabla_{v'} f_0$ is

$$\frac{\partial f_0}{\partial v_x'} = \frac{\partial f_0}{\partial w_\perp} m v_x' - \frac{\partial f_0}{\partial Y}\frac{1}{\Omega_e}, \tag{3}$$

where $w_\perp = \frac{1}{2}mv_\perp^2 = \frac{1}{2}m(v_x^2 + v_y^2)$ is also a constant of motion. Since the Larmor radius ρ_e has been assumed much smaller than the scale of the transverse density variation, which is taken to be of the order of the plasma width or radius R, we can Taylor expand f_0, retaining only the lowest- and first-order terms:

$$f_0(\epsilon, X, Y) = f_0(\epsilon, x, y) + \frac{v_y}{\Omega_e}\frac{\partial f_0}{\partial x} - \frac{v_x}{\Omega_e}\frac{\partial f_0}{\partial y}. \tag{4}$$

When f_1 from Eq. (2) is substituted in Poisson's equation, the gradient terms yield corrections of order ρ_e/R to the dielectric tensor for a homogeneous plasma. Likewise, the constants of motion X and Y become x and y, respectively, to the same order; if we drop corrections $\sim\rho_e/R$ in both places, Eq. (1) in the usual form is still valid, with f_0 now an arbitrary function of the coordinates, subject to $\rho_e/R \ll 1$.

We discuss systems with two-dimensional geometry first, then outline the analogous treatment of cylindrical systems.

For two-dimensional geometry we write the potential as

$$\varphi = \psi(x)e^{ik_\parallel z - i\omega t}. \tag{5}$$

$\psi(x)$ should vary smoothly over the cross section of the plasma, so we can speak of an effective transverse wavenumber $k_\perp \sim 1/R$. We assume Maxwellian velocity distributions with ion temperatures not substantially larger than electron temperatures, so only the electron contribution to $\boldsymbol{\varepsilon}$ need be retained. Then for long wavelengths

$$\omega/k_\parallel \gg v_T, \tag{6}$$

and small electron Larmor radius

$$\rho_e/R \ll 1, \tag{7}$$

$\boldsymbol{\varepsilon}$ simplifies to[7]

$$\boldsymbol{\varepsilon} = \hat{x}\hat{x}\epsilon_\perp + \hat{z}\hat{z}\epsilon_\parallel, \tag{8}$$

where

$$\epsilon_\parallel = 1 + \sum_{n=-\infty}^{\infty} \frac{2\omega_p^2}{\omega k_\parallel v_T} e^{-z} I_n(z) x_n [1 + x_n Z(x_n)] \tag{9}$$

and

$$\epsilon_\perp = 1 + \sum_{n=-\infty}^{\infty} \frac{\omega_p^2}{\omega k_\parallel v_T} Z(x_n) e^{-z} \frac{n^2}{z} I_n(z). \tag{10}$$

Here ω_p is the electron plasma frequency, $\omega_p^2 = (4\pi e^2/m)n(x)$; Ω_e is the electron cyclotron frequency; $v_T^2 = 2T/m$;

$$z = k_\perp^2 T/\Omega_e^2 m \ll 1,$$

by (7);

$$x_n = (\omega - n\Omega_e)/k_\parallel v_T \gg 1$$

(unless $\omega \approx n\Omega_e$), by (6);
Z is the plasma dispersion function of Fried and Conte[8], defined by

$$Z(\zeta) = \pi^{-\frac{1}{2}} \int_{-\infty}^{\infty} dx \frac{e^{-x^2}}{x - \zeta - i\epsilon} \to i\pi^{\frac{1}{2}} e^{-\zeta^2} - \frac{1}{\zeta}\left(1 + \frac{1}{2\zeta^2} + \frac{3}{4\zeta^2} + \cdots\right) \tag{11}$$

asymptotically for $\mathrm{Re}\,\zeta \gg 1 \gg \mathrm{Im}\,\zeta$; and I_n is the Bessel function of imaginary argument of nth order

$$I_n(z) \sim (\tfrac{1}{2}z)^{|n|}[1 + O(z^2)]$$

for small z.

In Eq. (8) diagonal terms and corrections to $\epsilon_\parallel$ and $\epsilon_\perp$ arising from the variation of the density n

[7] A. B. Mikhailovskii, in *Topics in Plasma Theory*, M. A. Leontovich, Ed. (State Atomic Press, Moscow, 1963), Vol. 3.

[8] B. D. Fried and S. D. Conte, *The Plasma Dispersion Function* (Academic Press Inc., New York, 1961).

have been dropped by Eq. (6) and Eq. (7); inclusion of the latter can lead in some cases to the existence of unstable drift modes, the universal instability.

Next we expand Eq. (9) and Eq. (10) for large x_n and small z, using the asymptotic form Eq. (11). If in addition we write $\omega = \omega_0 + i\gamma$, $\gamma/\omega_0 \ll 1$, and retain only terms to first order in γ/ω_0 and $\exp(-x_n^2)$, the result is

$$\epsilon_\parallel = 1 - \frac{\omega_p^2}{\omega_0^2} + i\left[2\pi^{\frac{1}{2}}\omega_p^2 \frac{\omega_0}{(k_\parallel v_T)^3} e^{-(\omega/k_\parallel v_T)^2} + \frac{\gamma\omega_p^2}{\omega_0^3}\right], \quad (12)$$

$$\epsilon_\perp = 1 - \frac{\omega_p^2}{\omega_0^2 - \Omega_e^2} + i\left(\tfrac{1}{2}\pi^{\frac{1}{2}} \frac{\omega_p^2}{\omega_0 k_\parallel v_T}\left\{\exp\left[-\left(\frac{\omega_0 - \Omega_e}{k_\parallel v_T}\right)^2\right] + \exp\left[-\left(\frac{\omega_0 + \Omega_e}{k_\parallel v_T}\right)^2\right]\right\} + \frac{2\gamma\omega_0\omega_p^2}{(\omega_0^2 - \Omega_e^2)^2}\right). \quad (13)$$

In Eq. (13), contributions from higher harmonics ($|n| > 1$) are exponentially small unless $n\Omega_e \simeq \omega$; then they are small like some power of z. Unless the magnetic field is very weak, it is usually possible to neglect the $n = -1$ term as well, and this is done in what follows.

Substitution of Eq. (8) in Eq. (1) yields

$$(d/dx)(\epsilon_\perp\, \partial\psi/\partial x) - k_\parallel^2 \epsilon_\parallel \psi = 0. \quad (14)$$

For given boundary conditions and density profile $n(x)$, this equation is an eigenvalue problem which in principle yields the analytic form of ψ and a dispersion relation for complex ω as a function of $k_\parallel$. In general it is not possible to carry out this calculation exactly, even in the limit $T \to 0$ where ω is real and the modes propagate undamped.

Nevertheless it is possible to utilize Eq. (14) in a perturbation approach. To do this, we rewrite it in the form

$$L\psi = (L_0 + iL_1)\psi = 0. \quad (15)$$

Here L_0 and L_1 are the real and imaginary parts of L:

$$L_j = (d/dx)\epsilon_\perp^{(j)}(d/dx) - k_\parallel^2 \epsilon_\parallel^{(j)}, \qquad j = 0, 1;$$

$$\epsilon_\perp^{(0)} = 1 - \omega_p^2/(\omega_0^2 - \Omega_e^2), \qquad \epsilon_\parallel^{(0)} = 1 - (\omega_p^2/\omega_0^2);$$

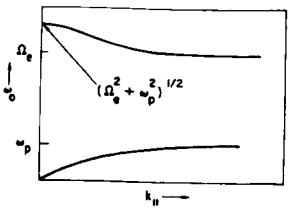

FIG. 1. Dispersion curve for homogeneous plasma in strong field.

$$\epsilon_\perp^{(1)} = \frac{2\gamma\omega_0\omega_p^2}{(\omega_0^2 - \Omega_e^2)^2} + \tfrac{1}{2}\pi^{\frac{1}{2}} \frac{\omega_p^2}{\omega_0 k_\parallel v_T} \exp\left[-\left(\frac{\omega_0 - \Omega_e}{k_\parallel v_T}\right)^2\right];$$

$$\epsilon_\parallel^{(1)} = \frac{2\gamma\omega_p^2}{\omega_0^3} + 2\pi^{\frac{1}{2}}\omega_p^2 \frac{\omega_0}{(k_\parallel v_T)^3} \exp\left[-\left(\frac{\omega}{k_\parallel v_T}\right)^2\right].$$

Now consider the equation

$$L_0\psi_0 = 0 \quad (16)$$

which describes undamped waves propagating at $T = 0$. Multiply Eq. (15) by $\psi_0^*(x)$, Eq. (16) by $\psi^*(x)$, and integrate over x from $-\infty$ to $+\infty$:

$$\int_{-\infty}^{\infty} dx\, \psi_0^* L_0 \psi + i \int_{-\infty}^{\infty} dx\, \psi_0^* L_1 \psi = 0, \quad (17)$$

$$\int_{-\infty}^{\infty} dx\, \psi^* L_0 \psi_0 = \int_{-\infty}^{\infty} dx\, \psi_0^* L_0 \psi = 0, \quad (18)$$

since L_0 is self-adjoint. Finally, subtracting Eq. (18) from Eq. (17), approximating $\psi_0 \approx \psi$ and integrating by parts yields

$$\int_{-\infty}^{\infty} dx\, \frac{2\omega_p^2 k_\parallel^2 \gamma}{\omega_0^3} |\psi(x)|^2 + \int_{-\infty}^{\infty} dx\, \frac{2\omega_p^2\gamma\omega_0}{(\omega_0^2 - \Omega_e^2)^2} \left|\frac{d\psi}{dx}\right|^2 = -\int_{-\infty}^{\infty} dx\, \frac{\frac{1}{2}\pi^{\frac{1}{2}}\omega_p^2}{\omega_0 k_\parallel v_T} \exp\left[-\left(\frac{\omega_0 - \Omega_e}{k_\parallel v_T}\right)^2\right] \left|\frac{d\psi}{dx}\right|^2 - \int_{-\infty}^{\infty} dx\, \frac{2\pi^{\frac{1}{2}} k_\parallel^2 \omega_p^2 \omega_0}{(k_\parallel v_T)^3} \exp\left[-\left(\frac{\omega_0}{k_\parallel v_T}\right)^2\right] |\psi(x)|^2. \quad (19)$$

This may be solved for γ as

$$\frac{\gamma}{\omega_0} = -\left\{\pi^{\frac{1}{2}} \frac{\omega_0^3}{(k_\parallel v_T)^3} \exp\left[-\left(\frac{\omega_0}{k_\parallel v_T}\right)^2\right] G + \frac{\pi^{\frac{1}{2}}}{4} \frac{\omega_0}{k_\parallel v_T} \cdot \exp\left[-\left(\frac{\omega_0 - \Omega_e}{k_\parallel v_T}\right)^2\right] F\right\}\left[G + \frac{\omega_0^4}{(\omega_0^2 - \Omega_e^2)^2} F\right]^{-1}, \quad (20)$$

where

$$F = \int_{-\infty}^{\infty} dx\, \omega_p^2 \left|\frac{d\psi}{dx}\right|^2, \quad (21)$$

$$G = k_\parallel^2 \int_{-\infty}^{\infty} dx\, \omega_p^2 |\psi(x)|^2. \quad (22)$$

For an approximately homogeneous plasma in which $\Omega_e \gg \omega_p$, the dispersion curve looks as shown in Fig. 1. On the lower branch, $\omega_0 \ll \Omega_e$, and the equation for γ reduces to

$$\frac{\gamma}{\omega_0} = -\frac{\pi^{\frac{1}{2}}[\omega_0^3/(k_\parallel v_T)^3] e^{-(\omega_0/k_\parallel v_T)^2} G}{(\omega_0/\Omega_e)^4 F + G}. \quad (23)$$

The calculations of Trivelpiece and Gould[3] and of Gould[4] show that for small $k_\parallel$, ω_0/Ω_e goes like $k_\parallel R$. Since $F/G \sim (k_\parallel R)^{-2}$, we see that Eq. (23) reduces to the familiar expression for the Landau damping of a homogeneous plasma in this limit, as it also does

in the limit $R \to \infty$. On the upper branch, $\omega_0 \sim \Omega_e$, and

$$\frac{\gamma}{\omega_0} = -\frac{\frac{1}{4}\pi^{\frac{1}{2}}(\omega_0/k_\parallel v_T)e^{-[(\omega_0-\Omega_e)/k_\parallel v_T]^2}F}{[\omega_0^4/(\omega_0^2-\Omega_e^2)^2]F+G}, \tag{24}$$

which is valid provided $|\omega_0 - \Omega_e|$ is not small compared with $k_\parallel v_T$.

If $\omega_p \gg \Omega_e$ through the bulk of the plasma, there are still two branches; on the lower one, $\omega_0 \lesssim \Omega_e$, and on the upper one, $\omega_0 \gg \Omega_e$. Now Eq. (20) does not simplify.

For the case of cylindrical symmetry we assume the potential is azimuthally symmetric:

$$\varphi = \psi(r)e^{ik_\parallel z - i\omega t}, \tag{25}$$

and Eq. (14) becomes

$$(1/r)(d/dr)[r\epsilon_\perp(d\psi/dr)] - k_\parallel^2\epsilon_\parallel\psi = 0. \tag{26}$$

Here $\epsilon_\parallel$ and $\epsilon_\perp$ are again given by Eq. (9) and Eq. (10), since in three dimension $\boldsymbol{\epsilon}$ is diagonal and $\epsilon_{yy} \approx \epsilon_{xx} \simeq \epsilon_\perp$ in the approximations Eq. (6) and Eq. (7).

The perturbation calculation goes through unchanged, except that now

$$L_0 = (d/dr)[r\epsilon_\perp^{(0)}(d/dr)] = k_\parallel^2\epsilon_\parallel^{(0)};$$

$$L_1 = (d/dr)[r\epsilon_\perp^{(1)}(d/dr)] - k_\parallel^2\epsilon_\parallel^{(1)}.$$

The result is identical with Eq. (20), where now we must replace Eq. (21) and Eq. (22) by

$$F' = \int_0^\infty dr\, r\omega_p^2 \left|\frac{d\psi}{dr}\right|^2; \tag{27}$$

$$G' = k_\parallel^2 \int_0^\infty dr\, r\omega_p^2\, |\psi|^2. \tag{28}$$

The formula for γ simplifies as before when we specialize considerations.

This case may be generalized without difficulty to include azimuthal dependence in ψ.

III. GROWTH RATE FROM BEAM INJECTION

We imagine that a low-temperature beam of electrons moving parallel to **B** is superposed on the Maxwellian which was considered in Sec. II. If we ignore thermal motion within the beam altogether and assume it is cylindrically symmetric, the part of the electron distribution function arising from the beam has the form

$$f_b(v, r) = D(r)\ \delta[v_\parallel - v_0 - \alpha(r)]\ \delta(v_\perp^2), \tag{29}$$

where $\alpha(r) + v_0$ is the velocity with which particles at a distance r from the axis of the system are moving; we assume $\alpha(0) = 0$. In general, $\alpha(r)$ will increase with r, since we may imagine the beam to have arisen as a result of shooting electrons from an electron gun into a potential profile something like that shown in Fig. 2.

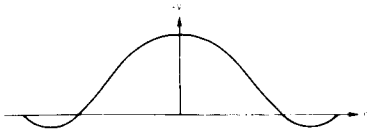

FIG. 2. General form of observed potential in plasma confined by magnetic field.

We are primarily interested in simple modes which propagate through the plasma as a whole, that is, in which all the electrons in a cross-sectional slice participate. This being the case, we may expect that for a beam distribution function which varies radially as does (29), the wave will see an effective distribution averaged over r. In the case of interest, the local beam density is much smaller than the density of the background Maxwellian,

$$D(r) \ll 1. \tag{30}$$

To include the effects of the beam, we retrace the argument leading to Eq. (20). If we let $\Omega_e \gg \omega_0$ in order to concentrate attention on the contribution of the lower branch to γ, Eq. (15) is still valid; but now

$$\epsilon_\perp^{(0)} \approx 1; \qquad \epsilon_\perp^{(1)} \approx 0;$$

and

$$\epsilon_\parallel^{(1)} = \frac{\gamma\omega_p^2}{\omega_0^3} + \pi\frac{\omega_p^2}{k_\parallel^2}\int_{-\infty}^{\infty} d^3v\, \frac{\partial f_0}{\partial v_\parallel}\, \delta\left(v_\parallel - \frac{\omega_0}{k_\parallel}\right), \tag{31}$$

with $f_0 = f_{\max} + f_b$. The second term in Eq. (31) is the usual expression for the imaginary part of the parallel component of the dielectric tensor with a general velocity distribution f_0 when $\gamma/\omega_0 \ll 1$. If f_b vanishes, repeating the operations of Eqs. (15)–(20) yields the formula for the Landau damping of an infinite homogeneous Maxwellian plasma, identical with that which is obtained when $\Omega_e \to \infty$ in Eq. (20) and G cancels in numerator and denominator. However, the same manipulations applied to the radially dependent beam component result in a contribution to the decay rate

$$\left(\frac{\gamma}{\omega_0}\right)_{\text{beam}} = \frac{1}{G'}\int_0^\infty r\, dr\, |\psi|^2\, \omega_p^2\, \frac{\pi}{2}\, \omega_0^2 \cdot \int_{-\infty}^{\infty} dv\, \frac{\partial g}{\partial v}\, \delta\left(v - \frac{\omega_0}{k_\parallel}\right), \tag{32}$$

where

$$g = D(r)\ \delta[v - v_0 - \alpha(r)].$$

and

$$G' = k_\parallel^2 \int_0^\infty r\, dr\, \omega_p^2\, |\psi|^2.$$

In calculating $1/G'$, we can ignore f_b since the beam density is negligible compared with the background density.

Equation (32) may be rewritten in order to investigate particular choices of $\alpha(r)$ and $D(r)$. To do this we assume that $\alpha(r)$ is monotone increasing, so that

$$\delta[v - v_0 - \alpha(r)] = [1/\alpha'(r_0)]\, \delta(r - r_0),$$

where $\alpha(r_0) = v - v_0$ and $\alpha' = d\alpha/dr$, and

$$\frac{\partial}{\partial v} = \frac{\partial r}{\partial v}\bigg|_{r_0} \frac{\partial}{\partial r} = \frac{1}{\alpha'(r_0)} \frac{\partial}{\partial r}.$$

Then integrating by parts we have

$$\left(\frac{\gamma}{\omega_0}\right)_{\text{beam}} = \frac{1}{G'} \frac{\pi}{2} \omega_0^2 \frac{1}{\alpha'(r_0)} \left\{ \frac{r_0\, |\psi|^2\, \omega_p^2\, D(r_0)\, \delta(r_0)}{\alpha'(r_0)} + \theta(r_0) \frac{\partial}{\partial r} \left[\frac{r\, |\psi|^2\, \omega_p^2\, D(r)}{\alpha'(r)} \right] \right\}_{r = \alpha^{-1}[(\omega_0/k) - v_0] = r_0}, \quad (33)$$

where $\theta(r_0)$ is the Heaviside step function. This shows that the contribution to γ for a particular phase velocity $\omega_0/k_\parallel$ comes from particles at a distance r_0 sufficient to make

$$v_0 + \alpha(r_0) = \omega_0/k_\parallel.$$

For $\omega_0/k < v_0$, there are no such particles, since $\alpha(r) > 0$; so if $rD(r)/\alpha'(r) \neq 0$ in the limit $r \to 0$, there is a jump in the effective velocity distribution, yielding a δ-function dependence in γ. Such a singularity is inconsistent with our assumption that $\gamma/\omega_0 \ll 1$. In order to ensure that formula (33) will be valid, it is necessary to introduce finite beam temperature or make $D(r)$ vanish sufficiently fast that the δ function does not appear. Applications of Eq. (33) are thus subject to a self-consistency condition. This condition is not satisfied by the simplest models of radial dependence of the beam, as we see later. It is necessary to make additional refinements in choosing $\alpha(r)$ and $D(r)$ in order that γ/ω_0 be small everywhere.

Following Fig. 2, let us examine some plausible choices for $\alpha(r)$. We assume $D(r) = D$, a constant, and assume that ω_p^2 and $|\psi|^2$ are roughly constant out to some value $r = R$. This implies that the densities of both beam and plasma are constant out to $r = R$, then drop off abruptly to zero.

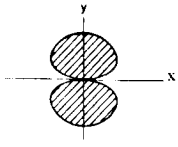

FIG. 3. Outline of a template with shape described by $r^2 = a^2 \sin\theta$.

The first choice is

$$\alpha(r) = Ar^2, \qquad A = \text{const.} \quad (34)$$

Then $\alpha'(r) = 2Ar$, and $r_0 = [(v - v_0)/A]^{\frac{1}{2}}$. We see that there is a jump in the effective distribution, since

$$\lim_{r \to 0+} \left(\frac{r}{\alpha'(r)}\right) = \frac{1}{2A} = \text{const.}$$

Formula (33) yields

$$\left(\frac{\gamma}{\omega_0}\right)_{\text{beam}} = \frac{1}{G'} \frac{\pi}{2} \omega_0^2 \frac{1}{2[A(v - v_0)]^{\frac{1}{2}}} \frac{D\, |\psi|^2\, \omega_p^2}{2A} \cdot [\delta(r_0) - \delta(r_0 - R)]. \quad (35)$$

In this model, the self-consistency of the treatment is violated at two points, defined by the arguments of the two δ function in Eq. (35). The first singularity is a consequence of the behavior of $\alpha(r)$ for small values of the radius. The peak at $r_0 = R$ may be flattened out simply by retaining a realistic radial dependence for $\omega_p^2\, |\psi|^2$.

For the second choice of $\alpha(r)$, we argue as follows: an electron will have kinetic energy

$$\tfrac{1}{2}mv^2 = E_0 - V, \quad (36)$$

where E_0 is the "muzzle" energy of the electron gun and V is shown in Fig. 2. If V has roughly parabolic dependence or r, then

$$v = [(2E_0/m) - (2V/m)]^{\frac{1}{2}} \approx [v_0^2 + \nu^2 r^2]^{\frac{1}{2}}. \quad (37)$$

Thus

$$\alpha(r) = (v_0^2 + \nu^2 r^2)^{\frac{1}{2}} - v_0;$$

$$\frac{1}{\alpha'(r)} \frac{d}{dr} \left[\frac{r}{\alpha'(r)}\right] = \frac{1}{\nu^2}.$$

Now formula (33) tells us that for $0 < r_0 < R$,

$$(\gamma/\omega_0)_{\text{beam}} = (1/G')(\tfrac{1}{2}\pi)\omega_0^2\, D\omega_p^2\, |\psi|^2\, (1/\nu^2).$$

Note that the δ-function singularities at $r_0 = 0$ and $r_0 = R$ still appear, for the same reasons as before, so this model is still not consistent with the assumptions used in the derivation of Eq. (33).

It is not necessary to treat finite beam temperature to remove the sharp peak in γ which arises in both of these examples. Thus far we have taken $D(r)$ to be a constant. If a template is placed before the stream of electrons from the electron gun, it can screen some out, so that $D(r)$ may vanish at $r = 0$. For example, let the template be in the form of a screen whose edges have roughly the shape shown in Fig. 3, satisfying the equation $r^2 = a^2 \sin\theta$.

Then

$$D(r) \sim 4 \int_0^{\sin^{-1} r^2/a^2} d\theta \approx 4 \frac{r^2}{a^2}$$

for r small.

Now, taking $\omega_p^2 \, |\psi|^2$ gradually decreasing as r increases (instead of a sudden drop at $r = R$), we have for γ a curve of the form shown in Fig. 4.

Note that the area under the curve sums to zero. This follows from the calculation leading to Eq. (33), which expresses γ as a total derivative with respect to v of a quantity which vanishes as $v \to v_0$ and $v \to \infty$.

IV. SUMMARY

We have discussed plasma waves propagating parallel to a uniform magnetic field in a system whose density is a function of the transverse coordinates. For a zero-temperature plasma, no Landau damping or growth occurs. When a finite spread (finite temperature) is introduced in the velocity distribution of the electrons, the eigenfrequencies become complex; however, if the spread in the distribution is small ($v_T \ll \omega_0/k_\parallel$, etc.), γ, the imaginary part of the wave frequency will be small and the shape of the potential eigenmodes of the system as functions of transverse coordinates will not be greatly altered. The effect of wave-particle resonance is to cause the zero-temperature eigenmodes to grow or decay slowly in time as a whole, without changing otherwise. The rate of decay or growth depends on the slope of the velocity distribution function at the velocities where resonance can take place, weighted by the electrostatic energy as a function of transverse displacement and averaged over the density profile of the plasma. The average is quite insensitive to the exact shape of the transverse profile, and the resulting formula for γ is not qualitatively different from that obtained for infinite homogeneous plasmas. It can be applied to predict the growth or decay of plasma waves in an electron plasma confined by a magnetic field, provided that the density and potential profiles, shape of the electron velocity distribution and dependence of the real part of the wave frequency on $k_\parallel$ are known.

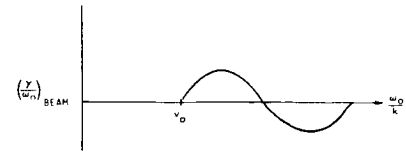

FIG. 4. γ/ω_0 modified by template and radial dependence of plasma.

For a thermal plasma with Maxwellian f_0, γ is negative and damping occurs. If an electron beam is injected into the plasma with radially dependent velocity determined by the transverse variation in potential, the averaging process described above smears it into a "gentle bump" on the tail of the Maxwellian, so that waves with the proper phase velocity experience slow growth, just as in the idealized gentle bump problem with an infinite homogeneous plasma. Note that if the plasma profile were not finite and varying, this smearing would not take place; the injected beam would be a sharp spike on the velocity distribution function, producing a two-stream instability. As the amplitude of the unstable spectrum grows, the resonant particles lose energy and slow down, flattening down the positive bump in the growth rate indicated in Fig. 4. The end result is a stationary wave spectrum and a stable velocity distribution, the quasilinear limit. This approach is the basis for an experimental study of the quasilinear theory.[9,10]

ACKNOWLEDGMENTS

The author wishes to thank Dr. William E. Drummond for suggesting the approach used in this work and Dr. John H. Malmberg and Professor Marshall N. Rosenbluth for useful discussion. A number of suggestions of the referee were incorporated to clarify the analysis and results presented.

This research was supported in part by the National Aeronautics and Space Administration under Contract NAS7-275 and in part by the United States Air Force Office of Scientific Research of the Office of Aerospace Research under Contract AF49(638)-1546.

[9] W. E. Drummond, Phys. Fluids 7, 816 (1964).
[10] C. B. Wharton and J. H. Malmberg, private communication.

APPENDIX IV

THE DISPERSION OF THE UPPER HYBRID MODE IN A SPATIALLY INHOMOGENEOUS PLASMA

by

L. D. Pearlstein and D. Bhadra

General Atomic Report
GA-8347
August 25, 1967

The Dispersion of the Upper Hybrid Mode In
A Spatially Inhomogeneous Plasma†

L. D. Pearlstein‡ and D. Bhadra

General Dynamics, General Atomic Corporation
John Jay Hopkins Laboratory for Pure and Applied Science
San Diego, California

We calculate the dispersion of the normal mode at the upper hybrid frequency propagating parallel to a uniform magnetic field in a spatially inhomogeneous plasma. For the case where the density varies in a direction perpendicular to the magnetic field, it becomes necessary to solve a fourth order differential equation for the perturbed potential. Our method of solution is a WKBJ analysis of this equation. We consider a Maxwellian plasma and a Maxwellian plasma with a superimposed beam parallel to the magnetic field. Finally, we solve the relevant dispersion relations in a UNIVAC 1108 digital machine. A comparison is made with results of a recent experiment.

†This research has been sponsored by the Defense Atomic Support Agency under Contract DA-49-146-XZ-486.

‡New Address: Lawrence Radiation Laboratory, Livermore, California

PRECEDING PAGE BLANK NOT FILMED.

I. INTRODUCTION

Recently, there has been considerable interest in measuring the dispersion of the upper hybrid mode in a uniformly magnetized plasma.[1,2,3] In this paper, we calculate the behavior of the normal modes of a spatial inhomogeneous plasma in this frequency range.

In the limit in which the density is constant across the plasma, the eigenmodes of the uniform infinite medium can be used to determine the dispersion. Such an analysis produces a theory in good agreement with experiment.[4,5] However, for the case in which the density varies in a direction orthogonal to the uniform magnetic field it becomes necessary to solve a differential equation which is characterized by the vanishing of the coefficent of the second derivative of the perturbed potential[6] at a frequency near the local upper hybrid frequency. Since the differential equation is obtained (in the small Larmor radius limit) from a convergent expansion of an integral equation, it is now necessary to go to higher order in the derivatives of the perturbed potential. In general, such an analysis leads to a fourth order differential equation in which the coefficient of the fourth derivative is down by the Larmor radius squared; however, due to the accidental cancellation in the second derivative, the higher order term can no longer be neglected. To date, the analyses[1,6] have been limited to one dimensional models in which the wavelength of the perturbed wave is in the direction of the density gradient. In this limit the differential equation factors and one needs only solve a second order equation.

In the present calculation we incorporate the effect of wavelengths parallel to the magnetic field. We concern ourselves with two different regimes. In one, the plasma is Maxwellian and Landau damping is introduced. In the other, a beam with a velocity parallel to the ambient magnetic field is superimposed upon a Maxwellian plasma and instability occurs. Our primary purpose is to explain the results obtained in the Malmberg-Wharton experiment.[7]

The theory for the spatially inhomogeneous Maxwellian plasma predicts the presence of a mode whose frequency increases with increasing parallel wavenumber. In addition, the inhomogeneous theory predicts a dispersion in which the frequency is an extremely flat function of the parallel wavenumber for small values of the latter. In fact, the group velocity goes to zero in this range, implying strong spatial damping and thus the absence of a wave in this region. Consequently, what should be observed is the onset of a wave at finite k with the frequency increasing with k, the behavior of the M-W experiment.[8]

Our method of solution is a WKBJ analysis of the fourth order differential equation. Since it turns out that the eigenmode is exponentially small outside the turning point of the fourth order equation, but well within the plasma, the analysis leads to reliable values of the eigenvalue but not of the eigenfunction. The answer occurs as an integral from the origin to the turning point of a modified phase equal to $(n + \frac{1}{2})\pi$.

In Section II we derive the fourth order differential equation. Section III contains the WKBJ analysis for cylindrical symmetry; to be complete we include the dispersion relation for slab symmetry. Section IV includes the effect of the beam.

II. FOURTH ORDER DIFFERENTIAL EQUATION

The starting point is the linear perturbed Vlasov equation. We assume the equilibrium quantities vary only in the radial direction. The ambient field is uniform and in the z-direction. We do not include any effects of an equilibrium electric field. If we Fourier analyze in z and t $(e^{-i\omega t+ikz})$, we have

$$f_k = + \frac{e}{m} \int_{-\infty}^{\infty} dt' \, \underset{\sim}{\nabla} \cdot \left[\varphi\left(\xi - \frac{v_y}{\Omega}, \eta \frac{v_x}{\Omega}\right) e^{+i(\omega t - kz)} \right] e^{-i\omega t' + ikz'} \underset{\sim}{\nabla}_v f(v^2, w, \xi, \eta) \tag{1}$$

for the solution to the linear Vlasov equation. The constants of motion are

$$\xi = x + \frac{v_y}{\Omega} \quad , \quad \eta = y - \frac{v_x}{\Omega}$$

$$v^2 = v_x^{\,2} + v_y^{\,2} \quad , \quad w = v_z \quad . \tag{2}$$

Also, the integral in Eq. (1) is along the unperturbed orbits defined by

$$z' - z = w(t - t')$$

$$v_x = v \cos(\Phi - \Omega(t' - t))$$

$$v_y = v \sin(\Phi - \Omega(t' - t)) \quad . \tag{3}$$

If we write

$$f(v^2,w,\xi,\eta) = g(\xi,\eta)\left(\frac{\alpha}{\pi}\right)^{3/2} e^{-\alpha(v^2+w^2)} \tag{4}$$

for a Maxwellian velocity distribution, we can integrate Eq. (1) by parts to obtain

$$f_k = -\frac{e}{m}\left(\frac{\alpha}{\pi}\right)^{3/2} e^{-\alpha(v^2+w^2)}\left\{2\alpha g(\xi,\eta)\left[\varphi(x,y) - i\omega\int_{-\infty}^{t} dt'\ \varphi\left(\xi - \frac{v_y}{\Omega},\ \eta\ \frac{v_x}{\Omega}\right)e^{-i\bar{\omega}(t'-t)}\right]\right.$$

$$\left. - \frac{1}{\Omega}\int_{-\infty}^{t} dt' \left(\frac{\partial g}{\partial \xi}\frac{\partial}{\partial \eta} - \frac{\partial g}{\partial \eta}\frac{\partial}{\partial \xi}\right)\varphi\left(\xi - \frac{v_y}{\Omega},\ \eta + \frac{v_x}{\Omega}\right)e^{-i\bar{\omega}(t'-t)}\right\} , \tag{5}$$

where we have defined

$$\bar{\omega} = \omega - kw \quad . \tag{6}$$

To proceed we use the small Larmor radius limit, i.e., $v/\Omega \ll \xi,\eta$, and Taylor expand φ inside the orbit integral as

$$\varphi = \sum\left(-\frac{v_y}{\Omega}\right)^n\left(\frac{v_x}{\Omega}\right)^m \frac{1}{n!}\frac{1}{m!}\frac{\partial^n}{\partial\xi^n}\frac{\partial^m}{\partial\eta^m}\varphi(\xi,\eta) \quad , \quad 0 \le m+n \le 4 \tag{7}$$

keeping terms up to $1/(\bar{\omega}+\Omega)$. That is, we drop terms of order $1/(\omega\pm 2\Omega)$ and higher since we are concerned with behavior near the upper hybrid frequency in the limit $\omega_p/\Omega < 1$.

If Eq. (7) is substituted into Eq.(5) and integrated we obtain

$$f_k = -\frac{e}{m}\left(\frac{\alpha}{\pi}\right)^{3/2} e^{-\alpha(v^2+w^2)}\Bigg\{2\alpha g(\xi,\eta)\varphi(x,y) - \Bigg[2\alpha g\,\frac{\omega}{\bar{\omega}}\left(1 + \frac{v^2}{4\Omega^2}\nabla_\perp^2\right.$$

$$\left. + \frac{v^4}{\Omega^4}(\nabla_\perp^2)^2\right) - \frac{i}{\Omega\bar{\omega}}\left(\frac{\partial g}{\partial\xi}\frac{\partial}{\partial\eta} - \frac{\partial g}{\partial\eta}\frac{\partial}{\partial\xi}\right)\left(1 + \frac{v^2}{4\Omega^2}\nabla_\perp^2\right)$$

$$+ \frac{v\omega}{2i\Omega}\left(\frac{e^{i\Phi}}{\bar{\omega}-\Omega} - \frac{e^{-i\Phi}}{\bar{\omega}+\Omega}\right)\Bigg[g\left(\frac{\partial}{\partial\xi} + \frac{v^2}{8\Omega^2}\frac{\partial}{\partial\xi}\nabla_\perp^2\right)2\alpha$$

$$+ \frac{1}{\Omega\omega i}\left(\frac{\partial g}{\partial\xi}\frac{\partial}{\partial\eta} - \frac{\partial g}{\partial\eta}\frac{\partial}{\partial\xi}\right)\frac{\partial}{\partial\xi}\Bigg] - \frac{v\omega}{2\Omega}\left(\frac{e^{i\Phi}}{\bar{\omega}-\Omega} + \frac{e^{-i\Phi}}{\bar{\omega}+\Omega}\right)\Bigg[g\left(\frac{\partial}{\partial\eta} + \frac{v^2}{8\Omega^2}\frac{\partial}{\partial\eta}\nabla_\perp^2\right)2\alpha$$

$$+ \frac{1}{\Omega\omega i}\left(\frac{\partial g}{\partial\xi}\frac{\partial}{\partial\eta} - \frac{\partial g}{\partial\eta}\frac{\partial}{\partial\xi}\right)\frac{\partial}{\partial\eta}\Bigg]\Bigg]\varphi(\xi,\eta)\Bigg\} \tag{8}$$

with

$$\nabla_\perp^2 = \frac{\partial^2}{\partial\xi^2} + \frac{\partial^2}{\partial\eta^2} \quad . \tag{9}$$

Next, we integrate over v^2 and Φ to obtain, with $a^2 = 1/2\alpha\Omega$ and the density given by

$$n(x,y) = \left(1 + \frac{a^2}{2}\nabla_\perp^2 + \frac{a^4}{4}(\nabla_\perp^2)^2\right) g(x,y) \quad ,$$

$$\int d^2v\, f_k = -\frac{e}{m}\left(\frac{\alpha}{\pi}\right)^{\frac{1}{2}} e^{-\alpha w^2}\Bigg\{2\alpha\varphi(x,y)n(x,y) - \frac{\omega}{\bar{\omega}}\Bigg[2\alpha n(x,y) + \frac{1}{\Omega^2}\underset{\sim}{\nabla}_\perp\cdot n\nabla_\perp + \frac{3}{4}\frac{a^2}{\Omega^2}\nabla_\perp^2 n\nabla_\perp^2$$

$$- \frac{i}{\omega\Omega}\underset{\sim}{b}\cdot(\underset{\sim}{\nabla}_\perp n)\times\underset{\sim}{\nabla}_\perp\left(1 + \frac{a^2}{2}\nabla_\perp^2\right) + \frac{1}{2}\frac{a^2}{\Omega^2}(\underset{\sim}{\nabla}_\perp\underset{\sim}{\nabla}_\perp n):\nabla_\perp\nabla_\perp - \frac{1}{2}\frac{a^2}{\Omega^2}(\nabla_\perp^2 n)\nabla_\perp^2\Bigg]\varphi$$

$$+ \frac{\omega}{(\bar{\omega}^2-\Omega^2)\Omega^2}\Bigg[\frac{\bar{\omega}}{\Omega}\left(\underset{\sim}{\nabla}_\perp\cdot n\underset{\sim}{\nabla}_\perp + a^2\nabla_\perp^2 n\nabla_\perp^2 + a^2(\underset{\sim}{\nabla}_\perp\underset{\sim}{\nabla}_\perp n):\underset{\sim}{\nabla}_\perp\underset{\sim}{\nabla}_\perp - a^2(\nabla_\perp^2 n)\nabla_\perp^2\right)$$

$$+ i\left(\underset{\sim}{b}\cdot\underset{\sim}{\nabla}_\perp\times n\underset{\sim}{\nabla}_\perp\left(1 + \frac{a^2}{2}\right)\nabla_\perp^2 - \frac{a^2}{2}\nabla_\perp^2\underset{\sim}{b}\cdot\underset{\sim}{\nabla}_\perp\times n\underset{\sim}{\nabla}_\perp\right) + i\frac{a^2\bar{\omega}}{\omega}\underset{\sim}{\nabla}_\perp\cdot\underset{\sim}{b}\cdot(\underset{\sim}{\nabla}_\perp n)\times\underset{\sim}{\nabla}_\perp\underset{\sim}{\nabla}_\perp\Bigg]\varphi(x,y)\Bigg\}. \tag{10}$$

If we now make use of Poisson's equation and incorporate the plasma dispersion function of Fried and Conte[9]

$$Z(\xi) = \frac{1}{\sqrt{\pi}}\int_{-\infty}^{\infty} dx\, e^{-x^2}\frac{1}{x-\xi}\quad, \tag{11}$$

we have for $k_\perp = 0$

$$a^2\frac{1}{r}\frac{\partial}{\partial r}r\frac{\partial}{\partial r}D^2(r)\frac{1}{r}\frac{\partial}{\partial r}r\frac{\partial\varphi}{\partial r} + \frac{1}{r}\frac{\partial}{\partial r}r\,k_o(r)\frac{\partial\varphi}{\partial r} + \frac{k_1^2(r)}{D^2(r)}\varphi = 0 \tag{12}$$

for cylindrical symmetry and

$$a^2\frac{\partial^2}{\partial x^2}D^2(x)\frac{\partial^2\varphi}{\partial x^2} + \frac{\partial}{\partial x}k_o(x)\frac{\partial\varphi}{\partial x} + \frac{k_1^2(x)}{D^2(x)}\varphi \tag{13}$$

for slab geometry. We have defined

$$D^2(r) = \frac{\omega_p^2(r)}{\Omega^2}\left[\frac{3}{4}\, Z\left(\frac{\omega}{k}\sqrt{\alpha}\right) - \frac{1}{2}\left(Z\left(\frac{\omega-\Omega}{k}\sqrt{\alpha}\right) + Z\left(\frac{\omega+\Omega}{k}\sqrt{\alpha}\right)\right)\right]\frac{\omega}{k}\sqrt{\alpha} \quad ,$$

$$k_o(r) = -\frac{\omega_p^2(r)}{\Omega^2}\,\frac{\omega}{k}\sqrt{\alpha}\left[-\, Z\left(\frac{\omega}{k}\sqrt{\alpha}\right) + \frac{1}{2}\left(Z\left(\frac{\omega-\Omega}{k}\sqrt{\alpha}\right) + Z\left(\frac{\omega+\Omega}{k}\sqrt{\alpha}\right)\right)\right] - 1$$

and

$$k_1 = k\left[1 + \frac{2\alpha}{k^2}\,\omega_p^2(r)\left(\frac{\omega}{k}\sqrt{\alpha}\, Z\left(\frac{\omega}{k}\sqrt{\alpha}\right) + 1\right)\right]^{\frac{1}{2}} D(r) \tag{14}$$

with $\omega_p^2(r) = \frac{4\pi e^2}{m}\, n(r)$ the local plasma frequency. Note that we have dropped terms of order a^2/R^2 in the definition of k_o. R is the plasma radius and is of order $\{\frac{1}{\omega_p}\,(\partial^2\omega_p/\partial r^2)\}^{-\frac{1}{2}}$.

III. WKBJ ANALYSIS

As previously mentioned, it is the vanishing of k_o, the coefficient of the second derivative, which dominates the structure of the eigenmodes. To obtain the eigenvalue we need only connect, to the well behaved solution at the origin, that solution about the turning point $(k_o \approx 0)$ which vanishes outside of the plasma. To do this we make use of the WKBJ approximation in the region between the turning point and the origin and in the region beyond the turning point.

First, near the origin (we consider the cylindrical problem) we have

$$\left(\frac{1}{r}\frac{\partial}{\partial r} r \frac{\partial}{\partial r} - [k_+(0)]^2\right)\left(\frac{1}{r}\frac{\partial}{\partial r} r \frac{\partial}{\partial r} - [k_-(0)]^2\right)\varphi = 0 \quad ,$$

where

$$k_\pm^2 = \frac{k_o \pm \sqrt{k_o^2 - 4k_1^2 a^2}}{2a^2 D^2} \quad . \tag{15}$$

Thus, near the origin

$$\varphi = J_o(k_+(0)r) + AJ_o(k_-(0)r) \tag{16}$$

where we have excluded the ill behaved solutions.

To obtain the solution in the vicinity of the turning point, or rather how the solution on one side of the turning point connects on to the solution on the other side, it is convenient to make the substitution

$$\frac{r}{R} = e^{x} \quad ,$$

which leads to

$$\left[\frac{a^2}{R^2}\frac{\partial^2}{\partial x^2} e^{-2x} D^2(x) \frac{\partial^2}{\partial x^2} + \frac{\partial}{\partial x} k_o(x) \frac{\partial}{\partial x} + \frac{k_1^2(x)R^2}{D^2(x)} e^{2x}\right]\varphi(x) = 0 \quad . \quad (17)$$

Well away from the turning points we have for the WKBJ solutions

$$\varphi_{\pm}^{\pm} = \frac{R}{a} e^{-x/2} \frac{1}{D(x)} \frac{1}{\sqrt{k_{\pm}}} \frac{1}{\sqrt{k_+^2 - k_-^2}} \exp\left(\pm i \int^{x} dx e^{-x} k_{\pm}\right) \quad . \qquad (18)$$

To arrive at Eq. (18) we set $\varphi = e^{S(x)}$ and solve by iteration with $S'' \ll (S')^2$, etc. It should be pointed out that the derivative of the coefficients relative to the derivative of φ is small by at least $\sqrt{a/R}$ since, as will be subsequently seen, the wavelength of the mode in the direction of the density gradient is on the order of $\sqrt{aR}$. Moreover, as will be shown, k_o is on the order of a/R; and so we see that all terms of Eq. (17) are the order of unity, whereas the sixth derivative term (which we have not included) can easily be seen to be of order a/R and therefore can properly be dropped. Further note that for $r < r_{turn}$ the WKBJ solutions are oscillatory, while for $r > r_{turn}$ the solutions are exponential (recall r_{turn} is roughly the position at which $k_o = 0$).

To continue, we compare the asymptotic limit of Eq. (16) to Eq. (18) and obtain the appropriate linear combination of $\varphi_{\pm}^{\pm}$, namely

$$\varphi = \frac{2}{\sqrt{\pi}} \frac{R}{a} \frac{1}{D(r)\sqrt{r}} \frac{1}{\sqrt{k_+^2 - k_-^2}} \left[\frac{1}{\sqrt{k_+}} \cos\left(\int_o^r k_+ dr - \frac{\pi}{4}\right) + \frac{A}{\sqrt{k_-}} \cos\left(\int_o^r k_- dr - \frac{\pi}{4}\right)\right] \quad .(19)$$

To complete the program we need only determine how the asymptotic solution for $r < r_{turn}$ given by Eq. (19) connects on to the well behaved (exponentially decreasing) solution for $r > r_{turn}$. The procedure is to expand k_o about its zero (the turning point) and evaluate all other terms at the turning point which leads to an equation of the form

$$\left[\alpha \frac{\partial^4}{\partial x^4} - \beta \frac{\partial}{\partial x} x \frac{\partial}{\partial x} + \gamma\right] \varphi = 0 \quad . \tag{20}$$

α, β, γ are positive and constant. The solutions to Eq. (20) is given in terms of the contour integral.[10]

$$\varphi = A \int_c \frac{dp}{p} \exp\left(- \frac{\alpha p^3}{3\beta} + px + \frac{\gamma}{p\beta}\right) = A \int_c \frac{dp}{p} e^{\psi(p)} \quad . \tag{21}$$

Since an analysis of the above equation has been given by Brueckner and Rosenbluth in an unpublished report,[11] we shall only sketch the method here and present the desired connection formulae. Our interest is only in the asymptotic behavior, so we may evaluate the contour integral by the method of steepest descent. The independent solutions are determined by the four independent contours. The position of the saddles and contours of constant phase ($\mathrm{Im}\, \psi(p)$ a constant) for large x are sketched in Figs. 1 and 2. The contours which connect the exponentially decreasing solutions to the oscillatory solutions are easily seen to be

$$J_1 \rightarrow - I_4 + I_3 - I_2 + I_1$$

$$2J_2 \rightarrow I_4 - I_3 - I_2 + I_1 \quad . \tag{22}$$

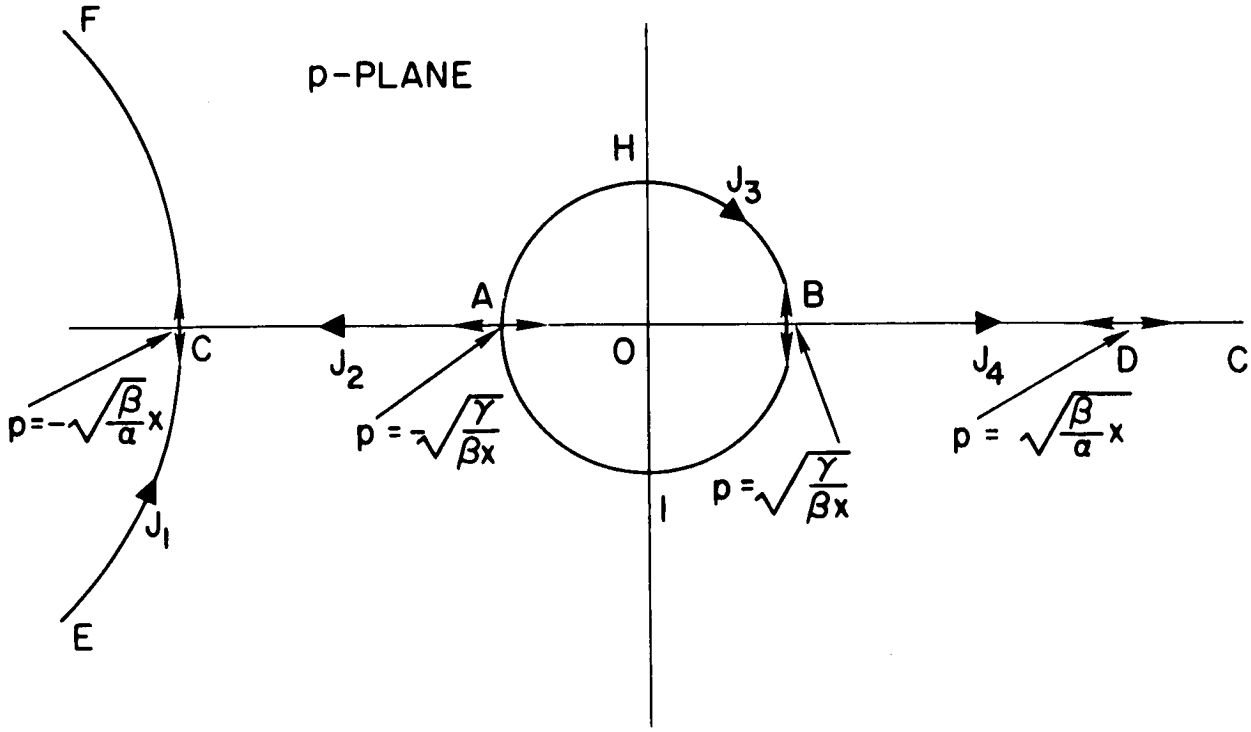

$J_1 = ECF$

$J_2 = \frac{1}{2}(OACF + OACG)$

$J_3 = OAHBIAO$

$J_4 = \frac{1}{2}(OAHBDG + OAIBDG)$

Fig. 1--Contours of constant phase for $x \gg 0$

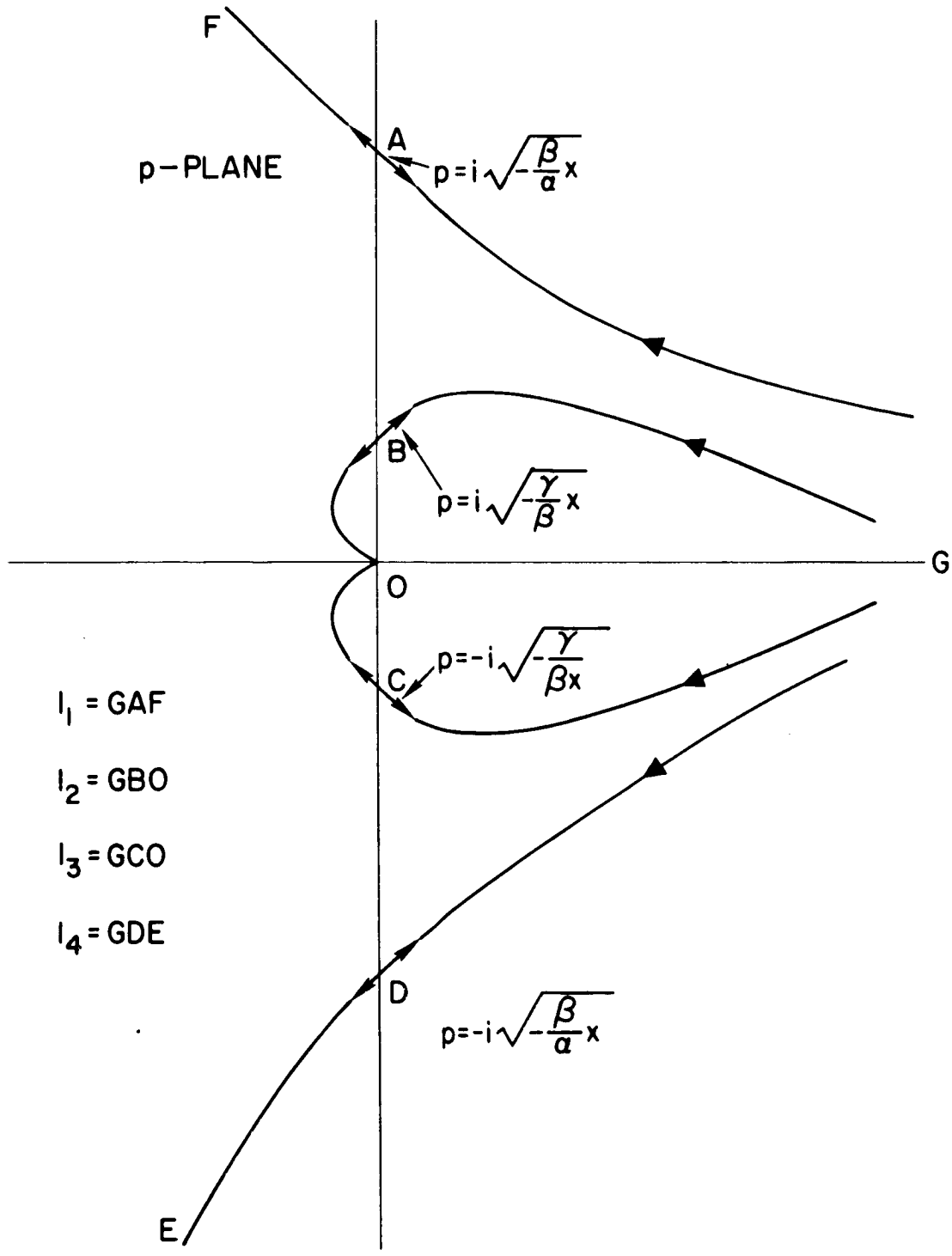

Fig. 2--Contours of constant phase for $x \ll 0$

Hence, the WKBJ solution which connects onto the decreasing solution is

$$\frac{1}{\sqrt{k_+^2-k_-^2}}\,\frac{2}{\sqrt{\pi}}\,\frac{R}{a}\,\frac{1}{D(r)\sqrt{r}}\left[A'\left(\frac{1}{\sqrt{k_+}}\sin w_+ + \frac{1}{\sqrt{k_-}}\cos w_-\right) + B'\left(\frac{1}{\sqrt{k_+}}\cos w_+ - \frac{1}{\sqrt{k_-}}\sin w_-\right)\right] , \tag{23}$$

where

$$w_\pm = \int_r^{r_{turn}} \left(k_\pm(r) - \frac{\pi}{4}\right) dr \quad . \tag{24}$$

Finally, to connect on smoothly with the solution of Eq. (19) we must have

$$\int_0^{r_{turn}} (k_+-k_-)^{\frac{1}{2}}\, dr = (n + \tfrac{1}{2})\pi \quad , \tag{25}$$

which with Eq. (15) can be written

$$\int_0^{r_{turn}} (k_o - 2k_1 a)^{\frac{1}{2}}\, \frac{dr}{D} = (n + \tfrac{1}{2})\pi a \quad , \quad n = 0,1,2,\ldots \tag{26}$$

The dispersion relation for slab symmetry is identical to Eq. (26) with $r \to x$.

A comparison of the above dispersion relation and that of the infinite medium, namely

$$k_-^2 = \frac{k_1^2}{k_o D^2} \quad , \tag{27}$$

immediately reveals that there is little similarity between the two. That this behavior is reasonable can be seen from the connection formula given by the contour relations of Eq. (22), which lead to

$$\frac{1}{\sqrt{k_+^2-k_-^2}}\left\{\frac{1}{\sqrt{-k_+}}\, e^{-\int^x |k_+|\,dx} \pm \frac{1}{2\sqrt{-k_-}}\, e^{-\int^x |k_-|\,dx}\right\}$$

$$\rightarrow \frac{1}{\sqrt{k_+^2-k_-^2}}\left\{\frac{1}{\sqrt{k_+}}\, e^{\pm i\left(\int_x |k_+|\,dx - \frac{\pi}{4}\right)} + \frac{1}{\sqrt{k_-}}\, e^{\pm i\left(\int_x |k_-|\,dx - \frac{\pi}{4}\right)}\right\}.$$

Now since k_+ is a backward wave (phase velocity of opposite sense to the group velocity) and k_- is a forward wave, we see that at the turning point the incident k_+ mode is converted into a reflected k_- mode and the converse. Hence, it is not possible to set up a standing k_- wave in the radial direction, but rather the only normal modes must be linear combinations of k_+ and k_- waves, which accounts for the new dispersion relation of Eq. (26).

We now return to the evaluation of Eq. (26). Assume

$$\omega_p^2(r) = \omega_p^2\left(1 - \frac{r}{R}\right)^2$$

and expand in the square root to order $(r/R)^2$. (Since as previously mentioned $\Delta r/R \approx \sqrt{a/R}$), treat D as constant (for the same reason) to obtain

$$k_o(0) - 2k_1(0)a = 2(2n+1)\,\frac{a}{R}\,D(0) \quad , \tag{28}$$

where the position of the turning point is given by

$$\frac{r^2}{R^2} = k_o(0) - 2k_1(0) \approx \frac{a}{R} \quad , \tag{29}$$

which demonstrates that $\Delta r/R \approx \sqrt{a/R}$. To arrive at these results, we have taken the asymptotic limit of all Z functions of Eq. (14) except those whose argument is $\frac{\omega-\Omega}{k_{\|}\alpha}\sqrt{\alpha}$, since we are concerned with frequencies around the upper hybrid frequency, which is in the vicinity of the cyclotron frequency. In this limit we have

$$D^2 = \frac{\omega_p^2(r)}{\Omega^2}\left[-\frac{3}{4} + \frac{\omega^2}{\omega^2-\Omega^2} - \frac{\xi Z(\xi)+1}{2}\,\frac{\omega}{\omega-\Omega}\right]$$

$$k_o(r) = \frac{\omega_H^2(r)-\omega^2}{\omega^2-\Omega^2} - \frac{\omega_p^2(r)}{\Omega^2}\,\frac{\omega}{\omega-\Omega}\,\frac{\xi Z(\xi)+1}{2}$$

$$\xi = \frac{\omega-\Omega}{k_{\|}}\sqrt{\alpha}$$

$$k_1 = k_{\|}\sqrt{1 - \frac{\omega_p^2(r)}{\omega^2}}\,D(r) \quad . \tag{14'}$$

To obtain the dispersion of the wave we have solved Eq. (21) numerically and have plotted $(\omega-\Omega)/\omega$ vs Re $ka\sqrt{2}$ for various values of the parameters in Fig. 3. In Fig. 4 we have plotted Im $ka\sqrt{2}$ vs Re $ka\sqrt{2}$ for the same parameters. Note, from Fig. 3, the flat behavior for small k,

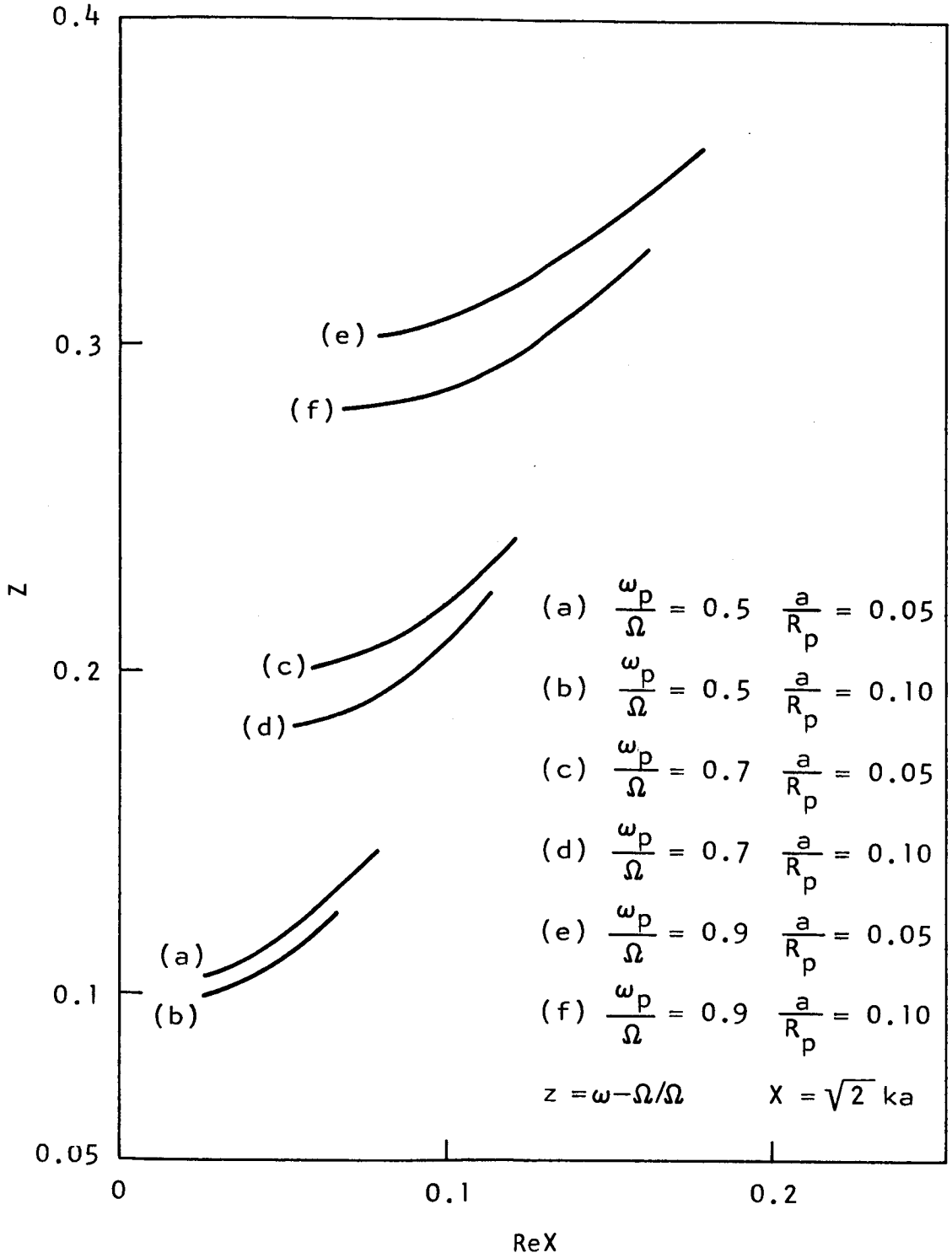

Fig. 3--Dispersion of the eigenmode n = 0

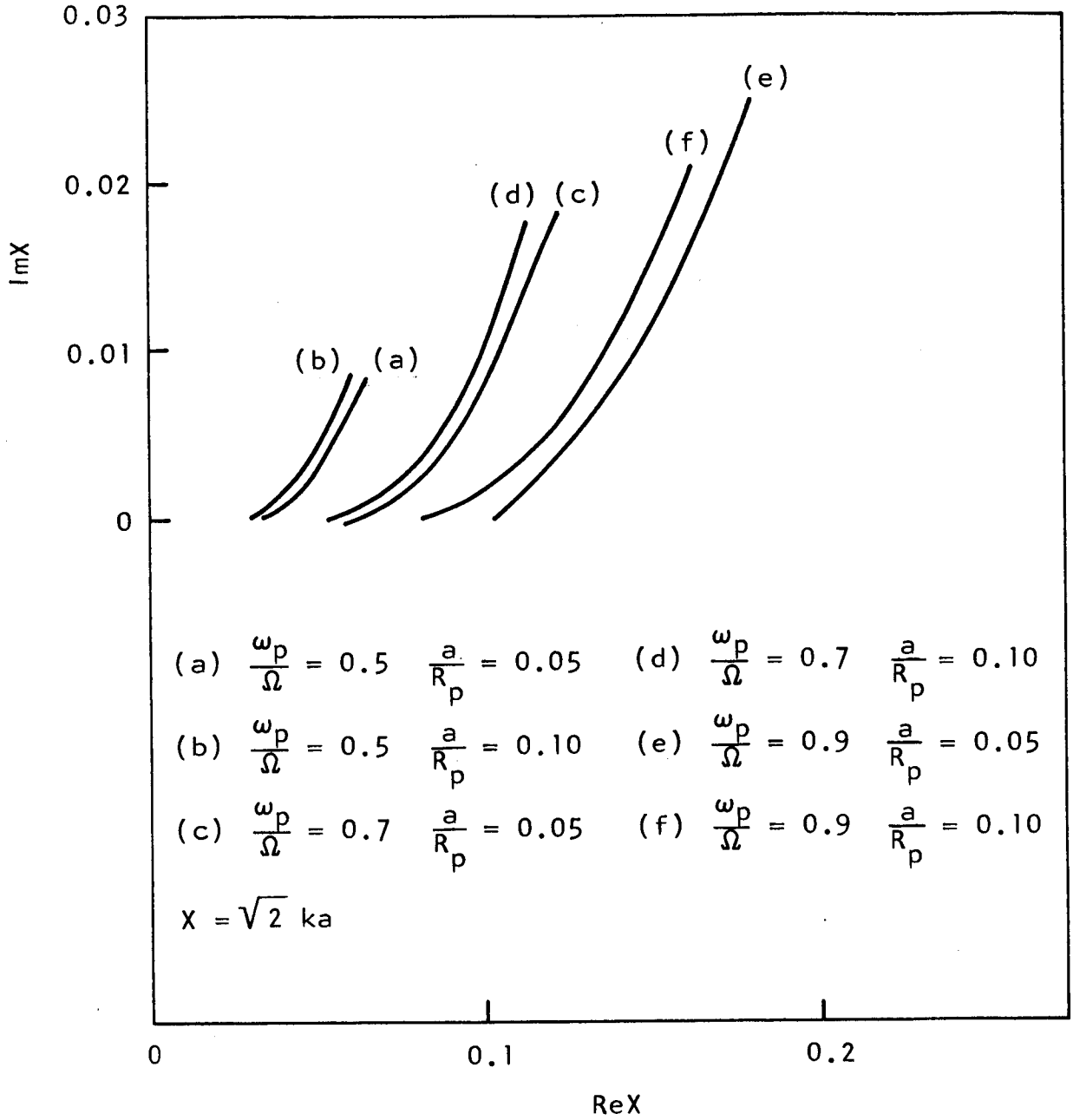

Fig. 4--Dispersion of the eigenmode $n = 0$

which indicates the sudden onset for finite k. We have limited the curves to $\mathrm{Im}\, k/\mathrm{Re}\, k < 0.15$, since the wave cannot reasonably be called a wave beyond this value. In Fig. 4 we see the monotonic increase of $\mathrm{Im}\, k$ with $\mathrm{Re}\, k$ above the onset. Just below this limit $\mathrm{Im}\, k$ becomes quite large. It should be pointed out that $n = 0$, the least damped solution, and the one we have depicted is the least accurate. For improved accuracy it would be necessary to solve the fourth order differential equation directly. The dispersion of this eigenmode is in qualitative agreement with the M-W experiment.[8]

IV. BEAM INTERACTION

To compute the effect of the beam interaction we must add to f_k the beam contribution. For the beam distribution we choose

$$f_B = \lim_{\alpha\to\infty} n_B\left(\frac{\alpha}{\pi}\right)^{3/2} e^{-\alpha[v_\perp^2+(w-V)^2]} \quad ; \tag{30}$$

that is, we assume a negligible thermal spread to the beam relative to that of the background. Further, we assume uniform density for the beam. These properties describe the unstable mode of operation of the M-W experiment. Utilizing Eq. (30), we find the perturbed density associated with the beam is

$$4\pi e n_B' = \left(\frac{\omega_{p_B}^2 k^2}{(\omega-kV)^2} + \frac{\omega_{p_B}^2}{(\omega-kV)^2-\Omega^2}\frac{1}{r}\frac{\partial}{\partial r} r \frac{\partial}{\partial r}\right)\varphi \quad , \quad \omega_{p_B} \ll \omega_p \quad , \tag{31}$$

and thus we have for the new coefficients of the fourth order differential

$$k_o' = k_o + \frac{\omega_{p_B}^2}{(\omega-kV)^2-\Omega^2}$$

$$k_\perp'^2 = k_\perp^2 - k^2 \frac{\omega_{p_B}^2}{(\omega-kV)^2} D^2(r) \quad . \tag{32}$$

We first consider the beam mode where $\omega \approx kV$. Again, we solve the dispersion relation numerically to obtain the results depicted in Figs. 5 through 7. We see that the unstable beam mode exists both above and below the plasma mode in contrast to the lower branch wherein the beam mode above the plasma mode is stable. In addition, there are two other damped modes. One is a beam mode below the plasma mode and transmutes into a plasma mode; the other, a plasma mode, becomes the other end of the beam mode. Once again the accuracy of the analysis is limited since we restrict attention to the $n = 0$ mode. Also, the WKBJ analysis breaks down at the upper and lower limits of the beam curves since k_o' becomes too large; however, in this range the second order differential equation becomes the appropriate equation to solve. Again, these predictions qualitatively match the experiment results. (See Fig. 7, with parameters similar to those in the M-W experiment.)

We have also considered the second beam mode for which $kV \sim \omega + \Omega$. A numerical solution of the corresponding dispersion relation has been obtained. Figure 8 shows the result for the parameters mentioned therein. We see that an unstable beam mode exists together with a similar mode which is damped.

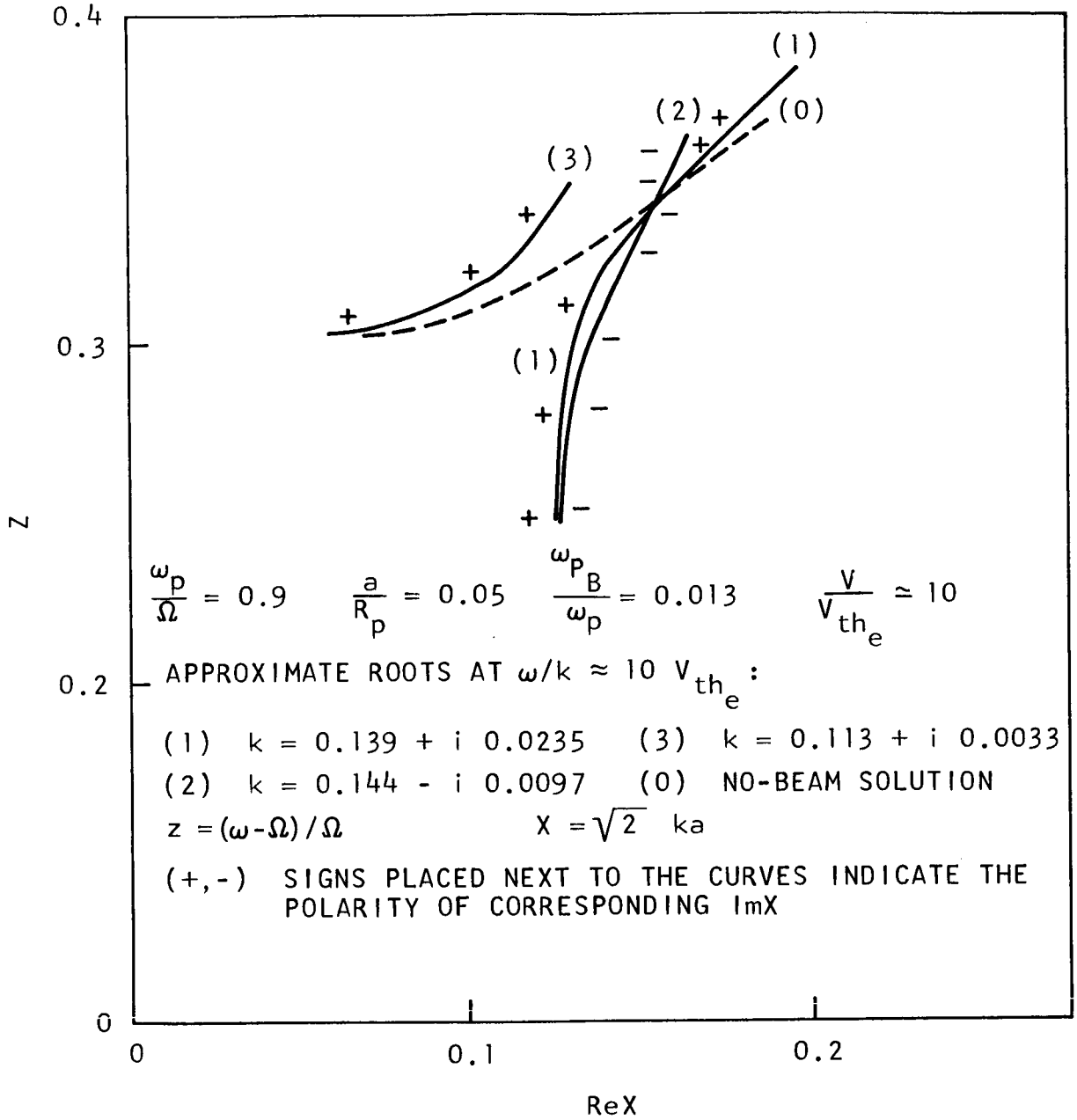

Fig. 5--Dispersion of the beam mode $\omega \simeq kV$. The minus sign corresponds to growth

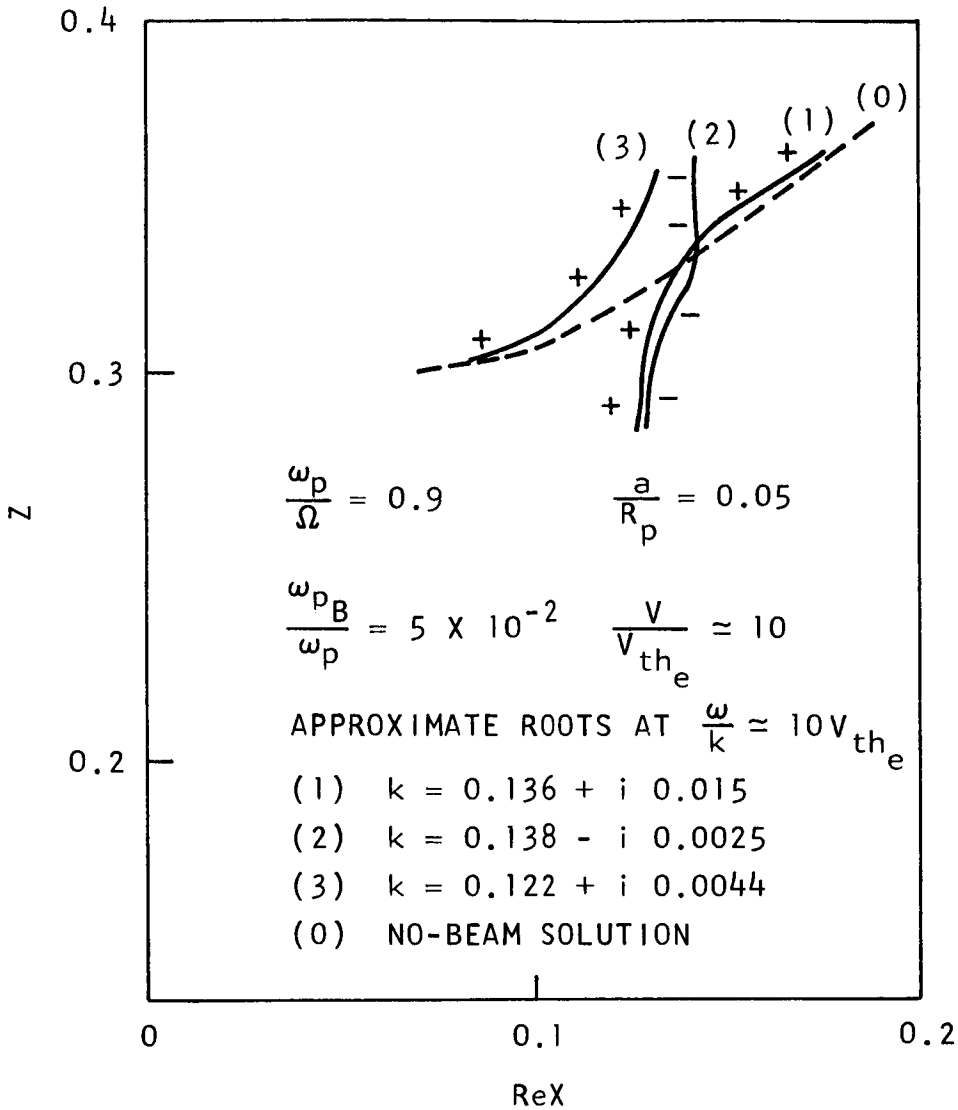

Fig. 6--Dispersion of the beam mode $\omega \simeq kV$. See Fig. 5 for definitions of parameters

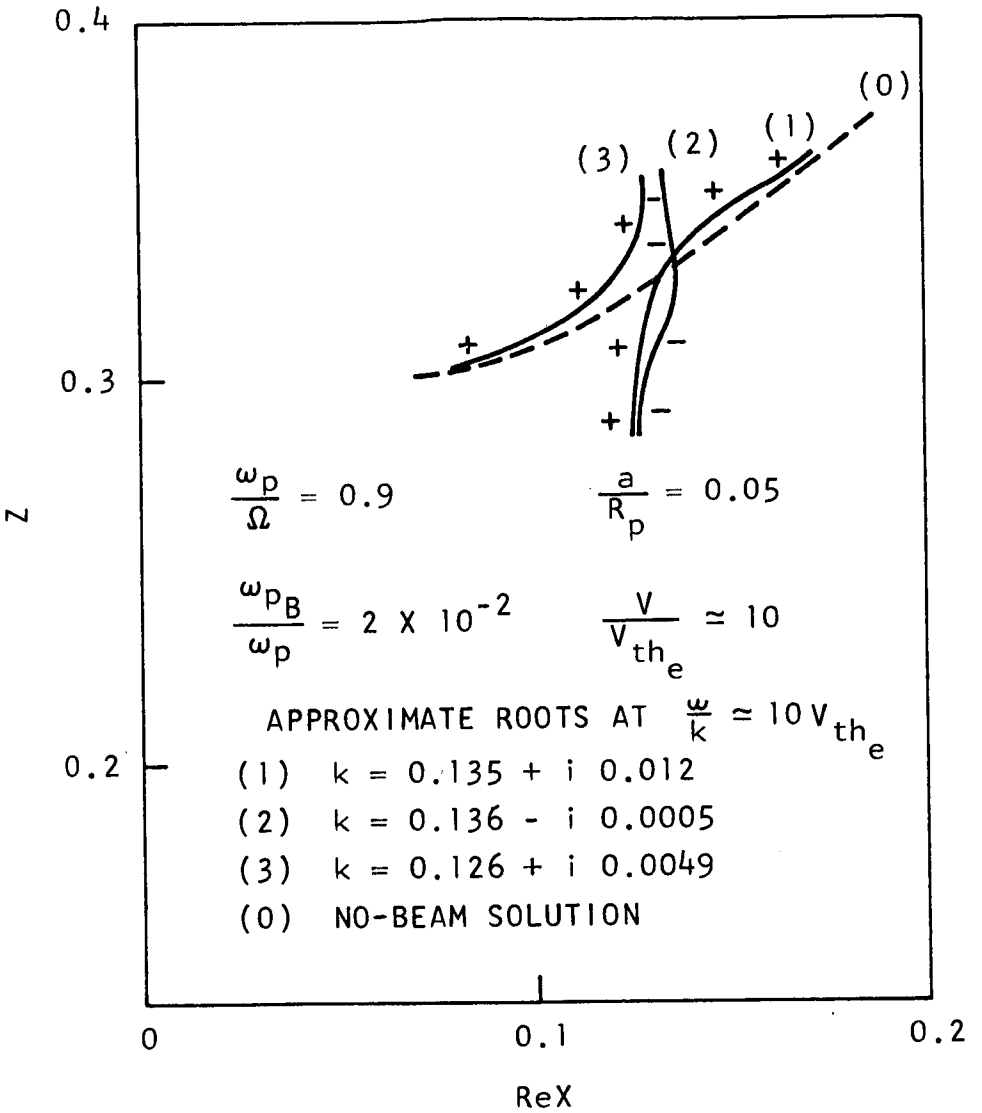

Fig. 7--Dispersion of the beam mode $\omega \simeq kV$. See Fig. 5 for definitions of parameters

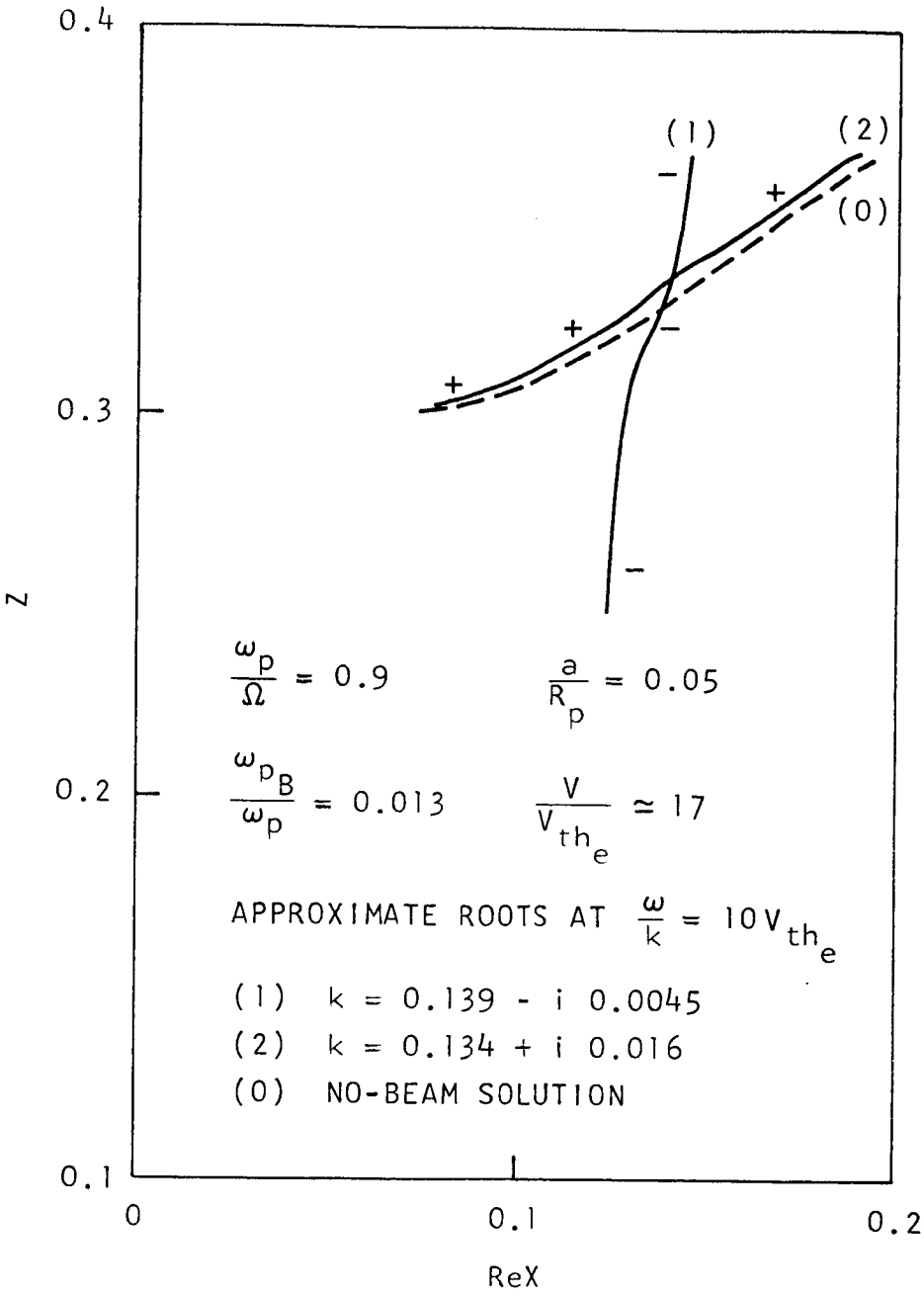

Fig. 8--Dispersion of the second beam mode $\omega+\Omega \simeq kV$. See Fig. 5 for definitions of parameters

V. RESULTS

There are three qualitative features which characterize the eigenmodes near the upper hybrid frequency: First, for the stable inhomogeneous Maxwellian plasma, the frequency is an extremely flat function of parallel wave number for small $k_{\parallel}$, leading to large spatial damping in this region. Second, for larger $k_{\parallel}$, ω increases with $k_{\parallel}$; simultaneously, the coefficient of spatial damping which goes from its extremely large value in the flat region to a small value beyond increases monotonically with $k_{\parallel}$. Finally, for the case in which a beam is added to the stable background plasma, we find an unstable beam mode both above and below the plasma mode.

APPENDIX XIV

REFERENCES

1. S. J. Buchsbaum and A. Hasegawa, Phys. Rev. 143, A303 (1966).
2. For a more extensive list of references, see Reference 1.
3. C. B. Wharton and J. H. Malmberg, Proceedings VIIth International Conference on Phenomena in Ionized Gases, Belgrade, 1965, Vol. II, 256 (1966).
4. I. B. Bernstein, Phys. Rev. 109, 10 (1958).
5. A. W. Trivelpiece and R. W. Gould, J. Appl. Phys. 30, 1784 (1959).
6. See for instance Reference 1 and Gary A. Pearson, Phys. Fluids 9, 2454 (1966).
7. J. H. Malmberg and C. B. Wharton, submitted for publication, hereafter referred to as M-W experiment.
8. A detailed comparison between the theory developed here and the M-W experiment is given in Reference 7.
9. B. D. Fried and S. D. Conte, The Plasma Dispersion Function, Academic Press (1961).
10. L. D. Landau and E. M. Lifshitz, Quantum Mechanics: Non-relativistic Theory (Addison-Wesley Publishing Company, Inc., Reading, Massachusetts 1958), Mathematical Appendix, p. 483.
11. K. A. Brueckner and M. N. Rosenbluth, SRI report (unpublished).

APPENDIX V

CYCLOTRON WAVES IN A COLLISIONLESS PLASMA

by

C. B. Wharton and J. H. Malmberg

General Atomic Report
GA-6584
July 30, 1965

Published in
NASA Contractor Report
NASA CR-348
December 1965

and

Proceedings of VII International Conference
on Phenomena in Ionized Gases, Beograd, Yugoslavia
Volume II, 256 (1966)

PRECEDING PAGE BLANK NOT FILMED.

CYCLOTRON WAVES IN A COLLISIONLESS PLASMA

C. B. Wharton and J. H. Malmberg

ABSTRACT

Experimental studies of plasma waves in a 2 meter long collisionless plasma column, over the frequency range 30 to 520 Mhz, are reported. Special attention is given to the frequencies neighboring the electron cyclotron frequency ω_b. At least three (and perhaps more) distinct waves having resonances at or near ω_b are found. Two waves lie above the cyclotron frequency. One has a velocity greater than that of light and is a forward wave, apparently an electromagnetic waveguide mode, perturbed by the plasma. The other is a slow, backward wave, having a propagation cutoff at the upper hybrid frequency $\omega_{uh} = (\omega_b^2 + \omega_p^2)^{1/2}$, with a dispersion curve resembling that of the C_{01} cyclotron wave. This wave is heavily damped in space, typically 10 to 20 dB per wavelength. The third wave is a slow forward wave, lying below ω_b and resembling a whistler. It is only moderately damped.

The measured dispersion curves of these waves are presented, and their relation to the predictions of theory is discussed.

INTRODUCTION

A plasma column confined by a magnetic field inside a conducting cylinder can support many modes of waves, both electrostatic and electromagnetic. The theory of electron plasma oscillations, ion sound waves, Alfven waves, whistlers and the ordinary and extraordinary modes of electromagnetic wave propagation, for many different combinations of parameters such as magnetic field strength and plasma density, have been considered in the literature, and excellent reviews of this work have been published (refs. 1, 2, 3, 4). However, detailed experimental confirmation of the theories is lacking in most cases. We have previously reported results on the dispersion and collisionless damping of longitudinal plasma waves (refs. 5, 6). We report here measurements of the dispersion relations of waves near the electron cyclotron frequency. Because the cyclotron wave is highly dispersive, with wavelengths varying from meters to centimeters over a small frequency range (or density change, for fixed-frequency), a long, very stable, quiet plasma was required for these measurements. This apparatus is discussed in the section below and in reference 12.

Growth and damping of spacecharge waves are easily seen qualitatively in our wave experiments. However, there are several waves propagating simultaneously at some frequencies, which makes quantitative measurements difficult. We have not yet been successful in identifying some of the wave types, but for most

PRECEDING PAGE BLANK NOT FILMED.

waves, the measured dispersion fits the theory in the vicinity of the electron cyclotron frequency. The wavelengths measured are long, yet the waves are heavily damped. In a collisionless plasma, such as in the experiment discussed here, collisional damping is not important; however, there may be Landau damping. The waves observed near the cyclotron frequency consist of cyclotron plasma waves, evanescent waves, and electromagnetic waves mixed together. Further, when an electron beam is injected, certain cyclotron waves are observed to increase in amplitude and others to decrease. Whether this is due to wave growth and damping or to variations in probe coupling caused by the beam, has yet to be determined. If the increase in amplitude is really due to wave growth, the effects may be understandable in terms of the theory of microinstabilities (refs. 7, 8, 9, 10, 11).

EXPERIMENTAL DETAILS

These investigations used the same apparatus as used for the research reported in references 5 and 12 with the addition of a 10 cm I.D. stainless steel pipe surrounding the plasma, to cut off electromagnetic wave coupling between the probes, and an insulating ring between the duoplasmatron and the main chamber, to permit a voltage difference to be applied between the duoplasmatron anode and the grounded pipe. A general view of the equipment is shown in Fig. 1. Four movable probes are guided by rails in the vacuum chamber and controlled externally by manipulators seen in the left of the picture. The probes are able to explore any region along the chamber, inside a 10 cm radius when the liner pipe is absent. When the slotted liner is in place, their angular variation is restricted by the slot width to about 10°, allowing only a slice of the column to be explored. The probes can be retracted radially completely out of the plasma.

The plasma density in the chamber near the duoplasmatron source is typically between 5×10^{7} and 5×10^{9} cm^{-3} for these experiments and is steady state. The density decreases downstream along the axis due to radial diffusion, producing a 25% drop from one end to the other. The radial density profile as indicated by the saturation ion current to a small Langmuir probe is given in Fig. 2. The plasma spatial potential profile may be inferred from the probe floating potential, also given in Fig. 2. The center of the column is about 15 volts positive with respect to the wall for these experimental conditions. The potential on axis is about $(V_A - 3kT)$, where V_A is the voltage applied to the anode of the plasma source and T is the electron temperature. We have observed that, when the axial potential is below about 10 volts, a rotational instability is excited. The rotational frequency is between 20 and 60 kc., depending on density, magnetic field strength and axial potential. As the duoplasmatron anode bias voltage is raised, the rotation ceases and the plasma noise, as picked up by probes, drops to a low level. Further increase in the bias voltage leads to a rotation in the opposite direction at a frequency of 50 to 100 kc. accompanied by a decrease in density. This effect will be described in more detail elsewhere. The profile of Fig. 2 was obtained in the "stable" condition. The profile is broader or even double-peaked when the column instability is present. When the column is rotating, a modulation of the transmitted waves and R.F. noise at the rotation frequency is observed.

The electron temperature is determined by Langmuir probes and by energy-analysis of electrons escaping through a hole in the ion trap at the downstream end. The electron temperature varies between 6 and 12 eV for various adjustments of the machine parameters.

The R.F. transmission circuitry uses a conventional interferometer (ref. 4), with 5 kc. modulation on the carrier, and a tuned video amplifier and phase-coherent detector in the receiver, to reject noise outside the narrow pass-band. The crystal detector in the interferometer is operated at a high level ($\sim$0.5 mA) by keeping the CW reference signal level at about 1 mW. This gives an overall system sensitivity almost as high as that of a superheterodyne. This high sensitivity and large dynamic range are necessary to follow the waves over their damping range. High frequency fluctuations in the density of the plasma in the transmission path result in corresponding changes in wave number (since the transmitter frequency is fixed) which leads in turn to noisy modulation of the phase of the received signal. Since the interferometer averages the received signal over a comparatively long time, in extreme cases, this effect can destroy the interference fringes even where appreciable power is still received. We call this phenomena "phase scrambling". The signal is finally lost by "phase scrambling" rather than in the receiver-generated noise.

Plasma waves are launched and received with the same probes used for current and potential measurements. These probes tend to excite a spectrum of plasma modes, and because of their small size, have rather poor coupling. Planar grids were tried but led to a serious loss of density, as well as to severe standing waves.

In an attempt to improve the coupling of our probes to the cyclotron waves, we tried launching from a matched slow-wave helix surrounding the plasma in front of the suppressor grid. The signal transmission level increased ten-fold, but the resulting wave-dispersion (plotted as an ω-β, or Brillouin diagram in Fig. 3) showed evidence of the presence of an electron stream. The "beam" velocity, as determined by the slope of the phase curves $\Delta\omega/\Delta\beta$, depended on the helix voltage, leading to the conclusion that the electron stream was due to ion-generated secondary electrons being liberated from the helix. The secondary electron energies computed from electrode potentials are compatible with wave group velocity for all of the data. Figure 3 shows an asymmetry about $\beta = 0$. In the "downstream" sense (from plasma source toward ion trap) the normal plasma waves were found, but in the "upstream" sense two sets of waves were found, one corresponding to more-or-less normal waves, and the other corresponding to plasma oscillations and cyclotron oscillations drifting on the beam of secondary electrons. To further demonstrate the drift modes, we turned off the plasma and turned on an electron beam from the electron gun, leaving the magnetic field and wave probes as before. Only upstream propagation was found, but the beam modes were present as expected. In the plasma experiment using the helix, without the electron gun the "lower branch" line of the beam mode is seen to intersect the $\beta = 0$ axis at ≈ 3 Mc, suggesting that the plasma frequency of the beam of secondary electrons was about this value. The "upper branch" line passes through the cyclotron frequency f_b.

The effects of these beam-waves in the plasma can be eliminated by using the wire probes to launch the waves. This reduces the wave launching efficiency,

but also lowers the current of secondary electrons to a negligible level. Secondary electrons from the ion trap suppressor grid and from the probe wires are then a minor problem for wave propagation in the upstream direction only, leading to abnormal damping, and in some cases wave growth. Their current density is too low to cause oscillations however, and no effect on downstream propagation is evident.

The lower branch plasma waves qualitatively fit a dispersion relation appropriate to the density profile sketched in Fig. 2. Further discussion of the dispersion is given in the section below and in reference 6.

CYCLOTRON WAVE OBSERVATIONS

At least three (and perhaps more) distinct waves having resonances (wavenumber becoming large) or cutoffs near the electron cyclotron frequency have been catalogued. Since two or three waves are present simultaneously at certain frequencies, we have had to develop rather sophisticated techniques to analyze the interferometer recordings. When two waves having widely different wavelengths are present, the analysis is straightforward. When the wavelengths are within a factor of 2 of each other, however, several measurements at closely spaced frequencies are required to follow the dispersion of the individual waves.

Two waves lie above the cyclotron frequency. One has a high phase velocity, ($v_\phi > c$), and is a forward wave. The other is a "slow wave", having a phase that retards with frequency, i.e., a backward wave. The fast wave apparently is an electromagnetic waveguide mode, perturbed by the plasma. The slow wave apparently is the C_{01} cyclotron wave (refs. 2, 4, 13, 14) having a propagation cutoff at the upper hybrid frequency, $f_{uh} = (f_b^2 + f_p^2)^{1/2}$. It is heavily damped at wavelengths shorter than about 8 cm and we have not yet been successful in plotting out the entire dispersion curve. Partial dispersion curves are shown in Figs. 4, 5, and 6. Only the "downstream" half of the ω-β diagrams are plotted. The "upstream" half looks similar, except for possible streaming effects of secondary electrons.

Below the cyclotron frequency there appear to be several waves. The fastest of these, fairly certainly, is a plasma perturbed TE_{mn} waveguide mode, mentioned above. Its dispersion curve matches that for a TE_{11} mode in a waveguide whose cross-section is 1/10 filled with plasma. The plasma density distribution shown in Fig. 2, inside a 10 cm diameter tube, gives a reasonable fit. The dispersion for this wave is very similar to that for a whistler (refs. 4, 15).

The other "cyclotron waves" have not been identified, but are strong waves, having only moderate damping. One of them, shown in Fig. 5, having a cutoff frequency between 200 and 300 Mc, seems to be a wave pair, with a frequency-separation depending on density. If so, it should exhibit Faraday rotation. The "whistler" mentioned above would also have Faraday rotation, except that the ordinary wave component is cut off by the waveguide cutoff, leaving only the elliptically polarized extraordinary component. No evidence for polarization rotation of these waves has been found in our experiment.

The "lower branch" waves--the conventional space charge or electron acoustic waves of a warm, finite plasma column--have been extensively investigated at General Atomic and elsewhere, and reported on in the literature (refs. 2, 5, 13). We have plotted the measured dispersion curves here, since we use these waves in a diagnostic manner, to aid us in understanding the cyclotron wave characteristics, and to determine the plasma density.

Figures 4, 5, and 6 show effects of various plasma densities and cyclotron frequencies on the cyclotron family of waves. The resonances and cutoffs of the waves move in the expected manner as the plasma and cyclotron frequencies are adjusted.

The above results were obtained using pure H_2 gas in the duoplasmatron. The waves were also investigated using a mixture of hydrogen and helium in the source. The pressure and mixture were adjusted empirically to obtain the same wavelength at some particular frequency as observed using pure hydrogen as a source gas. When this was done the damping length at that frequency did not change appreciably, but the signal-to-noise ratio was much improved, allowing waves to be observed at shorter wavelengths than before. The fluctuations in D.C. probe current were decreased by a large factor. The reduction in phase scrambling with the He-H_2 mixture permitted wavelengths as short as 6 cm to be observed just above the cyclotron frequency.

With the H_2-He mixture the adjustment of the duoplasmatron anode bias voltage is less critical than with pure H_2, to achieve the stable column condition in the previous section. In the unstable condition, the cyclotron waves have a small amplitude modulation imposed, but the time-averaged data looks similar to that obtained when the column was stable. This is not true with the "lower branch" spacecharge waves, whose short-wavelength characteristics are very much altered in some cases when the rotational instability is present.

APPENDIX V

REFERENCES

1. Stix, T. H.: The Theory of Plasma Waves. McGraw Hill Book Co., Inc., New York, 1962.

2. Allis, W. P.; Buchsbaum, S. J.; and Bers, A.: Waves in Anisotropic Plasmas. M.I.T. Pres , Cambridge, Massachusetts, 1963.

3. Ratcliffe, J. A.: The Magneto-Ionic Theory and Its Application to the Ionosphere. University Press, Cambridge, England, 1959.

4. Heald, M. A.; and Wharton, C. B.: Plasma Diagnostics with Microwaves. John Wiley and Sons, New York, 1965.

5. Malmberg, J. H.; and Wharton, C. B.: Collisionless Damping of Electrostatic Plasma Waves. Phys. Rev. Lett. vol. 13, no. 6, Aug. 1964, pp. 184-186.

6. Malmberg, J. H.; and Wharton, C. B.: Landau Damping of Electron Plasma Waves. Proceedings of Second Conference on Plasma Physics and Controlled Nuclear Fusion Research (Culham, England) September 6-10, 1965.

7. Rosenbluth, M. N., ed.: Topics of Microinstabilities. Advanced Plasma Theory. Academic Press, New York, 1964, pp. 137-158.

8. Harris, E. G.: The Two-Stream Instability in a Cold Inhomogeneous Plasma in a Strong Magnetic Field. Phys. Fluids vol. 7, no. 10, Oct. 1964, pp. 1572-1577.

9. Hall, L. S.; and Heckrotte, W.: Electrostatic Instabilities of a Plasma with Magnetically Supported Velocity-Space Anisotropy. Proceedings of Seventh International Conference on Phenomena in Ionized Gases (Beograd, Yugoslavia) August 22-September 1, 1965.

10. Drummond, W. E.; and Pines, D.: Non-Linear Stability of Plasma Oscillations. Proceedings of the Conference on Plasma Physics and Controlled Nuclear Fusion Research (Salzburg, Austria) September 4-9, 1961, Nuclear Fusion, Part 3, 1962 Supplement, pp. 1049-1057, conference paper CN-10/134.

11. Vedenov, A. A.; Velikhov, E. P.; and Sagdeev, R. Z.: A Quasi-Linear Theory of Plasma Oscillations. Proceedings of the Conference on Plasma Physics and Controlled Nuclear Fusion Research (Salzburg, Austria) September 4-9, 1961, Nuclear Fusion, vol. 1, no. 2, Mar. 1961, pp. 82-100.

12. Malmberg, J. H., et al: A Collisionless Plasma for Wave Propagation Studies. Proceedings of VI Conference Internationale Sur Les Phenomenes D'Ionisation Dans Les Gaz (Paris, France) July 8-13, 1963. P. Hubert, ed., S.E.R.M.A., Paris, France, 1964.

13. Trivelpiece, A. W.; and Gould, R. W.: Space Charge Waves in Cylindrical Plasma Columns. J. Appl. Phys., vol. 30, no. 11, Nov. 1959, pp. 1784-1793.

14. Bevc, V.; and Everhart, T. E.: Fast-Wave Propagation in Plasma-Filled Waveguides. J. Electronics and Control (GB), vol. 13, no. 3, Sept. 1962, pp. 185-212.

15. Budden, K. G.: Radio Waves in the Ionosphere. University Press, Cambridge, Massachusetts, 1961.

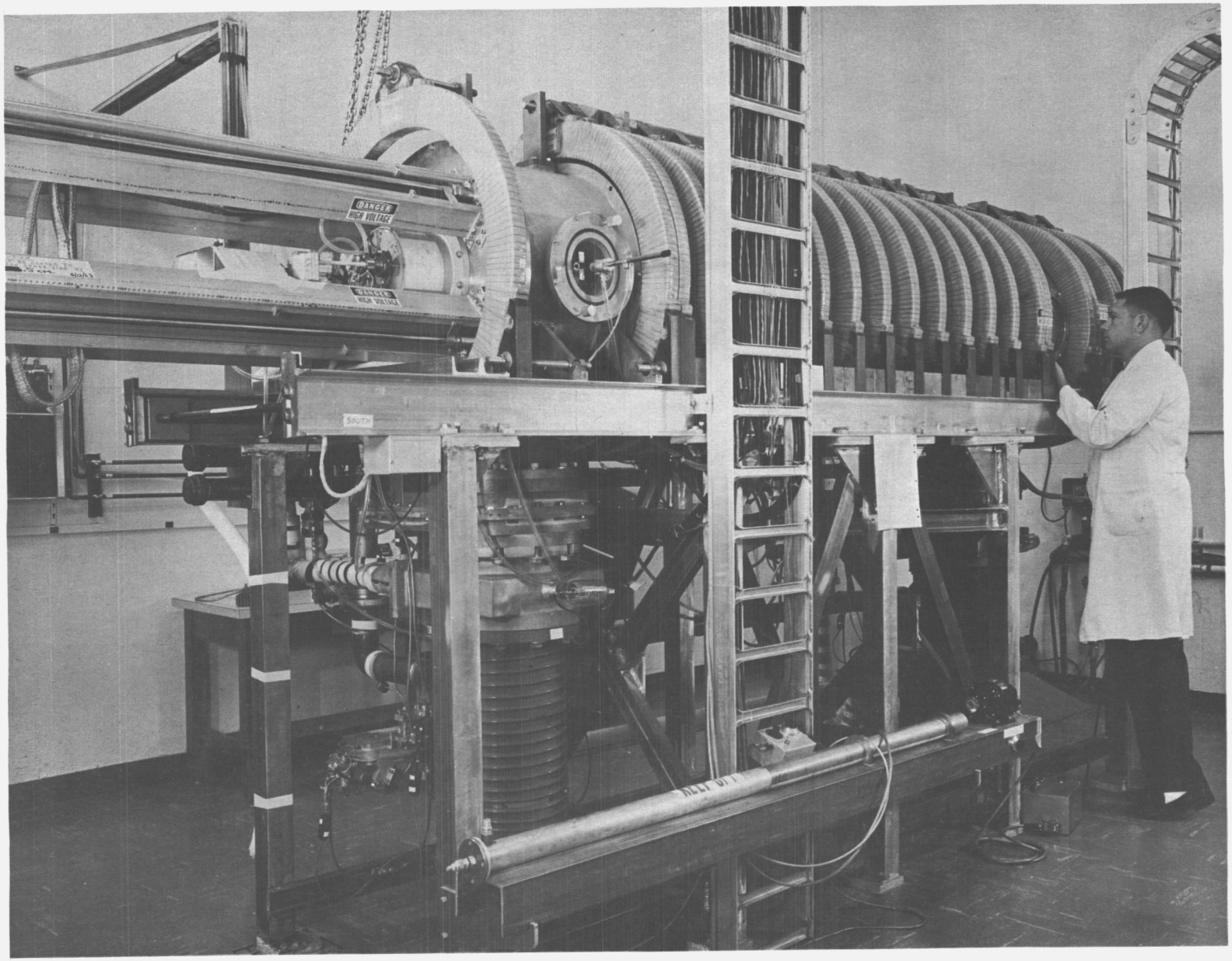

Fig. 1--Photograph of the apparatus used for studies of waves in the steady-state, collisionless plasma. The solenoidal field is uniform to ± 1% along the length. At far left are carriages for four movable probes. The plasma source is mounted on the left end of the vacuum chamber and the electron gun on the right end. (Not visible.)

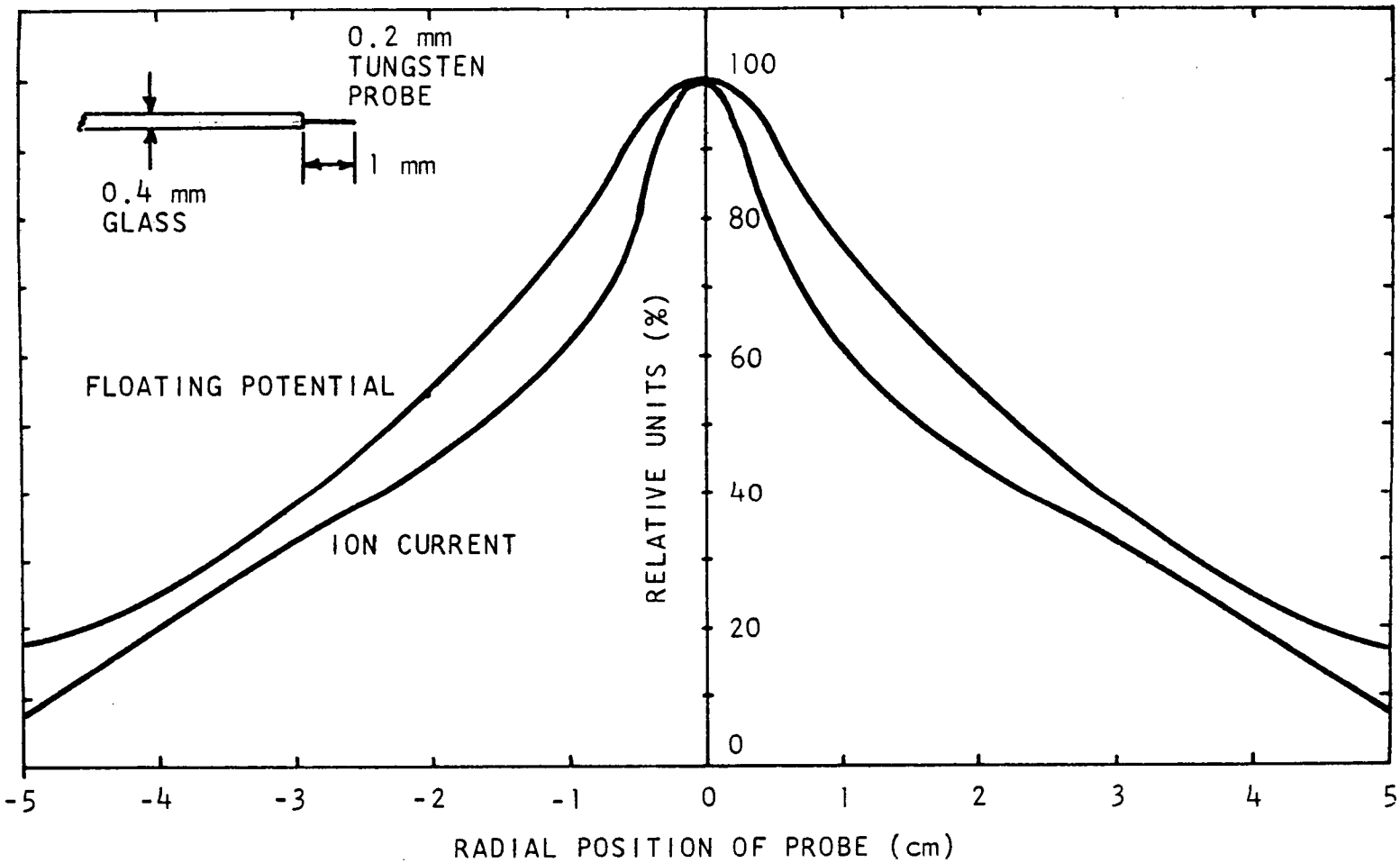

Fig. 2--Profile measurements of floating potential and saturation ion current, obtained by a small Langmuir probe. 100% refers to +16 volts and + 6 μamperes, respectively for these curves.

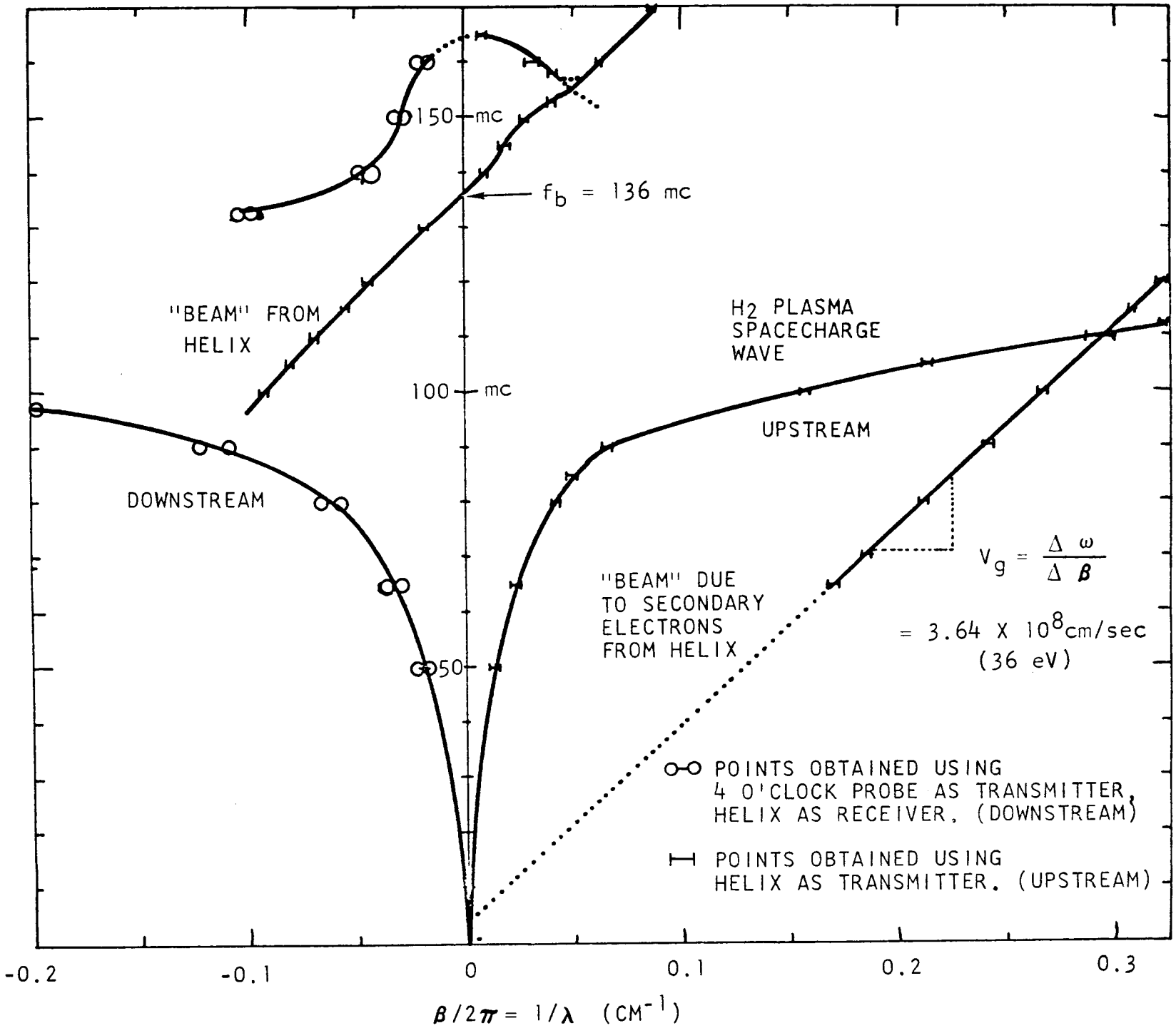

Fig. 3--Brillouin (ω-β) diagram for waves in the collisionless H_2 plasma, over the frequency range 0-170 Mc. The waves launched by a helix (upstream) show evidence of an electron stream, due

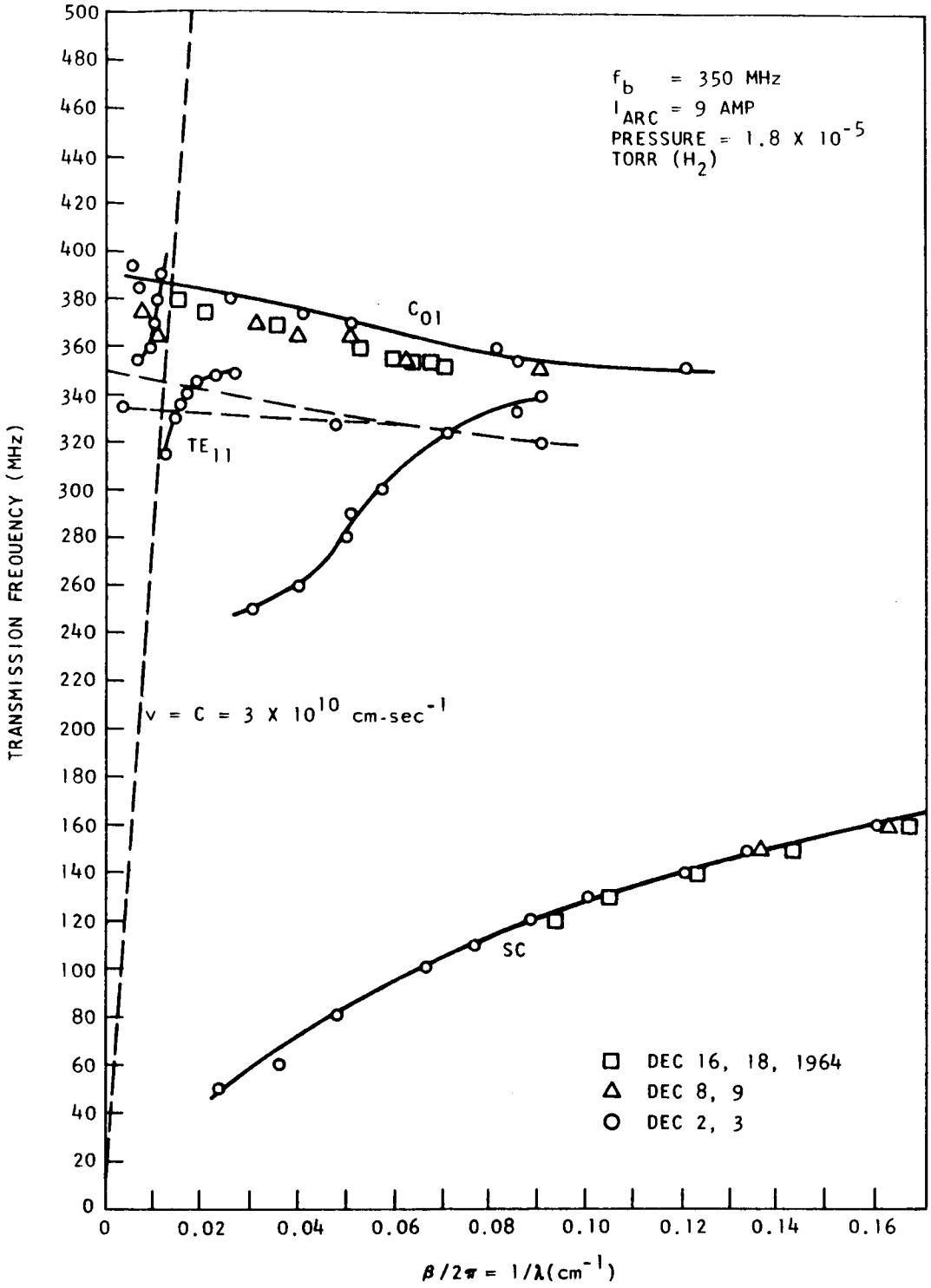

Fig. 4--ω-β diagrams for waves in the collisionless H_2 plasma, over the frequency range 0-500 MHz. Cyclotron frequency f_b was 350 MHz, and plasma density n_e was approximately 4.2×10^8 cm^{-3}

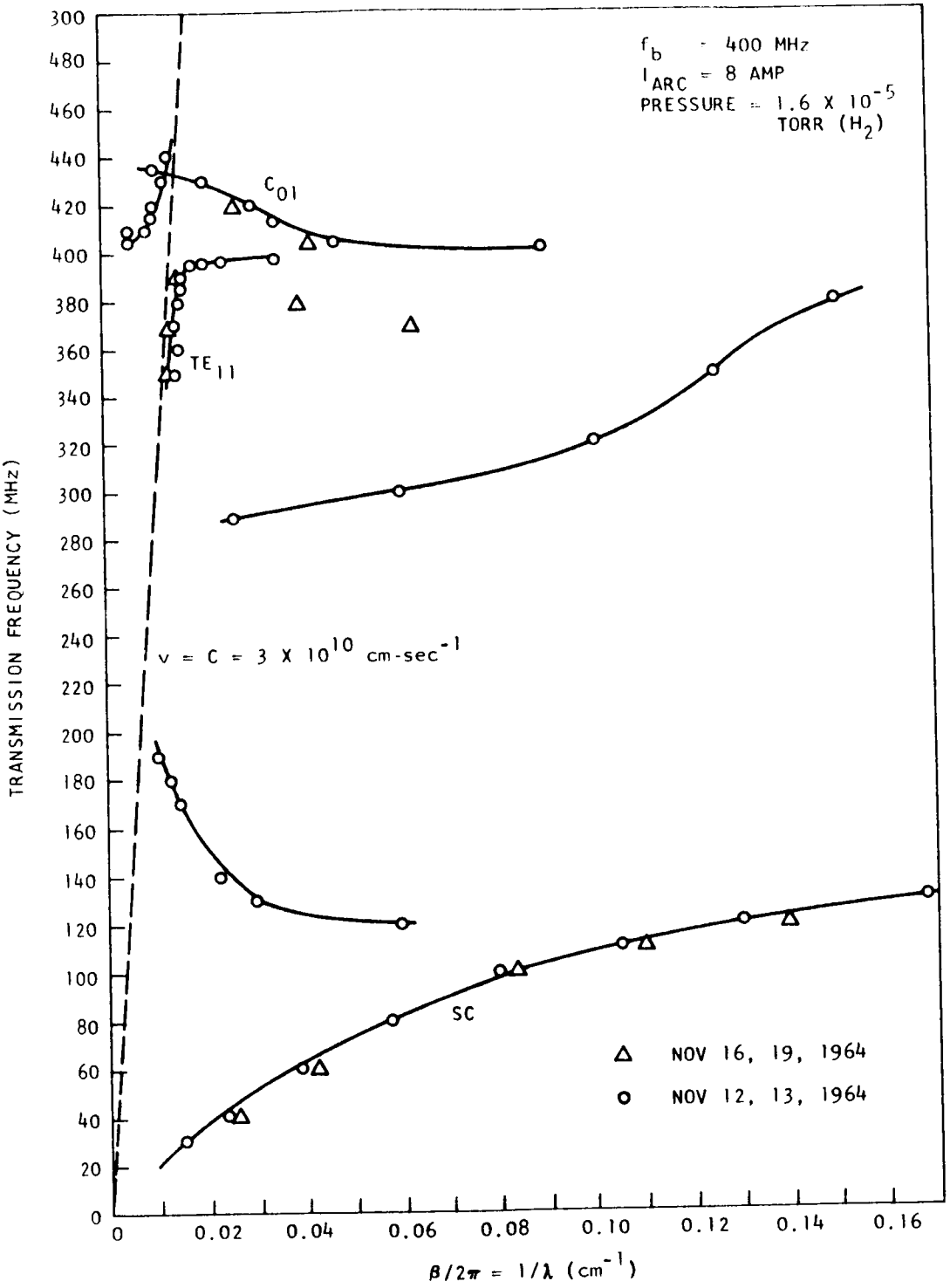

Fig. 5--ω-β diagrams as in Fig. 4, but f_b = 400 MHz, $n_e \approx 3.9 \times 10^8$ cm^{-3}

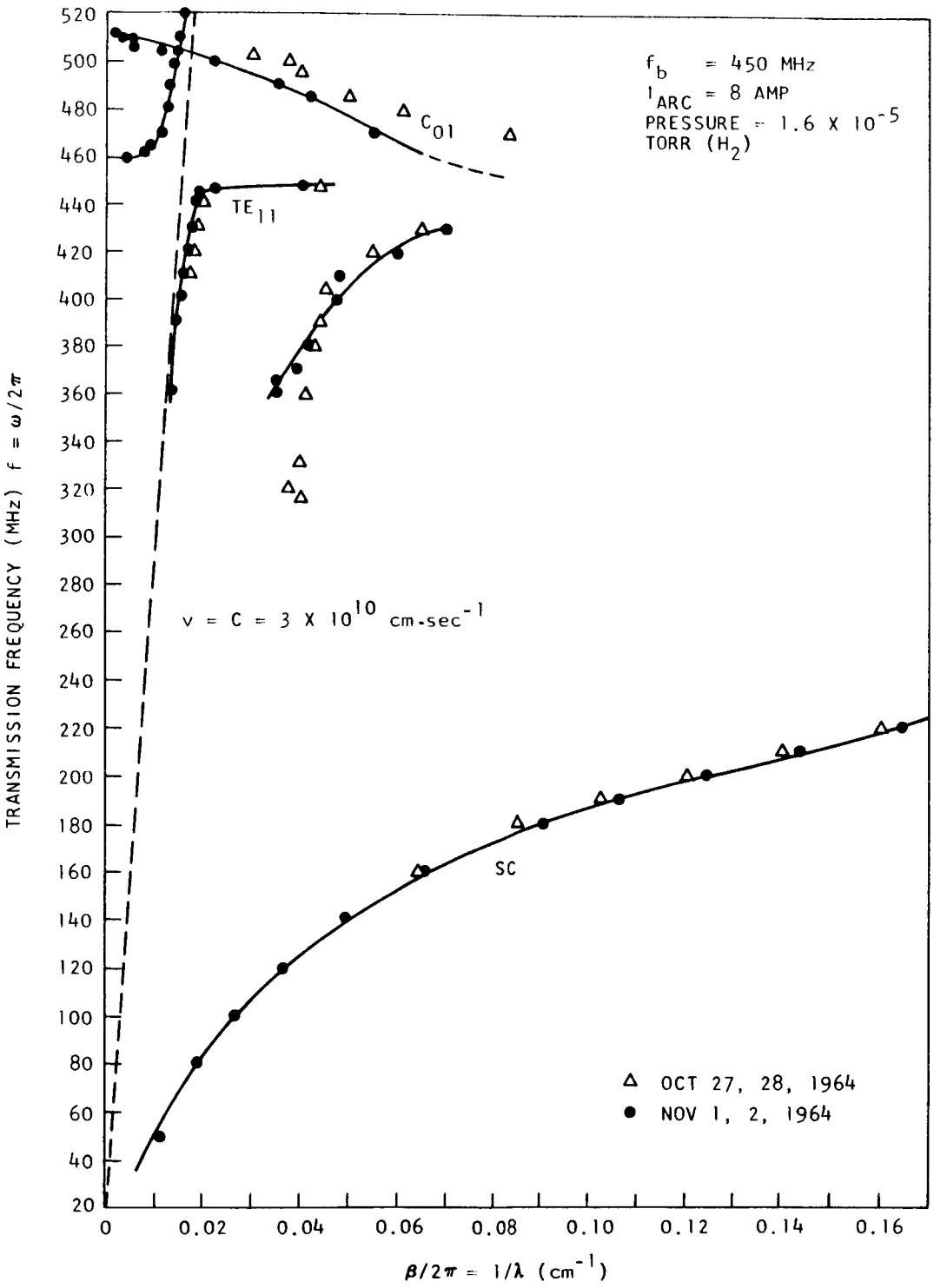

Fig. 6--ω-β diagrams as in Fig. 4, but f_b = 450 MHz, $n_e \approx 7.1 \times 10^8$ cm^{-3}

APPENDIX VI

CYCLOTRON WAVES IN A COLLISIONLESS PLASMA

by

C. B. Wharton and J. H. Malmberg

ABSTRACT

Presented at the Division of Plasma Physics
American Physical Society Meeting
New York, November 4, 1964

Published in
Bulletin of American Physical Society
Volume 10, 199 (1965)

PRECEDING PAGE BLANK NOT FILMED.

Cyclotron Waves in a Collisionless Plasma

C. B. Wharton and J. H. Malmberg

ABSTRACT

The propagation characteristics of spacecharge waves in a long collisionless plasma column[1] have been studied over the frequency range 90 to 520 Mc. The collisionless damping of these waves has previously been reported.[2] Recently the growth of the wave amplitudes in space, due to an injected electron beam having a velocity spread,[3] has been investigated.

In this paper we report the appearance of a wave at frequencies slightly above the cyclotron frequency ω_b. The wave appears to be longitudinal, with velocities ranging from 3×10^8 to 10^{10} cm/sec over the frequency range. There is also a wave at frequencies slightly below ω_b that seems to be directed by the plasma column and which may be a whistler.

---

[1]Malmberg, J. H., et al., Proceedings VI International Conference on Ionization Phenomena in Gases, Paris 1963, Vol. 4, 229 (1963).

[2]Malmberg, J. H. and C. B. Wharton, Phys. Rev. Letters 13, 184 (1964).

[3]Drummond, W. E., Phys. Fluids 7, 816 (1964), also Phys. Fluids 7, 816 (1964).

PRECEDING PAGE BLANK NOT FILMED.

APPENDIX VII

COMPARISON OF THE ELECTRON CYCLOTRON WAVE DISPERSION FOR VARIOUS BOUNDARY CONDITIONS

by

J. H. Malmberg

November 20, 1967

PRECEDING PAGE BLANK NOT FILMED.

Comparison of the Electron Cyclotron Wave Dispersion for Various Boundary Conditions

J. H. Malmberg†

Gulf General Atomic, Incorporated
P. O. Box 608
San Diego, California 92112

I. INTRODUCTION

A column of plasma immersed in a longitudinal magnetic field and surrounded by a conductor supports many electrostatic wave modes. In previous work we have investigated the dispersion and damping of the "lower branch" waves near the electron plasma frequency.[1-4] The properties of these waves are very insensitive to the details of the radial boundary condition. We have also previously made a detailed set of measurements on the waves near the electron cyclotron frequency.[5] It turns out that the observed properties of these waves are very sensitive to small changes in the radial boundary conditions. The dispersion and damping of the waves and their interaction with an electron beam are discussed.

†Also at the University of California, San Diego, La Jolla, California.

PRECEDING PAGE BLANK NOT FILMED.

II. EXPERIMENTAL PROCEDURE

The wave measurements are made in the following manner: Two radial probes are placed in the plasma column. One probe is connected by coaxial cable to a chopped signal generator. The other probe is connected to a receiver which includes a sharp, high-frequency filter, a string of broad-band amplifiers, an r-f detector, a video amplifier, and a coherent detector operated at the transmitter chopping frequency. Provision is made to add a reference signal from the transmitter to the receiver r-f signal; i.e., we may use the system as an interferometer. The transmitter is set at a series of fixed frequencies, and at each, the receiving probe is moved longitudinally. The position of the receiving probe, which is transduced, is applied to the x-axis of an x-y recorder, and the interferometer output or the logarithm of the received power is applied to the y-axis.

Typical raw data for the lower branch wave are shown in Fig. 1. The slope of the power curve is the rate of power damping of the wave. The distance between peaks on the interferometer curve is the wavelength. From the measured wavelengths and the transmitter frequencies we obtain the dispersion relation of the waves. For comparison with theory, we compute the dispersion relation for the wave numerically using the measured radial density distribution, the plasma temperature measured by the velocity analyzer, and the experimental value of the magnetic field. We choose an absolute density which normalizes the theory to the experimental dispersion

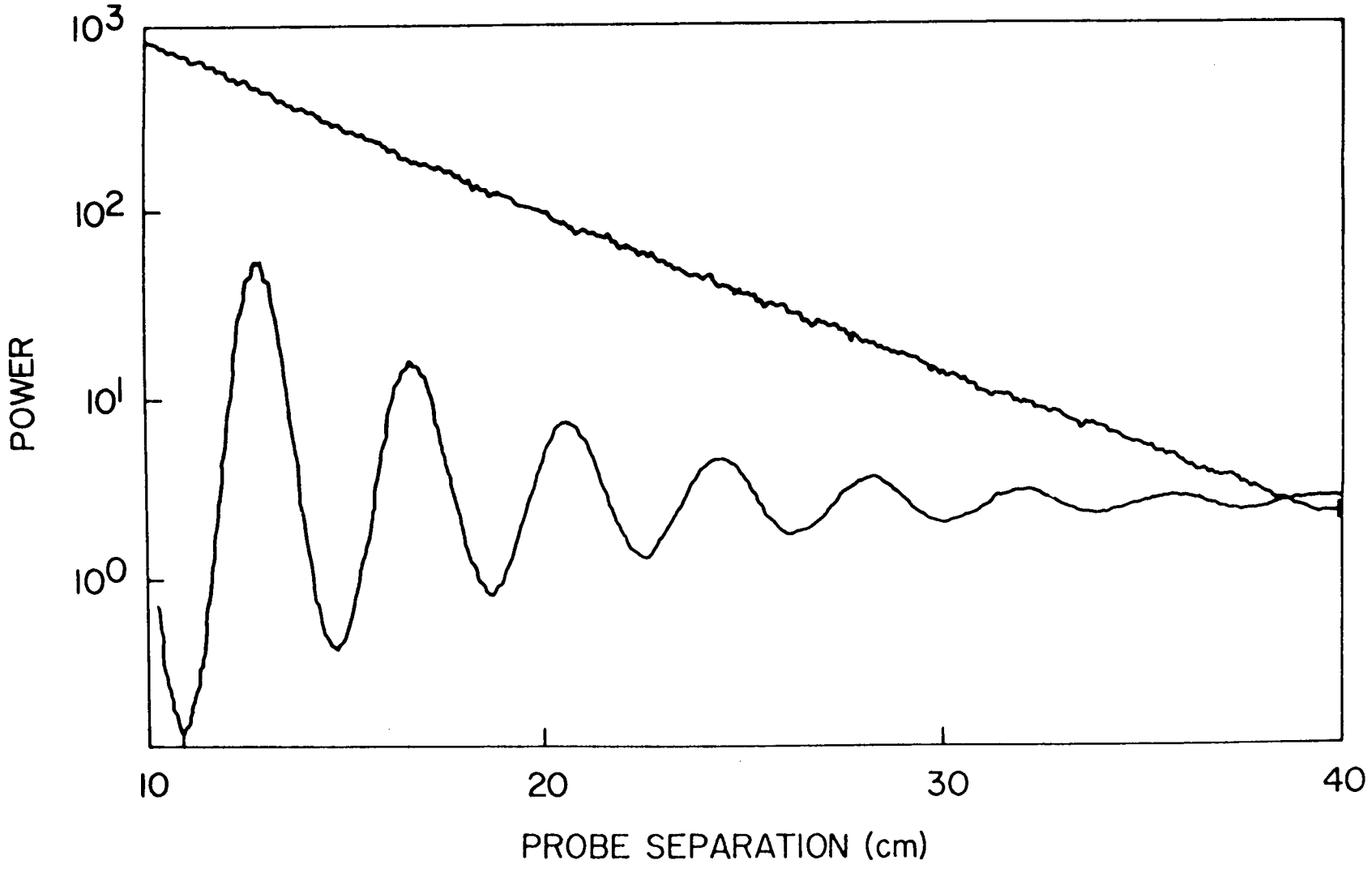

Fig. 1--Interferometer and logarithmic receiver responses as receiver probe is moved away from transmitter probe along machine axis

data at low frequencies (high phase velocities). The observed dispersion agrees to high precision with the theory.[3]

The Landau damping of these waves has been reported in detail in a previous paper.[2] We there showed that they exhibit heavy exponential damping under conditions where collisional damping is negligible, that the damping is caused by electrons traveling at the phase velocity of the wave, and that the magnitude of the damping, its dependence on phase velocity, and its dependence on plasma temperature, are accurately predicted by the theory of Landau.

There are a double infinity of solutions for the lower branch corresponding to various radial and angular eigenmodes. However, all higher modes at a given frequency are very heavily damped compared with the lowest mode, i.e., the one having angular symmetry and the simplest radial dependence. Hence, when we apply a given frequency to the transmitting antenna, only the lowest mode is observable a short distance away, and only its properties are measured.

We have described the experimental work on the lower branch waves because it demonstrates the power of the second order theory for explaining the dispersion and damping of the waves. The situation is substantially more complicated for the upper branch case. This is not because of additional terms in the equation, but because the eigenvalue equation at some radius is almost singular for the upper branch waves.

III. UPPER BRANCH DATA

In Fig. 2, a typical result for waves near the electron cyclotron frequency, for one set of plasma parameters, is reproduced from a previous paper.[5] The measurement of dispersion and especially of damping in that experiment was greatly complicated by the fact that more than one wave appeared at a given frequency. Thus we observed, when the transmitter was set at a given frequency, not an almost sinusoidal wave as in Fig. 1, but an interference pattern that had to be unscrambled. Also, the identity of all the waves near the cyclotron frequency was not firmly established. We have now established that the wave with one branch below and one above the cyclotron frequency, with phase velocity asymptotic to the velocity of light at low and high frequencies, is a plasma-perturbed electromagnetic mode, similar to a whistler. The tube surrounding the plasma is a waveguide beyond cutoff for these frequencies except slightly below the cyclotron frequency, where the refractive index becomes large. However, the tube is slotted to permit movement of the probe, and thus the waves are coupled through the slot into the 2 ft diam main chamber of the machine, which is not cut off. This is not the wave in which we are most interested, so to remove this interference we completely closed the slot associated with one of the probes and installed a large amount of damping material in the chamber proper. This seems to effectively remove this high-phase-velocity wave. The wave labelled TE_{11} in Fig. 2 is the whistler, which is still observed, as shown in Fig. 3. The other wave between the cyclotron frequency and the plasma frequency in

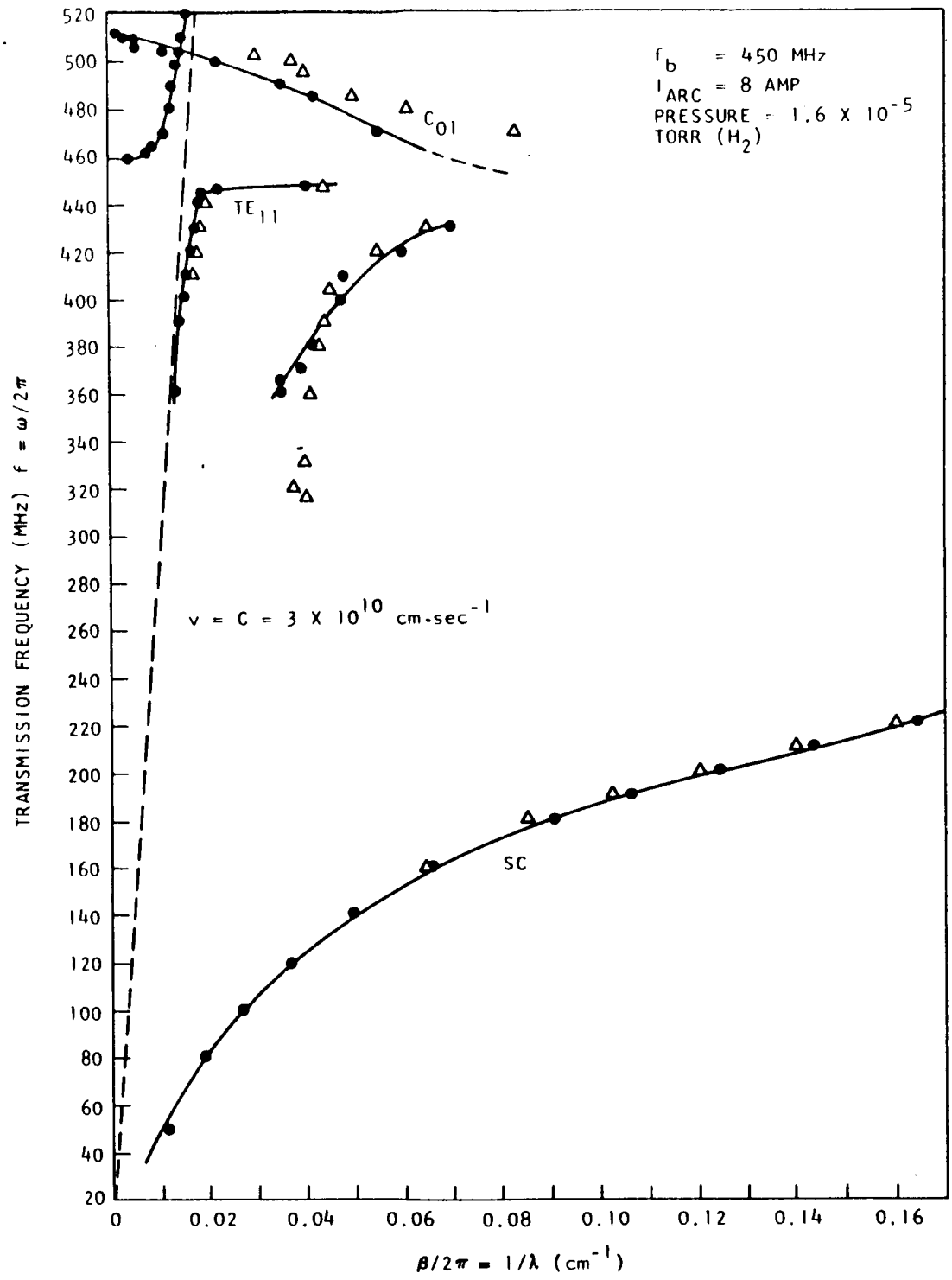

Fig. 2--Dispersion (ω-β) curves for plasma column in slotted metal shield. Cyclotron frequency f_b = 450 MH_z, ne ≈ 7.1 X $10^8/cm^3$

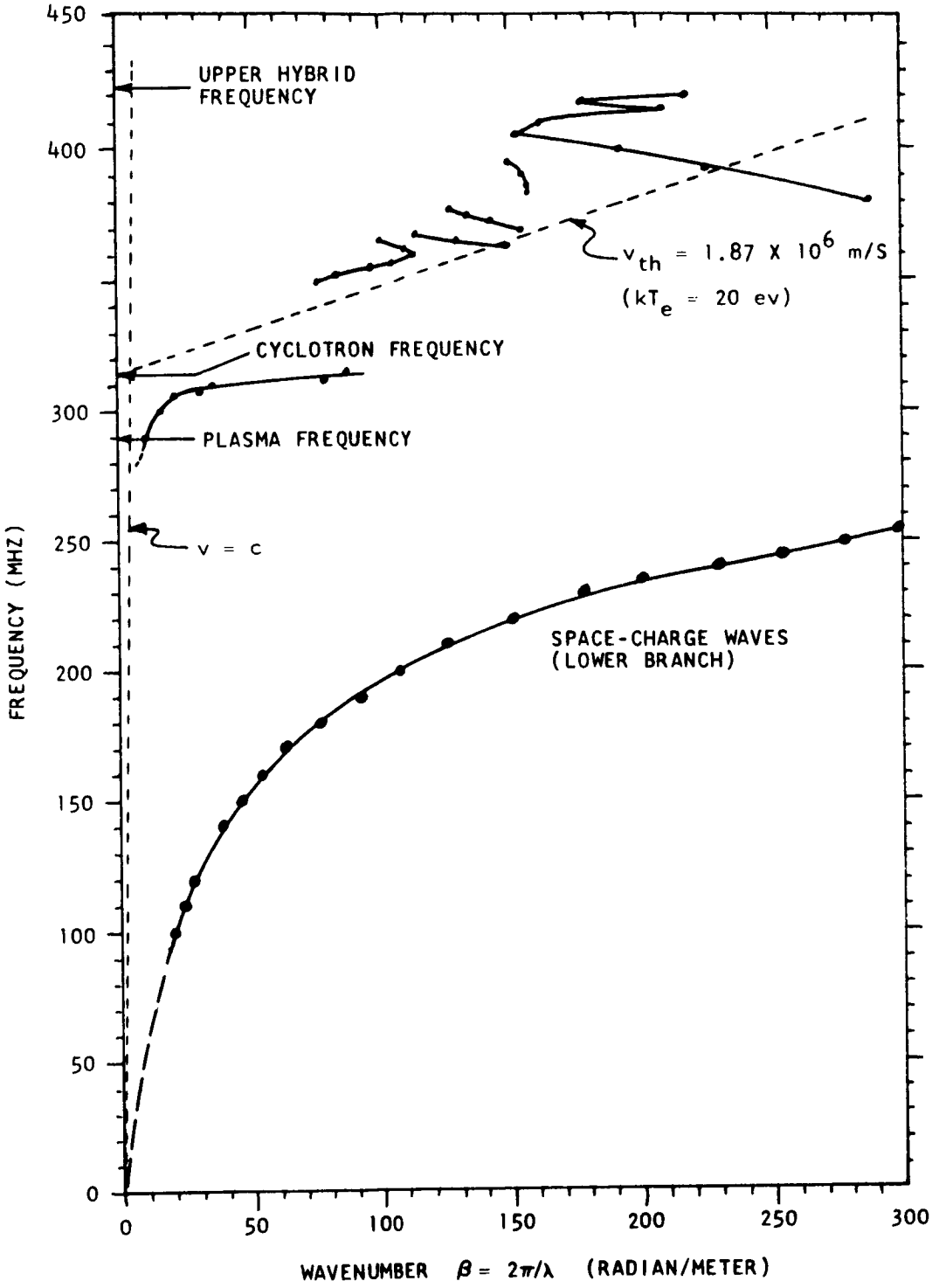

Fig. 3--Dispersion (ω-β) curves for plasma column injected through cusp into cylindrical metal shield having one slot closed and the other slot partially closed with damping material to decrease electromagnetic effects

Fig. 2 seems to be associated with a resonance of the remaining slot, loaded by the plasma. The wave appears when the length of the slot from its end to where it is shorted by the probe carriage is m half wavelengths for the wave. To reduce this effect, we have covered part of the slot with an absorbing material which tends to damp out the slot resonance.

The changes in the machine geometry also modified the upper branch cyclotron wave dispersion. These modifications changed the effective boundary condition for the waves, and they appear to make the upper branch cyclotron wave much more heavily damped. This may be associated with the fact that the singularity makes it difficult for the wave to find the eigenmode of the system which matches the boundary condition at the wall and still behaves properly at the singularity. The measured dispersion now shows evidence of a great many modes. Large, and often discontinuous, changes in wavelength result from small changes in frequency or density. The wave transmission thus is much more sensitive to noisy density fluctuations than are the lower branch waves. Severe phase scrambling (phase fluctuations of $> \pi/2$) make interferometer measurements of the wavelength difficult. In some portions of the frequency spectrum, the frequency of the transmitted wave becomes broadened or shifted by as much as 20%, presumably due to sidebands introduced by the large phase and amplitude modulations. The measured damping seems to be associated with both a scattering of energy from the initial frequency band into sidebands and spatial collisionless damping.

A second difficulty in analyzing the data of Fig. 2 is that the density of the plasma was not uniform in the z-direction. This is much more serious for the upper branch waves than for the lower branch because the observable wavelengths are much longer and hence span a greater variation in plasma density. The experiments on cusp injection[6] were motivated by a desire

to reduce the density gradient and in a large measure were successful. The second series of measurements on the upper branch (Figs. 3, 4) used the flattened density distribution obtained with the cusp configuration. With the improved density profile, we have made damping measurements on the cyclotron waves. The observed damping is given in Fig. 4. We have also observed the growth of these waves induced by a beam. When an electron beam of a few microamperes and 1 to 3 kV energy is injected into the plasma, a strong noise spectrum is observed at about 450 Mc even when the transmitter is off. This is close to the upper hybrid frequency for the parameters used and is presumably due to waves at the intersection of the dispersion curve of the beam and the dispersion curve for the cyclotron wave growing up from low level noise in the plasma. The frequency at which the waves grow is a weak function of beam velocity as expected.

Using somewhat lower beam energies,we observed growing waves from signals injected at discreet frequencies by the transmitting probe. These waves were seen to grow exponentially in space over several e-folds in the upstream direction, somewhat in the way that waves grow in the lower branch. In the downstream direction the growth is not exponential, but seems to demonstrate a start-oscillation condition as a certain beam current density is exceeded, much in the manner of a backward-wave oscillator, except that the oscillation ceases when the driving wave is removed. Because the wavelengths are long, the standing waves and feedback effects have made dispersion measurements very difficult. However, the few unambiguous results show the same trends as in the absence of the beam, namely that the interaction seems to be with a variety of modes rather than with a single one. The presence of a 50 μA beam may increase the wave amplitude by as much as 20 to 30 dB.

The growing noise at 450 Mc may provide a convenient measurement of the hybrid frequency and thus the plasma density. Since the plasma density is a function of radius, and since the beam is much smaller than the plasma, the waves may be well localized and thus measure the local density of the plasma.

After studying the data, of which Figs. 2, 3, and 4 are a sample, we decided to close the probe slots completely. Two thin beryllium-copper springs were affixed to the tube surrounding the plasma near each slot for the full length of the machine. In their normal positions they touch, closing the slot electrically. As the probe advances the spring is pushed out of the way but closes again behind it. The dispersion measurements were then repeated. The result for a series of arc currents is shown in Fig. 5. For the settings of the duoplasmatron used in this case, the major effect of increasing arc current is to increase the plasma density approximately proportionally. The lower branch dispersion curves are completely normal, as is their variation with plasma density. However, the waves around the cyclotron frequency (350 MHz) have completely changed character. In the region 350 MHz to 380 MHz some of the previously observed waves may still be present, but the interferometer data are now so confused in this region that reliable values of wavelength may no longer be extracted from the curves. Above 390 MHz a new wave has appeared. The quality of the interferometer data for this wave is excellent - just as good as that exhibited in Fig. 1 for the lower branch waves. The dispersion looks a bit like cyclotron waves on a drifting beam, especially for the highest currents, and we have seen this kind of dispersion when a low velocity electron beam is injected into the plasma. However, this explanation of the data is not correct: In the beam experiments the dispersion is always a perfectly

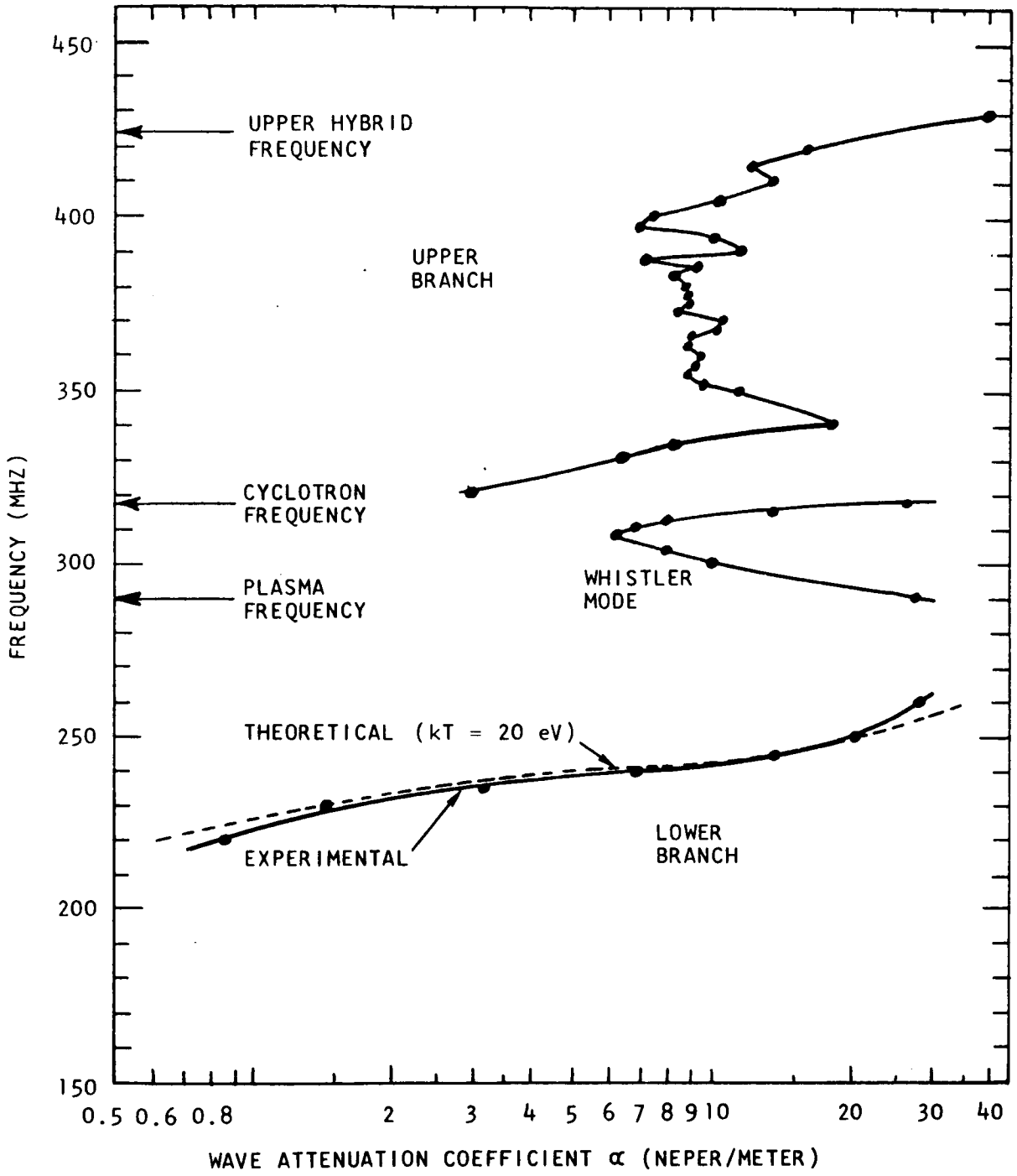

Fig. 4--Spatial attenuation (damping) of waves (ω-α curves) for same conditions as Fig. 3

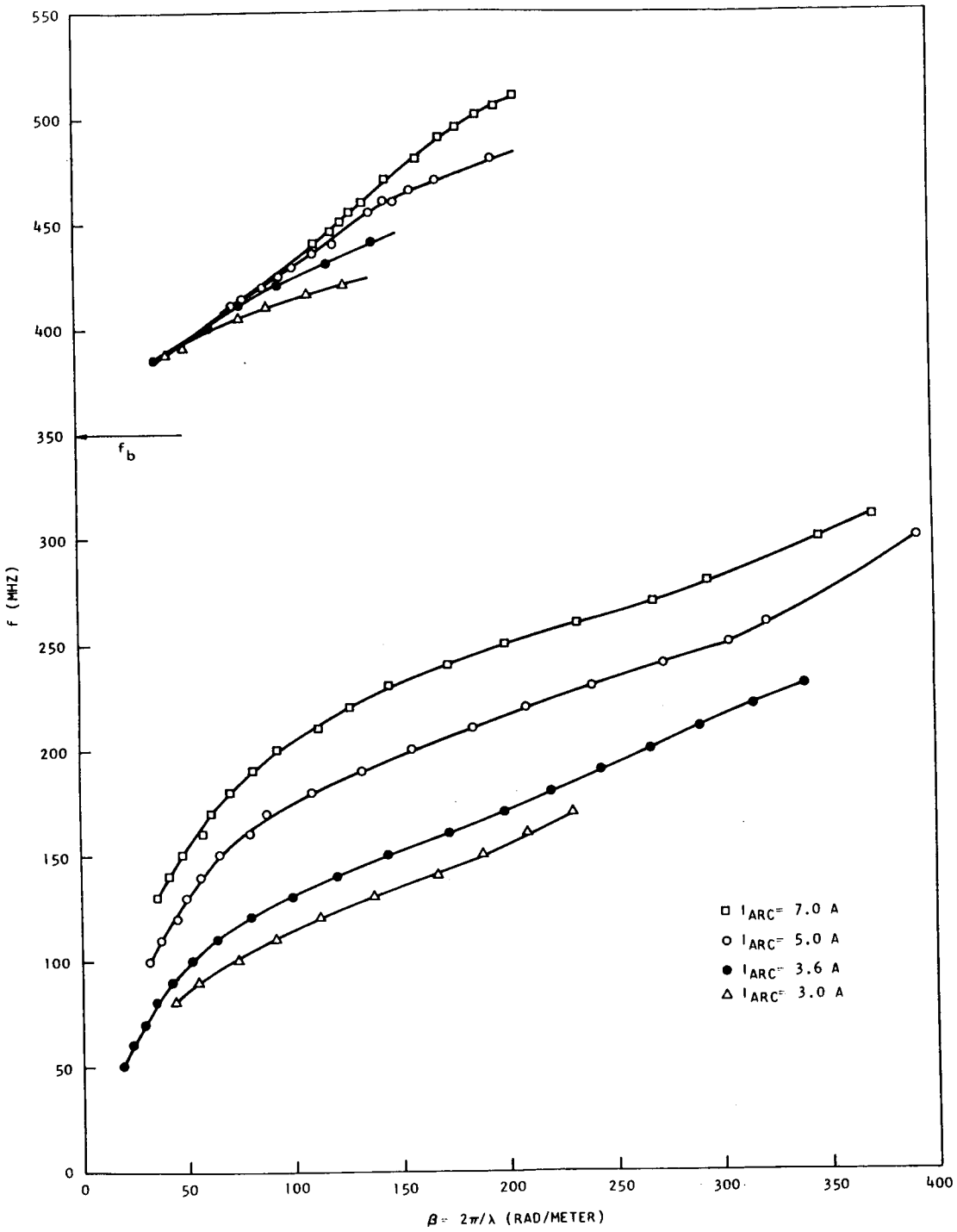

Fig. 5--Dispersion (ω-β) curves for plasma colunn injected through cusp into cylindrical metal shield having both probe slots closed

straight line which extrapolates to the cyclotron frequency at $k = 0$. The dispersion curves for these data are not straight lines and the upper parts of the curves do not extrapolate to the cyclotron frequency. In addition, we would not expect the geometric changes made to result in a low velocity beam in the plasma.

The interaction between this wave and a 1500 V, ~ 0.2 ma electron beam injected into the plasma has been measured. The dispersion of the combined beam-plasma system is shown in Fig. 6. Wave growth is also observed under these circumstances. The dispersion for the beam-plasma system is in quantitative agreement with the theory of Pearlstein and Bhadra.[7] The precision of their WKBJ analysis is not sufficiently good for the lowest radial mode to allow a detailed quanitative comparison. The qualitative comparison is discussed in their paper.

The second order theory predicts that the upper branch eventually becomes a forward wave even in a uniform density system when the thermal corrections get large enough. However, extensive numerical calculations using our actual density profile failed to find any set of parameters for which such a wave existed without being much more heavily damped than the experimentally observed result. The best explanation of the data appears to be the fourth order theory of Pearlstein and Bhadra. This would imply that the dispersion of the forward wave is dominated by the "almost singular" behavior at the radius for which the wave frequency equals the local hybrid frequency.

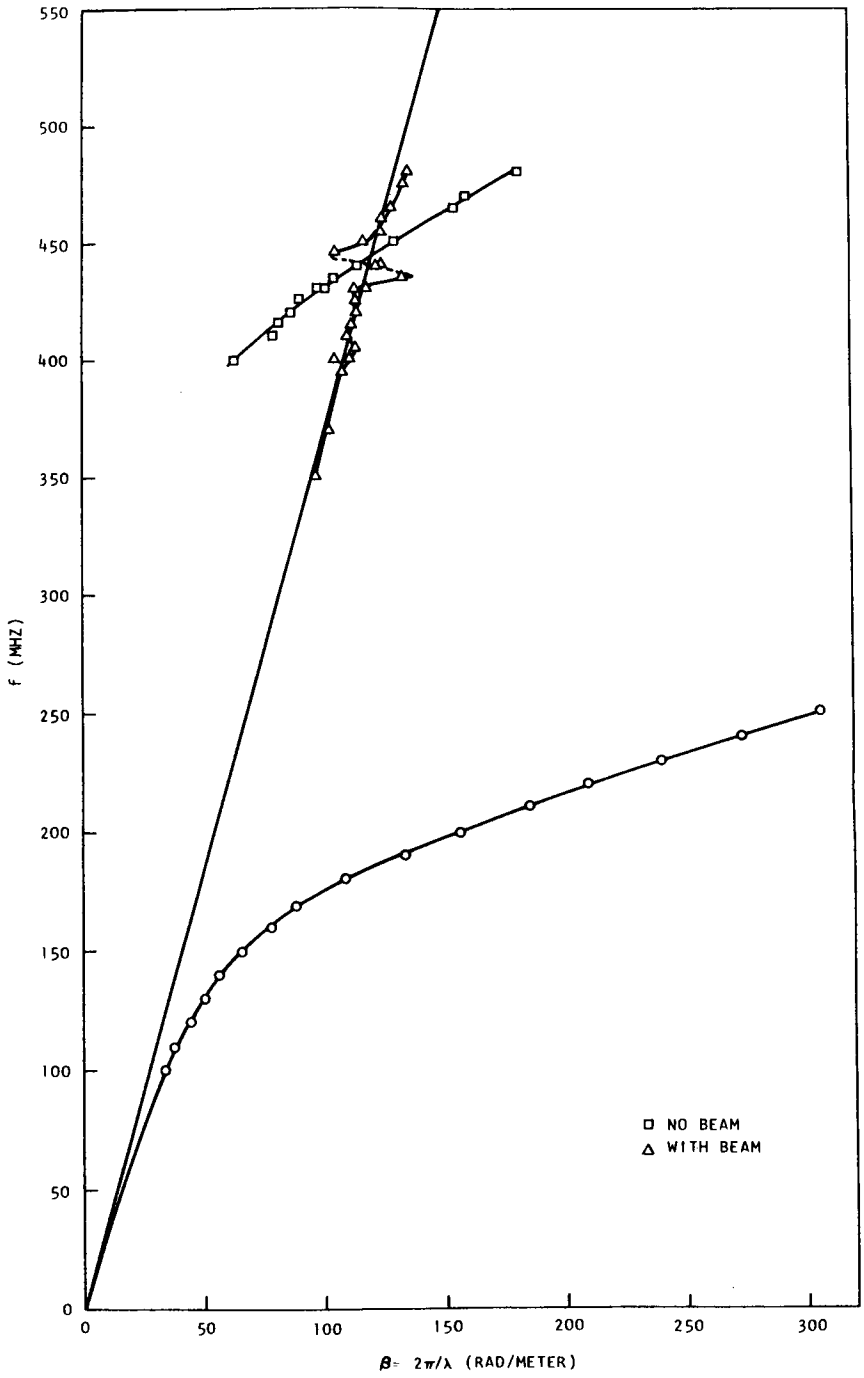

Fig. 6--Dispersion (ω-β) curves for plasma column injected through cusp into cylindrical metal shield having both probe slots closed. The triangles give the observed dispersion when a 1500 V, approximately 0.2 mA electron beam is injected into the plasma

APPENDIX VII

REFERENCES

1. J. H. Malmberg and C. B. Wharton, Phys. Rev. Letters 13, 184 (1964).
2. J. H. Malmberg and C. B. Wharton, Plasma Physics and Controlled Nuclear Fusion Research 1, 485 (1966).
3. J. H. Malmberg and C. B. Wharton, Phys. Rev. Letters 17, 175 (1966).
4. J. H. Malmberg and C. B. Wharton, Phys. Rev. Letters 19, 775 (1967).
5. C. B. Wharton and J. H. Malmberg, Proceedings VIIth International Conference on Phenomena in Ionized Gases, Beograd, Yugoslavia 1965, Vol. II, 256 (1966). (See Appendix V.)
6. J. H. Malmberg, "Rotation, Diffusion, and Noise of a Column of Plasma," (See Appendix I.)
7. L. D. Pearlstein and D. Bhadra, "The Dispersion of the Upper Hybrid Mode in a Spatially Inhomogeneous Plasma," General Dynamics, General Atomic Report No. GA-8347 (See Appendix IV.)

APPENDIX VIII

CURVE RESOLVER FOR MIXTURES OF DAMPED SINE WAVES

by

C. D. Moore and J. H. Malmberg

November 17, 1967

PRECEDING PAGE BLANK NOT FILMED.

Curve Resolver for Mixtures of Damped Sine Waves†

C. D. Moore and J. H. Malmberg‡

Gulf General Atomic, Incorporated
P. O. Box 608
San Diego, California 92112

A system for analyzing waveforms consisting of mixtures of exponentially damped sine waves is described. The instrument generates a series of damped sine waves of variable amplitude, frequency, damping decrement, and phase. These waveforms are added and displayed on an oscilloscope. Their parameters can then be adjusted to obtain a waveform which matches the curve to be analyzed. The component waveforms are then analyzed one at a time. The instrument has been used to analyze interferometer curves arising in the course of plasma wave experiments.

---

†This work was sponsored by the National Aeronautics and Space Administration under Contract NAS7-275.

‡Also at the University of California, San Diego, La Jolla, California.

PRECEDING PAGE BLANK NOT FILMED.

I

INTRODUCTION

In many experiments, the data are obtained in the form of a curve which is the sum of two or more simpler functions. The curve must be reduced to its component parts to be interpreted. In the particular case which led to the development of the present instrument, the composite curve is a sum of two or more exponentially damped sine waves with independent amplitudes, frequencies, damping rates, and phase. Such curves are generated in the application of radio-frequency interferometer techniques to the measurements of plasma wave propagation[1] when two or more modes at the same frequency, but with different wavelengths, are present in the plasma. The interferometer circuitry converts the signals to a curve $I(z)$ vs z, where z is the position in the plasma and $I(z)$ is of the form

$$I(z) = \sum_i A_i \exp(-\alpha_i z)\sin(k_i z+\varphi_i) \quad . \tag{1}$$

The problem is to extract the amplitudes, A_i, damping constants, α_i, wave numbers, k_i, and phases, φ_i, from the composite curve.

The most obvious method of extracting the parameters from the data is to digitize $I(z)$ vs z and do least squares calculation on a computer, but this method has disadvantages. The equipment for digitizing a waveform normally available only graphically and the necessity for writing a moderately complicated code do not present severe problems. However, with the

usual arrangements, some hours elapse between submission of the problem and return of the computer answer, so the results are not immediately available during the course of the experiment. In addition,the curve fitting is strictly mathematical: the experimenter cannot easily apply his judgment to the curve fitting in order to allow for non-ideal characteristics of the system under test. Graphical analysis of the curves is practical in simple cases, but is not sufficiently precise for the present experiment and is very involved in complicated cases. Another system is to store the data waveform on a rotating loop of magnetic tape and analyze the frequency spectrum of the output. This method lacks accuracy and is further complicated by the generation of extraneous frequencies due to the periodicity of the output associated with the rotation frequency.

The instrument here described generates an oscilloscope display which can be adjusted to match the original data. The synthesized waveform is the algebraic sum of up to three independent damped sine waves whose frequency, amplitude, damping rate, and phase are independently varied by adjusting the parameters of the gated LCR circuits producing them. The component waves are phase locked to present a static scope display, but their relative phase may be varied. The oscilloscope display is viewed through a tranparent tracing of the original data taped directly to the CRT tube. The parameters of the required number of waves are then varied to produce a best fit to the data. Polaroid photographs of the synthesized waveform and its components can then be made to serve as permanent records.

II
CIRCUIT DESCRIPTION

For this circuit, the problem is the generation of the component sine waves which must have individually variable frequency, amplitude, and damping rate. Their collective phase relation must be variable and coherent. Once the component waves have been generated, the complex waveform is obtained by algebraic addition with an operational amplifier. The waveforms must be generated at a rate convenient for viewing purposes, but otherwise the frequency range may be chosen with regard to circuit considerations. There are a variety of schemes for generating such waveforms including, for example, providing phase lock and exponentially variable gain to the required number of tunable CW oscillators. A simpler method is to abruptly gate off the current flowing through a parallel LCR circuit. If the "OFF" impedance of the gate is very high, an exponentially damped sine wave whose parameters are completely determined by the values of L, C, and R is generated. (The resistance of the inductor contributes to R.)

A functional diagram of the instrument is given in Fig. 1 and the circuit diagram for one channel is given in Fig. 2. Referring to these figures, a typical generation cycle proceeds as follows: Transistor Q3 is normally on, allowing current to flow through L1 (or L2 as selected for frequency range). A sawtooth voltage from the oscilloscope sweep output is fed to a Schmitt trigger circuit, Q1 and Q3, via potentiometer R2, to establish a delay time from start of the sweep. Firing of the trigger

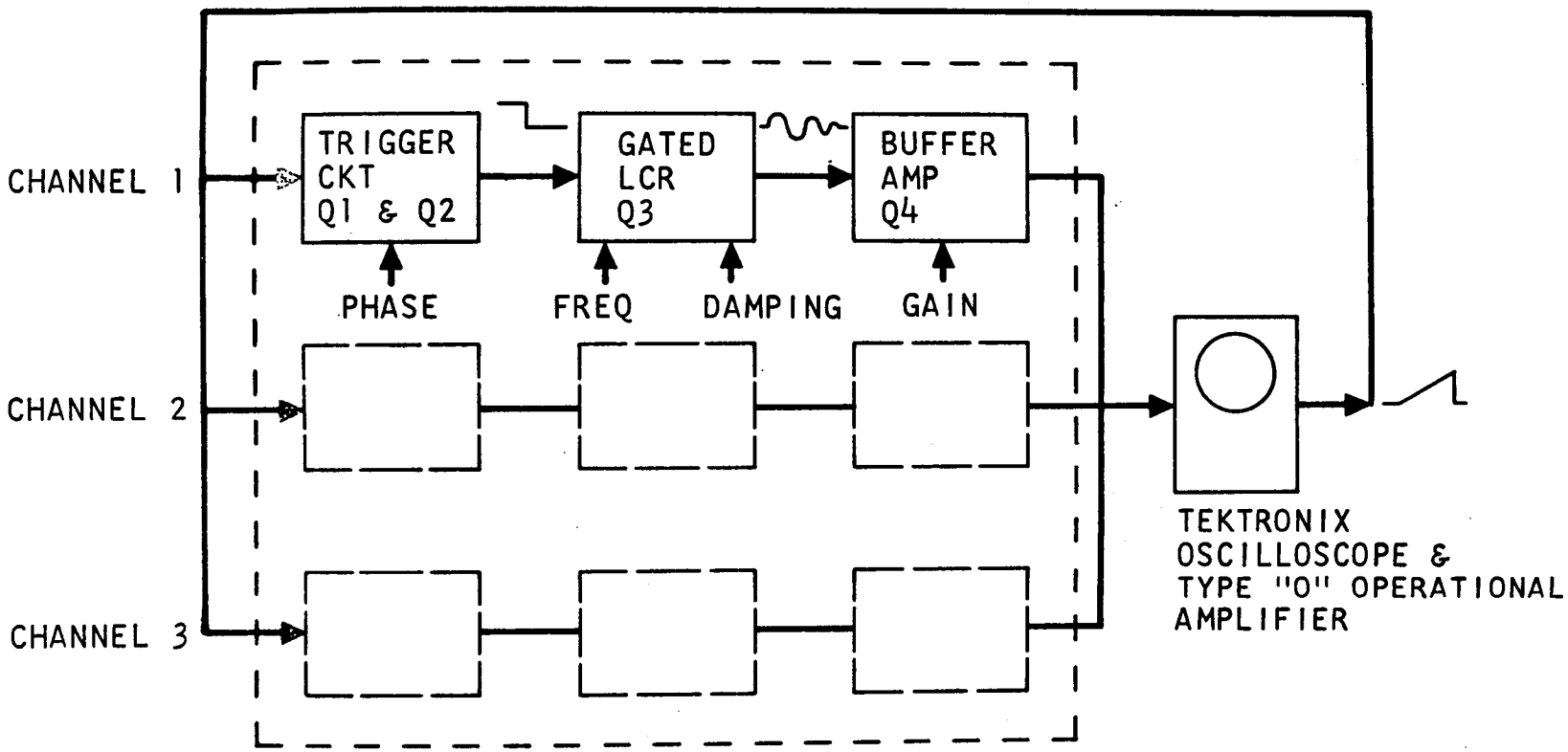

Fig. 1--Functional diagram of the curve resolver

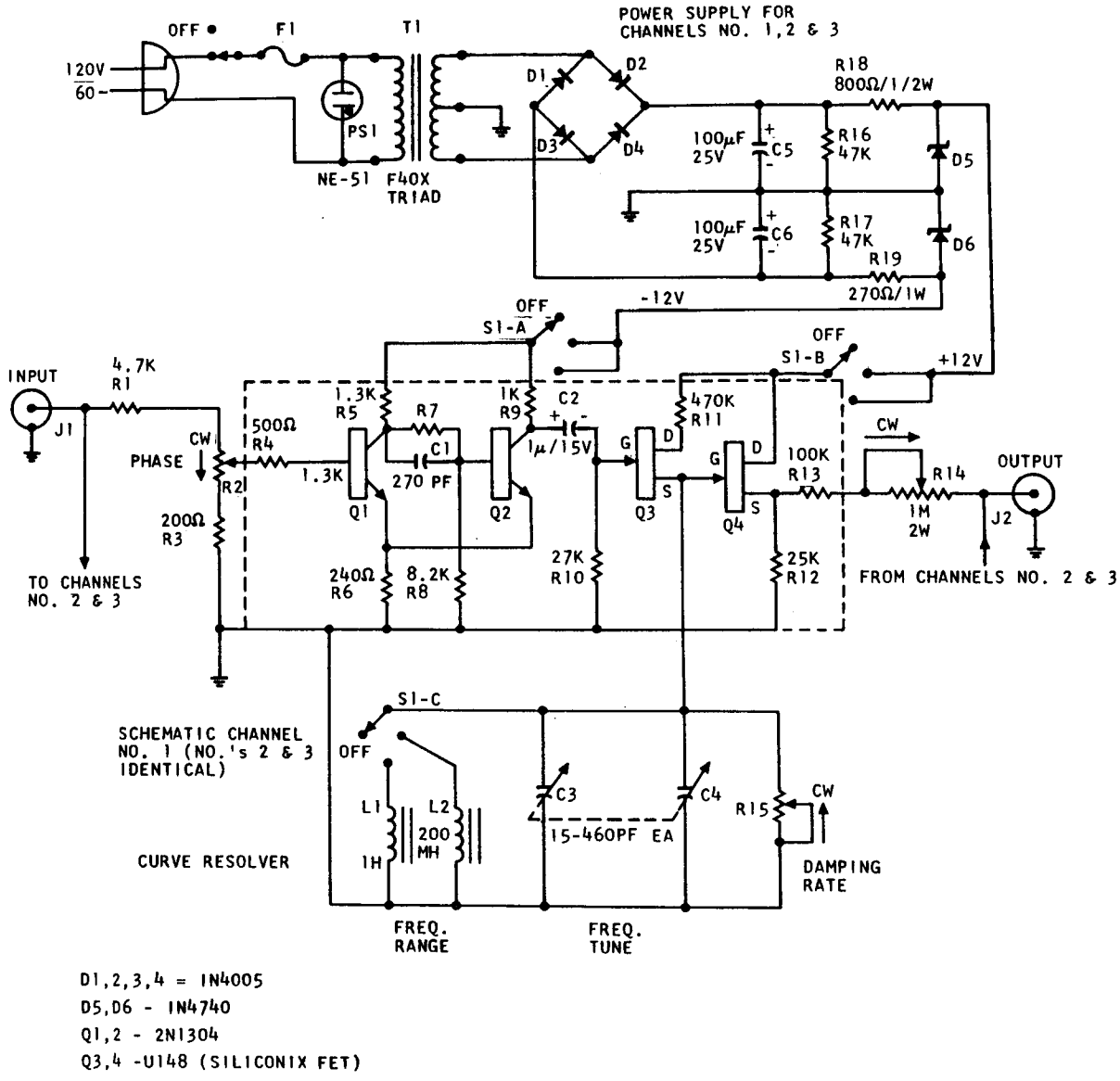

Fig. 2--Schematic diagram of one channel of the curve resolver

circuit applies a steep negative going step signal to the gate input of Q3, abruptly cutting off the current flow to L1, and initiating the characteristic damped sine wave of the simple parallel LCR "tank" circuit. The initial voltage value of the generated wave is essentially zero and the initial phase is at zero-crossing. The output voltage signal across the LCR circuit is coupled through the buffer amplifier Q4 and gain potentiometer R14 to the vertical amplifier of the oscilloscope. To sum the signals from several channels, we use a Tektronix Type "O" operational amplifier connected in the differentiating mode. This configuration eliminates the D.C. pedestal voltage component of the buffer amplifiers before summing. The gain potentiometers of the individual channels then become the weighting functions (z_{in}) of the operational amplifier summing circuit.

In order to generate lightly damped waveforms it is necessary that the unloaded Q of the LCR circuit be as high as possible. Ferrite toroidal core inductors were found to exhibit the best values of Q for the inductance range involved. Transistors Q3 and Q4 were chosen from FET types because of the high impedance characteristics of such devices. Q3 and Q4 are both shunt loads on the LCR circuit. Both devices exhibit shunt resistances in excess of 5 MΩ during the ringing time of the tank circuit. Measurement of the output of individual channels show that they are, very accurately, exponentially damped sine waves.

Figure 3a is an interferogram of a multiple-mode plasma wave and is typical of the data to be analyzed. An example of the circuit performance is exhibited in Fig. 3b. The circuit parameters have been adjusted to match the data shown in Fig. 3a. Comparison of the figures shows that a good fit has been obtained. The waveform of Fig. 3b is composed of three

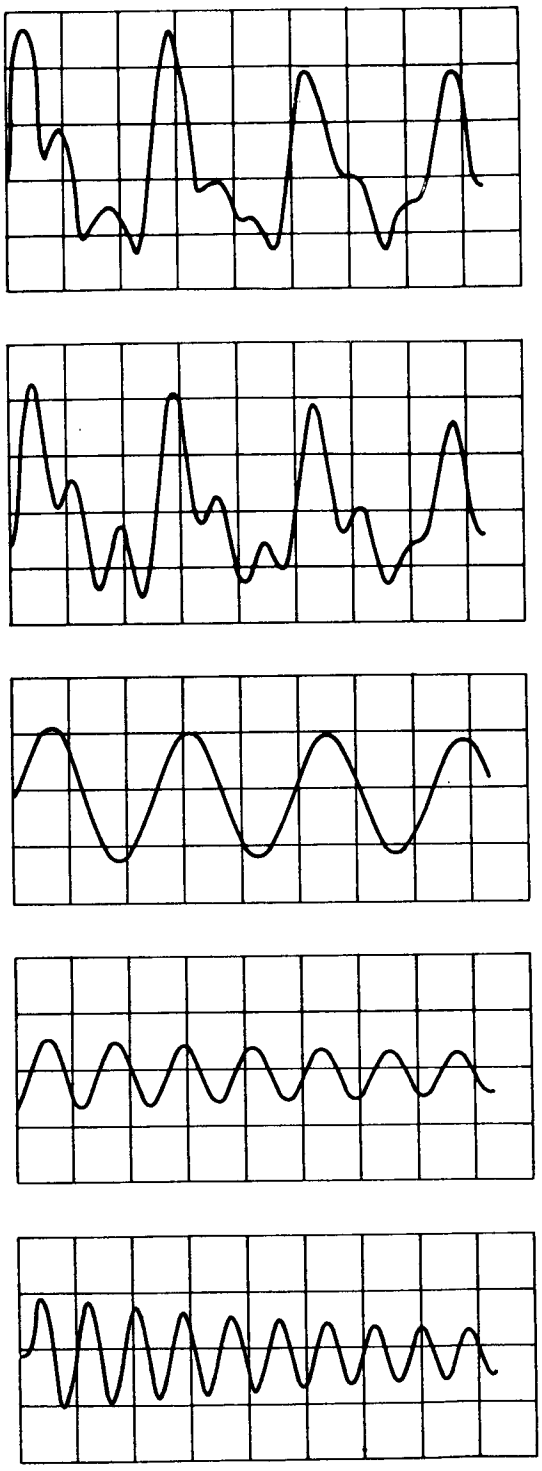

Fig. 3--Curve A is a interferogram of a multiple-mode plasma wave. Curve B is the combination waveform from the curve resolver. Curves C, D, and E are the individual components of Curve B

waves shown individually in Figs. 3c, 3d, and 3e. Each of these waves may be separately observed, photographed, and analyzed by turning off the other oscillator channels.

III
DISCUSSION

A question that naturally arises is whether the tuning converges rapidly. Even with only two component waves, this circuit has eight control parameters: i.e., the amplitude, frequency, damping, and phase of each channel. We have found that after a little practice at twisting the knobs, the data can be fit rapidly and accurately. Use of the device also rapidly educates the experimenter to recognize the probable components of waveforms which are rather complicated at first glance. A perfect fit to the data is not usually obtained. The residual discrepancies are not due to errors in the synthesized curve, but are caused by systematic experimental errors (i.e., a spatial variation in plasma density) which distort the data. An important advantage of the present method is that the experimenter can evaluate the importance of various distortions during the analysis and fit the data accordingly.

Channels to generate other types of functions could be added if required by the nature of the data.

APPENDIX VIII

REFERENCE

1. J. H. Malmberg and C. B. Wharton, Phys. Rev. Letters 17, 175 (1966); Phys. Rev. Letters 19, 775 (1967).